

**LIQUID PHASE ADSORPTION OF PURE, BINARY AND  
TERNARY SYSTEMS OF n-PARAFFINS ON LMS-5A**

**A Thesis Submitted  
In Partial Fulfilment of the Requirements  
for the Degree of  
DOCTOR OF PHILOSOPHY**

**By  
RAM KRISHNA GUPTA**

**to the  
DEPARTMENT OF CHEMICAL ENGINEERING  
INDIAN INSTITUTE OF TECHNOLOGY, KANPUR  
MARCH, 1979**

CHE-1979-D-GUP-LIQ

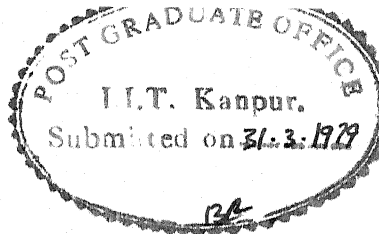
I.I.T. KANPUR  
CENTRAL LIBRARY

Acc. No. A 62147

3 MAY 1980

TO

MY PARENTS



CERTIFICATE

Certified that the work 'LIQUID PHASE ADSORPTION ON PURE, BINARY AND TERNARY SYSTEMS OF n-PARAFFINS ON LMS-5A' has been carried out under our supervision and that the work has not been submitted elsewhere for a degree.

*D. Kunzru*

[D. Kunzru]

Assistant Professor

Department of Chemical Engineering  
Indian Institute of Technology  
Kanpur-208016, India

*D.N. Saraf*

[D.N. Saraf]

Professor

Department of Chemical Engg.  
Indian Institute of Technology  
Kanpur-208016, India

Date: March 19, 1979

Date: March 19, 1979

POST GRADUATE OFFICE  
This thesis has been approved  
for the award of the Degree of  
Doctor of Philosophy (Ph.D.)  
in accordance with the  
regulations of the Indian  
Institute of Technology, Kanpur  
Dated: 25.10.1979 (3)

ACKNOWLEDGEMENTS

The author takes this opportunity, with great pleasure, to express his deep sense of gratitude to Professors D.N. Saraf and D. Kunzru for providing discerning guidance, flexibility in work, unfailing encouragement and constructive criticisms throughout the course of this research. Their clear, deep insight to many problems encountered during the period of this investigation has been a constant source of inspiration.

The author expresses his appreciation to his colleagues Drs. N. Choudhary, P.K. Bajpai and Mr. B.H. Jajoo who assisted him in many ways.

The cooperation rendered by the staff of Department of Chemical Engineering, Indian Institute of Technology, Kanpur is gratefully acknowledged.

The author is very much thankful to his wife, Sasha, for constant encouragement and patience shown by her during the course of this study. He also appreciates the entertainment provided by his son, MONU, on returning home after long hours of work in the laboratory.

Thanks are also due to Mr. B.S. Pandey for excellent typing, Mr. D.S. Panesar for preparing drawings, Mr. Hari Ram for cyclostyling, Mr. Jai Ballabh for making ammonia prints and Mr. T.R. Gupta who has helped him in many ways during his association with the department.

Author

CONTENTS

List of Tables	vi
List of Figures	viii
Synopsis	x
Nomenclature	xiv
CHAPTER 1 INTRODUCTION	1
References	6
CHAPTER 2 LITERATURE REVIEW	
2.1 Historical	7
2.2 Structure of Zeolites	
2.2.1 Introduction	10
2.2.2 Structure of Molecular Sieves 5A	15
2.3 Applications of Zeolites as Adsorbents	
2.3.1 Hydrocarbon Separation	
2.3.1.1 n-Paraffins Separation	19
2.3.1.2 Separation of p- and o-xylenes	22
2.3.1.3 Olefins Separation	23
2.3.2 Drying Gases and Liquids	24
2.3.3 Separation and Purification of Industrial Streams	
2.3.3.1 Purification of Air Prior to Liquefaction	24
2.3.3.2 Natural Gas Purification	25
2.3.3.3 Oxygen Enrichment of Air	25
2.3.4 Pollution Control	26
References	27
CHAPTER 3 EXPERIMENTAL RESULTS ON ADSORPTION OF PURE COMPONENTS	
3.1 Introduction	34
3.2 Experimental	35

3.3 Results and Discussion	
3.3.1 Breakthrough Curves	38
3.3.2 Adsorption Isotherms	38
References	48
CHAPTER 4	EXPERIMENTAL RESULTS ON ADSORPTION OF MULTI COMPONENT SYSTEMS
4.1 Introduction	49
4.2 Experimental	51
4.3 Results and Discussion	
4.3.1 Equilibrium Curves for Binary Systems	51
4.3.2 Separation Factors for Binary Systems	59
4.3.3 Adsorption in Ternary Systems	67
References	72
CHAPTER 5	MATHEMATICAL MODEL FOR ADSORPTION OF PURE AND MULTI COMPONENT HYDROCARBON SYSTEMS
5.1 Introduction	73
5.2 Mathematical Model for Adsorption of Pure n-Paraffins	76
5.3 Extension of the Model to Binary Systems	82
5.4 Extension of the Model to Ternary Systems	88
5.5 Results and Discussion	
5.5.1 Adsorption of Pure Hydrocarbons	95
5.5.2 Adsorption of Binary Systems	101
5.5.3 Adsorption of Ternary Systems	109
References	115
CHAPTER 6	CONCLUSIONS AND RECOMMENDATIONS
6.1 Conclusions	117
6.2 Recommendations	118
APPENDICES	120

LIST OF TABLES

TABLE		Page
2.1	Properties of Selected Natural and Synthetic Zeolites	11
4.1	Separation Factor, $K_r$ , for Binary Systems	66
4.2	Experimental Results for Ternary Systems at 6°C	68
4.3	Experimental Results for Ternary Systems at 18°C	69
4.4	Experimental Results for Ternary Systems at 30°C	70
5.1	Values of $\alpha$ and $\beta$ at Different Temperatures	99
5.2	Comparison of Experimental and Predicted Values for Binary Systems at 6°C	102
5.3	Comparison of Experimental and Predicted Values for Binary Systems at 18°C	104
5.4	Comparison of Experimental and Predicted Values for Binary Systems at 30°C	106
5.5	Comparison of Experimental and Predicted Values for Binary Systems at 42°C	108
5.6	Comparison of Experimental and Predicted Values for Ternary Systems at 6°C	110
5.7	Comparison of Experimental and Predicted Values for Ternary Systems at 18°C	111
5.8	Comparison of Experimental and Predicted Values for Ternary Systems at 30°C	112
A3.2	Experimental Results for Breakthrough Curves of n-Heptane	123
A3.3	Experimental Results for Pure Components at 6°C	124
A3.4	Experimental Results for Pure Components at 18°C	126
A3.5	Experimental Results for Pure Components at 30°C	128
A3.6	Experimental Results for Pure Components at 42°C	130

## TABLE

		Page
A4.1	Experimental Results for Binary Systems at 6°C	131
A4.2	Experimental Results for Binary Systems at 18°C	133
A4.3	Experimental Results for Binary Systems at 30°C	135
A4.4	Experimental Results for Binary Systems at 42°C	137
A4.5	Operating Conditions for Ternary Systems at 6°C	138
A4.6	Operating Conditions for Ternary Systems at 18°C	139
A4.7	Operating Conditions for Ternary Systems at 30°C	140

LIST OF FIGURES

FIGURE	Page
2.1 Arrangement of Silicon-Oxygen and Aluminum-Oxygen Tetrahedra	14
2.2 Truncated Octahedron	14
2.3 Cubic Array of Truncated Octahedra in the Zeolite Type A	16
2.4 Arrangement of Truncated Cuboctahedron to Give Zeolite Type A	16
3.1 Assembly of Adsorption Cell	36
3.2 Breakthrough Curves for n-Heptane	39
3.3 Adsorption Isotherms of n-Pentane	40
3.4 Adsorption Isotherms of n-Hexane	41
3.5 Adsorption Isotherms of n-Heptane	42
3.6 Adsorption Isotherms of n-Octane	43
3.7 Adsorption Isotherms of Different n-Paraffins at 30°C	45
4.1 Equilibrium Curves for Pentane-Hexane System at Different Temperatures	52
4.2 Equilibrium Curves for Hexane-Heptane System at Different Temperatures	53
4.3 Equilibrium Curves for Heptane-Octane System at Different Temperatures	54
4.4 Equilibrium Curves for Pentane-Heptane System at Different Temperatures	55
4.5 Equilibrium Curves for Pentane-Octane System at Different Temperatures	56
4.6 Equilibrium Curves for Binary Systems Containing Pentane at 30°C	58
4.7 Effect of Pentane Concentration on Separation Factor. System: Pentane-Hexane	60

FIGURE	Page
4.8 Effect of Hexane Concentration on Separation Factor: System: Hexane-Heptane	61
4.9 Effect of Heptane Concentration on Separation Factor. System:Heptane-Octane	62
4.10 Effect of Pentane Concentration on Separation Factor. System: Pentane-Heptane	63
4.11 Effect of Pentane Concentration on Separation Factor. System: Pentane-Octane	64
5.1 Comparison Between Predicted and Experimental Isotherms at 18°C	97
5.2 Arrhenius Plot for $\alpha$	100
A3.1 A Typical Chromatogram for n-Paraffins-Benzene Mixture	121
A3.2 Calibration Curves for Different Paraffins	122

LIQUID PHASE ADSORPTION OF PURE, BINARY AND TERNARY  
SYSTEMS OF n-PARAFFINS ON LMS-5A

A Thesis Submitted  
In Partial Fulfilment of the Requirements  
For the Degree of  
DOCTOR OF PHILOSOPHY

by

RAM KRISHNA GUPTA

to the

DEPARTMENT OF CHEMICAL ENGINEERING  
INDIAN INSTITUTE OF TECHNOLOGY  
KANPUR-208016

March 1979

SYNOPSIS

Separation of n-paraffins from petroleum fractions has been of great importance in petroleum industry. Molecular sieves are being extensively used as adsorbent in these separation processes. Since most earlier processes use vapor phase adsorption, enough information has been generated on this aspect. However, present trend is towards the use of liquid phase adsorption which has been investigated by few workers. In the present study, liquid phase adsorption isotherms of several normal paraffins on LMS-5A were measured in the temperature range 6-42°C. A mathematical model based on statistical thermodynamics was developed to predict multi-component adsorption, using adsorption isotherms of pure

components. The model was validated by experimentally measuring binary and ternary data on the same hydrocarbons.

A glass adsorption cell was developed for the measurement of adsorption of pure and multicomponent hydrocarbon systems. n-Pentane, n-hexane, n-heptane and n-Octane were used for liquid phase adsorption at  $6^{\circ}$ ,  $18^{\circ}$ ,  $30^{\circ}$ , and  $42^{\circ}\text{C}$ . Benzene served as a diluent since its adsorption is negligibly small on LMS-5A.

The general trend of the isotherms for pure n-paraffins showed an initial increase in equilibrium loading (m moles adsorbed/g of zeolite) with increase in concentration followed by a relatively large range of concentration over which the equilibrium loading was nearly constant and then a further increase at higher concentrations. This upward trend in equilibrium loading at higher concentration was attributed to adsorption on external surfaces rather than intracrystalline adsorption. The effect of temperature on equilibrium loading was maximum for n-pentane and reduced for higher paraffins, being minimum for n-octane. For a particular temperature, the effect of concentration on equilibrium loading was most significant for n-pentane and decreased with increase in molecular size. At a given temperature and molar concentration, equilibrium loading for lower molecular weight paraffin was higher than that for larger molecules. This was explained in terms of steric effect which is more predominant for larger molecules.

Pure component adsorption data were represented by a statistical model with two parameters namely, slope of the isotherm at low concentration,  $\alpha$ , and volume of the adsorbed molecule,  $\beta$ . The grand partition function of the system defined in terms of  $\alpha$  and  $\beta$  was used to calculate the number of molecules adsorbed per cavity. The model accounted for adsorbate-adsorbent interaction and the reduction in free volume due to the finite size of the adsorbed molecules. Accuracy required by the model and nature of the adsorption isotherms did not permit direct measurement of the slope at low concentrations. Consistent and satisfactory values of the molecular volume of various n-paraffins were also not available. A least square minimization procedure, using Blind Search Technique, was employed to evaluate  $\alpha$  and  $\beta$  from the experimental data. For all the n-paraffins studied,  $\alpha$  was found to increase with decreasing temperature and increasing molecular weight. Molecular volume, as expected, monotonically increased with temperature. This model was then extended to predict the adsorption in binary and ternary systems using the values of  $\alpha$  and  $\beta$  obtained for pure components.

Experimental measurements on 5 binary and 3 ternary systems of these n-paraffins were made at four different temperatures. The effect of temperature and concentration on separation factor,  $K$ , defined below was studied |

$$K = \frac{y_L/x_L}{y_H/x_H}$$

where  $y$  and  $x$  are mole fractions in adsorbed and liquid phases and  $L$  and  $H$  are lighter and heavier components respectively. In all binary systems, lower molecular weight paraffins were preferentially adsorbed. The value of  $K$ , at the same temperature, decreased with increase in composition of preferentially adsorbed component. To make the separation factor independent of concentration it was redefined as

$$K_r = \frac{y_L/x_L}{y_H/(x_H+x_B)}$$

where  $x_B$  is the mole fraction of benzene in the liquid phase. Adsorption measurements on ternary systems showed that total hydrocarbon adsorbed increased with decrease in temperature.

The extended form of the model was then validated against the experimental measurements of the binary and ternary systems. For most of the data, the predicted values of the number of molecules adsorbed per cavity were within 10 per cent of the experimentally observed values. This prediction procedure can be extended to systems of practical importance like separation of n-paraffins from petroleum fractions, which will facilitate their design without extensive pilot plant studies.

NOMENCLATURE

a	activity of the sorbate, $p/kT$
c	average number of molecules adsorbed per cavity
$c_{\text{cal}}$	average number of molecules adsorbed per cavity (calculated)
$c_{\text{expt}}$	average number of molecules adsorbed per cavity (experimental)
E	sum of square of errors
$E_{\text{min}}$	minimum of sum of square of errors
G	grand partition function
K	separation factor
$K_r$	redefined separation factor
k	Boltzmann constant
M	number of cavities
m	maximum number of molecules adsorbed in a cavity
$\bar{N}$	average number of molecules adsorbed
n	number of data points in a adsorption isotherm
P	vapor pressure at adsorption temperature
p	partial pressure
Q	canonical ensemble partition function of the system
q	partition function of a cavity
$r_i$	position vector
s	number of molecules adsorbed in a cavity
T	absolute temperature, $^{\circ}\text{K}$
$U_s$	potential energy for the sub system

v volume of the cavity (= 776  $\text{\AA}^3$  for LMS-5A)  
x mole fraction in liquid phase  
y mole fraction in adsorbed phase  
Z configuration integral of a cavity

#### Greek Symbols

$\alpha$  Henry's constant, (molecules)/(cavity)(torr)  
 $\beta$  molecular volume,  $\text{\AA}^3$   
 $\epsilon$  molecular constant  
 $\sigma$  diameter of the molecule  
 $\mu$  chemical potential

#### Subscripts

A component A  
B component B  
C component C  
H higher molecular weight paraffin  
h number of molecules of C adsorbed in a cavity  
i number of molecules of A adsorbed in a cavity  
j number of molecules of B adsorbed in a cavity  
L lower molecular weight paraffin

## CHAPTER 1

### INTRODUCTION

Amorphous, gel type, alumino silicates have been used for years for water treatment. An extensive literature survey till 1930 on the use of natural minerals, such as green sand or glauconite, and natural zeolite water softeners is given by Shreve [2]. Although, zeolite minerals were first discovered and named in 1756 by Baron Cronstedt, first experiments on separation of mixtures using dehydrated zeolite mineral chabazite were performed by Barrer only in 1938 [1]. Synthesis of molecular sieve zeolite in 1946 can be termed as a revolution in chemical industry. The magnitude of interest shown by scientists and engineers is reflected in the fact that from the first industrial research in 1948, over 7000 papers have been published and 2000 U.S. patents obtained dealing with zeolite science and technology.

Due to their many unique properties, zeolites are being used in a variety of applications in chemical industry. Broadly speaking, zeolites are used as adsorbents for separation processes and as catalysts or catalyst supports. Separation processes using molecular sieves as adsorbents include separation of n-paraffins from various petroleum fractions, separation of p- and o-xylenes, oxygen enrichment of air, removing water from water-alcohol mixture, drying of

refrigerants and other chemicals, recovering radioactive ions from waste solutions, removing carbon dioxide and sulfur compounds from natural gas, separating hydrogen isotopes, removing sulfur dioxide from flue gases, etc. Since very large surface areas are available for adsorption, molecular sieve zeolites are also used as catalysts or catalyst supports. For example, in the catalytic cracking of gas oil, zeolites are much superior than the conventional silica-alumina catalysts.

Separation of n-paraffins from petroleum fractions has been of great interest industrially. Higher carbon number n-paraffins recovered from kerosene or gas oil are used in the manufacture of biodegradable detergents while lower ones are removed from gasoline to increase its octane number. These n-paraffins when separated further can be used as organic chemicals. n-paraffins can not be separated from petroleum fractions by other conventional adsorbents such as activated carbons, activated clays, inorganic gels, etc., because these adsorbents do not possess an ordered crystal structure and consequently the pores are non-uniform. Development of molecular sieves (LMS-5A) has made it possible to recover n-paraffins from petroleum fractions. Molecular sieves have a high internal area available for adsorption with uniform pore opening which makes them size selective. The adsorption takes place inside the cavity and the component

having a critical diameter less than the mouth opening of the cavity is adsorbed while larger molecules are excluded. The only other method of n-paraffin separation is by forming adducts with urea. The formation of the complex is due to the ability of urea to form a frame work containing channels within which the molecules of n-paraffins fit lengthwise. This framework can accommodate molecules of different lengths but not those of widely different cross sections, i.e., the cross sections of branched paraffins, cycloparaffins, and aromatics are too large to permit these hydrocarbons to form adducts with urea. However, separation of n-paraffins by molecular sieves is superior to urea adduct method because of higher selectivity and easier generative properties of molecular sieves.

All petroleum fractions are mixtures of n-paraffins, iso- and other branched chain paraffins, olefins, naphthenes, etc. Each class of these components consist of several different hydrocarbons and each of these adsorb on molecular sieves to a different degree. The adsorption of n-paraffins on LMS-5A is one to two orders of magnitude higher than that of other hydrocarbons. To design separation systems it is, therefore, necessary to study the multicomponent adsorption of these hydrocarbon mixtures on molecular sieves. Depending on the boiling range and origin, the composition of a petroleum fraction can vary widely and therefore there will be an

infinite number of multicomponent systems to be studied. It will be impossible to measure multicomponent adsorption data for each of these systems. However, the number of n-paraffins present in any petroleum fraction is small and adsorption studies can easily be made for each of these hydrocarbons. A model which could predict multicomponent adsorption using only pure component data would eliminate the need for multicomponent adsorption measurements.

The adsorption of n-paraffins can be performed in the vapor or liquid phase. Although vapor phase adsorption has been investigated by various workers, very little information is available on liquid phase adsorption. A systematic study on the liquid phase adsorption of n-paraffins on molecular sieves is very much needed.

#### Objectives of the Present Investigation:

In the present investigation, liquid phase adsorption studies on molecular sieves for the separation of n-paraffins from naphtha were envisaged. Since naphtha is a very complex mixture of hydrocarbons it was felt necessary to make rather simple mixtures of known components (n-pentane, n-hexane, n-heptane, n-octane and benzene) for this study. Benzene was used as a diluent since it is essentially not adsorbed on Linde Molecular Sieve 5A which was used as the adsorbent. Adsorption isotherms for these n-paraffins were measured at

several temperatures. These isotherms were then used in a mathematical model that was developed to predict the binary and ternary adsorption data. These predictions were verified by making actual measurements.

An overall literature review has been given in Chapter 2. Chapter 3 deals with the pure component liquid phase adsorption of these n-paraffins on molecular sieves. Experimental results of binary and ternary systems of these n-paraffins are given in Chapter 4. In Chapter 5 a mathematical model is described. Conclusions and recommendations have been discussed in Chapter 6.

## REFERENCES

- [1] Barrer, R.M., Proc. Roy. Soc. London, A167, 393 (1938).
- [2] Shreve, R.N., Green Sand Bibliography to 1930, U.S. Bureau of Mines Bulletin, 328 (1930).

## CHAPTER 2

### LITERATURE REVIEW

#### 2.1 HISTORICAL:

The phenomenon of adsorption was first discovered by Sheele and Fontana in 1777. The ability of charcoal to remove color from solutions was discovered by Lowtiz in 1785. deSaussure carried out the first systematic investigation of adsorption in 1814. The adsorption studies till 1930 have been reviewed by McBain [69]. A comprehensive review of physical adsorption was published in 1942 by Brunauer [26]. Later, Mantell reviewed adsorption as a unit operation of chemical engineering in 1951 [67].

The aluminosilicates were termed zeolites by Cronstedt [33] in 1756. He observed that certain mineral crystals when heated appeared to melt and boil at the same time. Thus, from the Greek Zeo, to boil, and lithos, stone, he coined the term zeolite. The phenomenon of melting and boiling at the same temperature is termed 'intumescence' and the zeolites are said to intumesce.

Initial investigations on crystalline zeolites were performed in 1840 by Damour [34] who reported on the reversible dehydration of the zeolite minerals. Damour noted that the transparency and crystal form did not change on heating.

In 1845, Thompson [98] conducted experiments which showed that certain soils have the power of decomposing and retaining ammonium salts. When a solution of ammonium sulfate was filtered through the soil, the filtrate contained calcium sulfate and ammonium salt was retained in the soil. Later, Way [101] showed that the hydrated silicates in the soil produced this phenomenon. He was able to show that only ammonium or potassium was exchanged for calcium in the soil.

Several years later Eichhorn [40] in 1858 published a paper on the action of dilute salt solutions on silicates, showing that the base exchange principle discovered by Way is reversible. He studied the quantitative behavior of the zeolite minerals, chabazite and natrolite, in contact with dilute salt solutions and found that sodium and calcium could reversibly replace each other in these zeolites.

The idea that the structures of dehydrated zeolite consists of open sponge frame works, was given by Friedel [49] in 1896. He observed that various liquids such as alcohol, chloroform, carbondisulfide and benzene were occluded by zeolites. In 1909 Grandjean [53] found that dehydrated zeolite crystals could reversibly adsorb inorganic vapors such as iodine, mercury, ammonia, air, hydrogen, carbon-disulfide and bromine.

Beginning in the 1920's, a large number of papers on crystalline zeolites began appearing in the scientific

literature. In 1925, Weigel and Steinhoff [104] reported that chabazite, rapidly adsorbed the vapors of water, methyl and ethyl alcohol and formic acid while acetone, ether, and benzene were excluded. This was the first report of the sieving action at molecular scale of anhydrous crystalline zeolites. Shortly, thereafter, McBain [69] recognized the importance of these results and deduced that the pore openings in the chabazite crystals must be less than  $5 \text{ \AA}^{\circ}$  in diameter. To describe this phenomenon of selective adsorption, or 'persorption', as he termed it, McBain originated the term molecular sieve.

An extensive literature on the use of natural materials such as green sand or glauconite and zeolite water softners has been reported by Shreve [90]. Smith [93] in 1963 has defined zeolite as 'an aluminosilicate with a framework structure enclosing cavities occupied by large ions and water molecules, both of which have considerable freedom of movement, permitting ion exchange and reversible dehydration.'

The application of x-ray diffraction techniques by Pauling [81] and Taylor [97] in the early 1930's led to the determination of the crystal structures of analcite and natrolite. The porous nature of zeolite crystals attracted the attention of a few physical chemists, in particular Barrer, who reported the results of his studies on the sorption of gases on crystals of chabazite and analcite [8].

In the beginning, attempts [75] were made to duplicate the hydrothermal processes by which zeolite minerals were assumed to have formed in nature. Earlier scientists attempted to synthesize zeolite crystals with partial success. Although the synthesis of many zeolites has been reported in literature, majority of these must be discredited on the basis of improper identification [9-11]. The advent of x-ray diffraction has enabled a more positive identification of complex compositions and structures than the methods used by the early investigators. By 1952, many different types of synthetic zeolites had been prepared in the laboratory [ 9, 10, 18, 20, 67]. Some of these were new varieties not found in nature, e.g., type A and X. Recently, Bajpai [6] synthesized mordenite starting from rice husk ash which is available in abundance in India. Different zeolites were produced by changing the chemical composition and molecular weight distribution of the starting species in the silicate solutions. A selected list of natural and synthetic zeolites with their properties is given in Table 2.1.

## 2.2 STRUCTURE OF ZEOLITES:

### 2.2.1 Introduction:

Crystalline zeolites are complex materials, chemically and structurally, comprising the major group of the framework silicates [17]. Other minerals included in this category

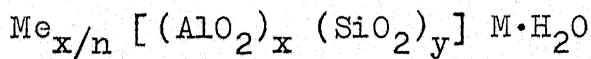
TABLE 2.1: SOME ZEOLITES WITH THEIR PROPERTIES

Name	Source	Composition	Density, g/cm <sup>3</sup>	Void Vol., cm <sup>3</sup> /g	Aperture, Å
alcire Group					
Analcime	Natural	Na <sub>16</sub> [ (AlO <sub>2</sub> ) <sub>16</sub> (SiO <sub>2</sub> ) <sub>32</sub> ]·16 H <sub>2</sub> O	1.85	0.099	2.8
dalite Group					
Zeolite A	Synthetic	Na <sub>12</sub> [ (AlO <sub>2</sub> ) <sub>12</sub> (SiO <sub>2</sub> ) <sub>12</sub> ]·27H <sub>2</sub> O	1.33	0.300	4.2
Faujasite	Natural	(Na <sub>2</sub> , Ca, Mg) <sub>60</sub> [ (AlO <sub>2</sub> ) <sub>60</sub> (SiO <sub>2</sub> ) <sub>132</sub> ]·260H <sub>2</sub> O	1.31	0.350	8.0
Zeolite X	Synthetic	Na <sub>86</sub> [ (AlO <sub>2</sub> ) <sub>86</sub> (SiO <sub>2</sub> ) <sub>106</sub> ]·264 H <sub>2</sub> O	1.29	0.360	8.0
Zeolite Y	Synthetic	Na <sub>56</sub> [ (AlO <sub>2</sub> ) <sub>56</sub> (SiO <sub>2</sub> ) <sub>136</sub> ]·264 H <sub>2</sub> O	1.30	0.350	8.0
abazite Group					
Chabazite	Natural	Ca <sub>4</sub> [ (AlO <sub>2</sub> ) <sub>8</sub> (SiO <sub>2</sub> ) <sub>16</sub> ]·26H <sub>2</sub> O	1.48	0.290	3.0x4.0
Erionite	Natural	(Ca, Mg, Na <sub>2</sub> , K <sub>2</sub> ) <sub>45</sub> [ (AlO <sub>2</sub> ) <sub>9</sub> (SiO <sub>2</sub> ) <sub>27</sub> ]·27H <sub>2</sub> O	1.50	0.210	3.6x5.2
illite Group					
Phillipsite	Natural	(K, Na) <sub>5</sub> [ (AlO <sub>2</sub> ) <sub>5</sub> (SiO <sub>2</sub> ) <sub>11</sub> ]·10H <sub>2</sub> O	-	-	-
Zeolite B	Synthetic	Na <sub>6</sub> [ (AlO <sub>2</sub> ) <sub>6</sub> (SiO <sub>2</sub> ) <sub>10</sub> ]·15 H <sub>2</sub> O	1.47	0.150	3.5

Name	Source	Composition	Density, g/cm <sup>3</sup>	Void Vol., cm <sup>3</sup> /g	Aperture, Å
Mordenite Group					
Mordenite	Natural	Na <sub>8</sub> [ (AlO <sub>2</sub> ) <sub>8</sub> (SiO <sub>2</sub> ) <sub>40</sub> ] · 24H <sub>2</sub> O	1.72	0.150	4.0
Mordenite	Synthetic	Na <sub>8</sub> [ (AlO <sub>2</sub> ) <sub>8</sub> (SiO <sub>2</sub> ) <sub>40</sub> ] · 24H <sub>2</sub> O	1.72	0.140	6.6

are feldspars and feldspathoids [36]. As a result of structural studies in the last three decades, using infrared, NMR and ESR in addition to x-ray diffraction, there is extensive information available on the structure of zeolites. Many zeolite properties can now be interpreted on the basis of their structure.

The first structural analysis of a synthetic zeolite, type A, was reported in 1956 [85] and was followed by the structures of faujasite [14], zeolite type X [19, 25] and chabazite [37]. These zeolites consist of a three dimensional frame work of  $\text{SiO}_4$  and  $\text{AlO}_4$  tetrahedra (Figure 2.1). Substitution of  $\text{Al}^{3+}$  for  $\text{Si}^{4+}$  in framework silicates is common. However, in order to maintain electrical neutrality, each substitution requires the presence of an alkali metal or alkaline earth ion, such as  $\text{Na}^+$ ,  $\text{K}^+$ ,  $\text{Ca}^{2+}$ ,  $\text{Sr}^{2+}$ . In zeolites, the maximum substitution of  $\text{Al}^{3+}$  for  $\text{Si}^{4+}$  in case of A type zeolite is in the ratio of 1:1 and leads to a complete ordering of Al and Si ions [85]. The minimum substitution is in the ratio of 1:5 in case of mordenite [70]. One unit cell of the zeolite structure is given by



where Me is the metal cation, x and y are constants, n is the valency of the metal cation and M is the number of water molecules. The bracketted term gives the frame work composition.

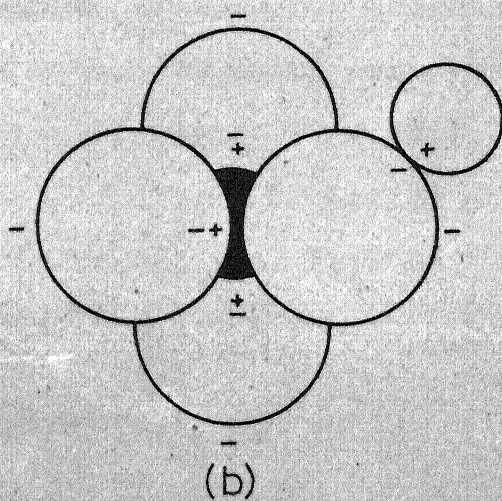
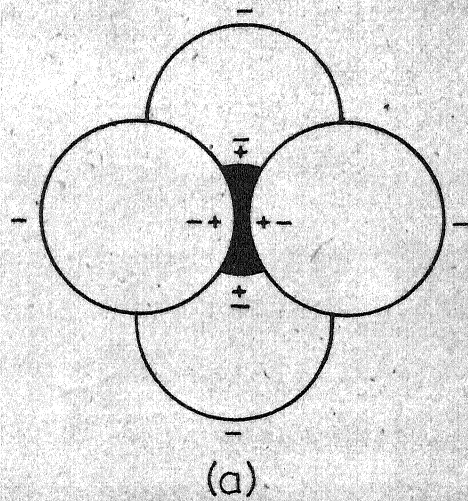
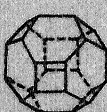


Fig. 2.1 - Tetrahedra of four oxygen ions surrounding a silicon or aluminum ion. (a) Silicon-oxygen tetrahedra. (b) Aluminum-oxygen tetrahedra with  $\text{Na}^+$  cation.



The ratio of Al to Si, as discussed earlier, varies from 1 to 5.

The structure of many zeolites consists of simple arrangements of polyhedra; each polyhedra itself is a three dimensional array of  $\text{Si AlO}_4$  tetrahedra in a definite geometric form. The sodalite group of zeolites (A, x and y types) are all based on frame works which are simple arrangements of truncated octahedra which contain eight hexagonal faces, six square faces, twenty four vertices and 36 edges [33] as shown in Figure 2.2. These truncated octahedra when interconnected in different ways form unit cells of different types of zeolites (A, x and y types).

#### 2.2.2 Structure of Molecular Sieves 5A:

In the structure of zeolite type A [85] as shown in Figure 2.3, the octahedra are linked in cubic array by joining them with cubes on the square faces. This produces a central truncated cube octahedron with an internal cavity of  $11\text{\AA}$  in diameter as shown in Figure 2.4. Each central cavity, termed the  $\alpha$  cage, is entered through six circular apertures formed by a nearly regular ring of eight oxygen atoms with a free diameter of  $4.2\text{\AA}$ . The cavities are, thus, arranged in a continuous three-dimensional pattern forming a system of unduloid-like channels with a maximum diameter of  $11\text{\AA}$  and a minimum of  $4.2\text{\AA}$ . The truncated octahedra

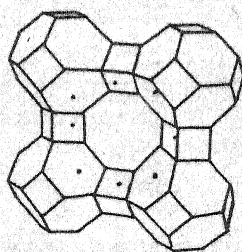


Fig. 2.3 - Cubic array of truncated octahedra in the zeolite type A.

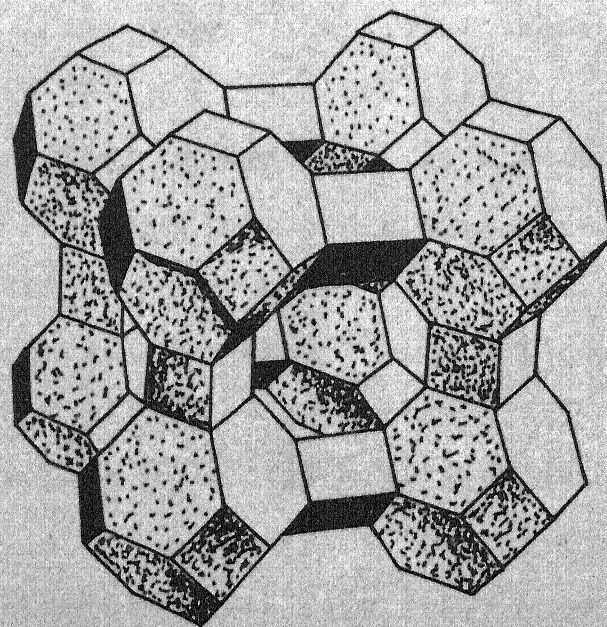


Fig. 2.4 - Arrangement of truncated cuboctahedron to give zeolite type A.

themselves enclose a second set of smaller cavities ( $\beta$  cages) with an internal diameter of  $6.6 \text{ \AA}$  which are connected to the larger cavities by means of a distorted ring of six oxygen atoms of  $2.2 \text{ \AA}$  free diameter.

In each crystallographic unit cell of zeolite type A, there are  $12 \text{ AlO}_4$  and  $12 \text{ SiO}_4$  tetrahedra and therefore 12 monovalent cations. Eight of these sodium ions lie in the centre of the six rings in the hexagonal faces and four occupy positions adjacent to the eight membered ring. When the zeolite is hydrated, these four cations are completely hydrated and float in the centre of their coordination sphere of water molecules. When the water is removed, the cations are found to be located on the walls of the cavity [85]. The eight  $\text{Na}^+$  ions in the six rings are referred to as type I and the remaining four as type II. As discussed earlier, the zeolites readily exchange the alkali metal cations originally present for many other species of cations. If the sodium ions in zeolite type A are replaced by calcium ions, the effective aperture size increases. The sodium form (effective aperture size  $4.0 \text{ \AA}$ ) does not adsorb linear hydrocarbons but after one-third of the sodium ions are replaced by calcium (four per unit cell) many straight chain paraffins are readily adsorbed. This calcium form of zeolite A has an effective diameter of  $5 \text{ \AA}$ .

## 2.3 APPLICATIONS OF ZEOLITES AS ADSORBENTS:

One of the major industrial applications of zeolites is in the area of adsorption processes. Zeolite adsorbents are not only the most important adsorbents today, but their importance is increasing, mainly because of the following unique adsorptive properties:

- (a) Selective adsorption of molecules based on molecular dimensions;
- (b) Highly preferential adsorption of polar molecules;
- (c) Highly hydrophilic surface;
- (d) Variation of properties by ion exchange;
- (e) Large void volume and
- (f) Well defined **crystalline** structure.

Zeolite adsorbents are mostly used in a fixed bed. A number of columns packed with the zeolite adsorbent are interconnected with an automatic valve system to facilitate a continuous flow of industrial stream being processed. Each bed, however, goes through a stepwise cyclic operation, and during each cycle the adsorbed molecules in the zeolite bed are desorbed either by raising the bed temperature, lowering the bed pressure, displacing the adsorbate with another adsorbate, or a combination of these.

Important properties of zeolite adsorbents for a fixed bed application are adsorptive capacity and selectivity, adsorption-desorption rate, physical strength, low catalytic

activity, thermal-hydrothermal stability, chemical stability, and particle size and shape. The ultimate basis in selecting a zeolite adsorbent for a specific application would be the performance, price, and the projected service life of a product. Important industrial adsorption processes using zeolite adsorbents may be classified as follows:

- (i) hydrocarbon separation processes
- (ii) drying gases and liquids
- (iii) pollution control applications
- (iv) separation and purification of industrial streams.

### 2.3.1 Hydrocarbon Separation:

#### 2.3.1.1 n-Paraffin Separation:

n-paraffins need to be separated from gasoline to increase its octane number and from kerosene to use them as a raw material for biodegradable detergents. A detailed discussion on n-paraffin separation processes has been given by Ries [37].

Many workers [39, 42, 57, 59, 99] have reported that n-paraffins can be separated from gasoline to increase its octane rating, using molecular sieve 5A as an adsorbent. These processes mainly differ in the operating conditions during the adsorption cycle and the type of desorbent used to recover n-paraffins. Avery and Lee [5] separated n-paraffins ( $C_5H_{12} - C_{12}H_{26}$ ) from a mixture of iso- and cyclic paraffins

present in naphtha and kerosene. Wolf, et al. [100], could increase the octane number of gasolines of various boiling ranges by 17-20 points. Adsorption was carried out in the vapor phase at 25-30°C higher than the boiling point of the least volatile component in gasoline. Desorption was carried out by nitrogen at 300-350°C. Galich, et al. [50] found that the adsorption of n-paraffins on Ca-A zeolite increased from C<sub>7</sub> to C<sub>10</sub> paraffins then decreased. They reported that the time to reach equilibrium increased with molecular weight of alkane. Charles [27] proposed a countercurrent adsorption scheme and then desorption of n-paraffins by heating the loaded molecular sieve 5A at a temperature 320°C.

Galich, et al. [51], have used steam as a desorbent. Investigations at ESSO [41] indicate that molecular sieve life is extended by using lower boiling olefins rather than steam as a desorbent. With propylene as a desorbent, they did not observe any change in adsorption capacity after 16 cycles while with steam, the sieve capacity was reduced to two thirds of the fresh sieves after 3 cycles. Desorption with different hydrocarbons was tried by Fleck [45]. Mirskii, <sup>that adsorbed paraffins were desorbed</sup> et al. [73] suggested with an excess of a lower boiling n-paraffin. They preferred butane in place of pentane for displacing, adsorbed hexane and/or heptane because of its lower boiling point. James and Lewis [46] reported desorption by straight chain hydrocarbons with 1 to 3 fewer carbon atoms.

ESSO [43] has used ammonia as a desorbent and found that desorption efficiency increased with decrease in pressure. Carbon dioxide was also used by several workers [38, 48, 74] as a desorbent. Plachenov, et al. [84] reported that when carbon dioxide was used as desorbing agent the desorption of octane and hexane was 9-10 per cent higher than when nitrogen was used.

Afanas'ev, et al. [1] reported that the desorption of paraffins from zeolite NaX is more complete compared to that from CaA. Plachenov, et al. [85] compared the thermo-displacement and vacuum-thermal methods of desorption and found that former is more effective at temperatures less than  $105^{\circ}\text{C}$  while at higher temperatures both methods are equally effective. Areshidze and Chivadze [2] desorbed the paraffins by increasing the temperature and reducing the pressure.

Kivitkovskii [63] reported that in case of n-heptane-n-octane system larger amounts of n-octane (higher molecular weight paraffin) were adsorbed while n-nonane (lower molecular weight component) was preferentially adsorbed from n-nonane-n-decane system.

Major commercial processes in n-paraffin separation are UOP's Molex process [21, 22, 23, 94], B.P's process [62, 105, 106], Exxon's Ensorb process [3, 86], Union Carbide's IsoSiv process [5, 54, 55], Texaco's T.S.F. process [31, 47], Shell's process [89], and VEB Leuna Werke's Parex process [104].

All processes, otherthan the Molex process, are in vapor phase and use fixed bed, cyclic technology. The processes are different, however, in operating pressure, temperature, desorption technique, and other operating conditions. Desorption is generally carried out by displacement. Displacement agents mentioned in patented literature are generally low boiling n-paraffins, and ammonia or alkylamines. Steam a cheaper source has also been used as a desorbing agent. Pressure swing operation is used for separating low carbon number n-paraffins. Purging, between adsorption and desorption cycles, is some times desirable when product purity is important.

In the Molex process [22, 23, 87] adsorption system consists of a single adsorption tower with multiple inlet-outlet points and a special rotary valve. The adsorption tower has many smaller adsorption chambers interconnected in series, and works under so called 'simulated moving bed' operation. Instead of moving the bed, the simulated moving bed operates by simultaneously advancing inlet-outlet points periodically.

#### 2.3.1.2 Separation of p- and o-xylanes:

The rapid increase in the use of p-xylene as a raw material for polyester products necessitated the development of a process for separating p-xylanes from a mixture of C<sub>8</sub> aromatics. Broughton, et al. [24] and Atkins [4], in 1970, have developed a process for separating p-xylanes from a

mixture of C<sub>8</sub> aromatics containing xylenes and ethylbenzene. The process has been commercialized by the name U.O.P.'s Parex process and the hardware for this process is similar to Molex process for separation of n-paraffins. The process is continuous liquid phase, simulated moving bed type. This process can separate p-xylene from various types of feedstocks with 99.5 per cent purity and recovery as high as 98.4 per cent [24]. The high recovery is certainly an improvement over the conventional crystallization processes. The adsorbent used in U.O.P. process is a synthetic faujasite containing cations of groups IA, IIA, or both [76-78]. U.S. Patents [14, 28] issued in 1972 also claim that sodium mordenite and modified type-Y zeolite containing predominantly potassium ions can separate p-xylenes from a mixture of p- and o-xylenes, and a C<sub>8</sub> aromatic mixture, respectively.

#### 2.3.1.3 Olefin Separation:

For the separation of olefins from a feedstock containing olefins and paraffins, the zeolite adsorbent used, according to patent literature, [79,80], is a synthetic faujasite with 1-40 weight per cent of atleast one cation selected from groups IA, IIA, IB, and IIB. The process is known as the U.O.P.'s Olex process. This process is also believed to use the same simulated moving bed operation in liquid phase as U.O.P.'s other hydrocarbon separation processes. Union Carbide's OlefinSiv process [7] is used to separate

n-butlenes from isobutylene. Product purities are claimed to be above 99 per cent for both n-butylene and isobutylene streams.

### 2.3.2 Drying Gases and Liquids:

Zeolites have a highly hydrophilic surface and are very efficient desiccants. Contrary to other non-zeolitic desiccants, such as silica gel and activated alumina, zeolite adsorbents have type I adsorption isotherm for water, which means a high water adsorption capacity at a low concentration. The zeolite type 3A, in particular, has the additional advantage of selective adsorption of water because of its small pore size. Although, in the past, alumina has been the most commonly used desiccant in drying cracked gas, 3A molecular sieve adsorbents have an overall economic advantage [82]. The main advantages of 3A molecular sieve over alumina and silica gel are its higher capacity and, therefore, smaller adsorption tower and its longer service time. Applications of zeolite adsorbents in drying other industrial gases and liquids have been discussed elsewhere [29, 30, 72].

### 2.3.3 Separation and Purification of Industrial Streams:

#### 2.3.3.1 Purification of Air Prior to Liquefaction:

Liquefaction of air by cryogenic processes requires removal of water vapor and carbon dioxide to avoid heat exchanger freeze-up. A 13X molecular sieve has

been used for separation of water vapor and carbon dioxide from air in a single adsorption step. The 13X molecular sieves have not only higher adsorptive capacities but also faster rates of  $\text{CO}_2$  adsorption compared to type A. The optimum operating temperature for  $\text{CO}_2$  removal by 13X molecular sieve is reported as 160-190°K [102].

#### 2.3.3.2 Natural Gas Purification:

Natural gas containing water vapor, carbon dioxide, hydrogen sulfide, etc. is purified by passing through either 4A or 5A molecular sieve bed. Other important applications of molecular sieves in natural gas purification [56, 58, 64,85] include purification of pipeline natural gas for liquefaction, drying natural gas prior to cryogenic hydrocarbon recovery using a turboexpander, and sweetening natural gas feed to ammonia plants.

#### 2.3.3.3 Oxygen Enrichment of Air:

The increase in demand of oxygen or oxygen-rich air in biological waste water treatment plants generated a necessity for a low cost, on site oxygen generator. Other applications of oxygen enrichment of air are secondary smelting plants, river and pond aeration, pollution control in the pulp and paper industry, etc. Pressure swing adsorptive process using zeolite adsorbents [63, 66] is found to be advantageous over the conventional cryogenic air separation

process. Commercial processes known today are: Union Carbide process [33], the W.R. Grace process [63], the Bayer-Mahler process [13], the Nippon steel process [96, 95], and ESSO Research and Engineering processes [16, 44, 91, 92]. These processes differ in the type of zeolites used, operating pressures, number of adsorbent beds, and cyclic operating steps.

#### 2.3.4 Pollution Control:

Zeolite adsorbents are effectively used to remove pollutants such as  $\text{SO}_2$ ,  $\text{H}_2\text{S}$ , and  $\text{NO}_x$  from industrial off-gas streams nearly at ambient temperature [52, 60, 65, 68]. Since water vapor usually exists along with these acidic compounds, an acid stable or acid resistant zeolite adsorbent is necessary for a long service life. Union Carbide offers three new processes for pollution control, namely, the PuraSiv-Hg process for mercury vapor removal, the PuraSiv-N process for  $\text{NO}_x$  removal from nitric acid plant off-gas, and the PuraSiv-S process for  $\text{SO}_2$  removal from sulfuric acid plant off-gas.

## REFERENCES

1. Afanas'ev, Yu. M., Zhukova, Z.A., Kel'tsev, N.V., Materialy Vses. Soveshch po Tseolitam, 2nd Leningrad 1964, 352 (Pub. 1965); Chem. Abstr. 64: 17310 (1966).
2. Arsehidze, Kh.I., Chivadze, G.O., Materialy Vses. Soveshch po Tseolitam, 2nd Leningrad 1964, 294 (Pub. 1965); Chem. Abstr. 65: 544 (1966).
3. Asher, W.I., et. al., U.S. Patent 3,070,542 (Dec. 25, 1962).
4. Atkins, R.S., Hydrocarbon Proc. 49, 132 (1970).
5. Avery, W.F., Lee, M.N.Y., OilGas J., 60, 121 (1962).
6. Bajpai, P.K., Ph.D. Thesis, Chemical Engineering, Indian Institute of Technology, Kanpur, 1977.
7. Barber, J.B., et al., 68th National Meeting of the American Institute of Chemical Engineers, Houston, Tex., 1971.
8. Barrer, R.M., Proc. Roy. Soc. London, 4167, 393 (1938).
9. Barrer, R.M., Discussions Faraday Soc., 40, 206 (1944).
10. Barrer, R.M., J. Chem. Soc., 2158 (1948).
11. Barrer, R.M., Discussions Faraday Soc., No. 5, 326 (1949).
12. Barrer, R.M., Ibbitson, D.A., Trans. Faraday Soc., 40, 195 (1944).
13. Bayer, F., Mahler, J.F., Chem. Eng., 77, 54 (Oct. 5, 1970).
14. Bearden, R., Jr., DeFeo, R.J., Jr., U.S. Patent 3,686,343 (Aug. 22, 1972).
15. Bergerhoff, G., Baur, W.H., and Nowacki, W., News Jahrb. Mineral. Mh., 9, 193 (1958).

16. Berlin, N.H., U.S. Patent 3,280,536 (Oct. 25, 1966).
17. Bragg, L., and Claringbull, G.F., 'The Crystalline State', Crystal Structure of Minerals, Vol.IV, Cornell Univ. Press, Ithaca, 1965.
18. Breck, D.W., Eversole, W.G., and Milton, R.M., J. Am. Chem. Soc. , 78, 2338(1956).
19. Breck, D.W., et al., Abstracts of Papers, 134th Meeting of the ACS, Sept. 1958, Chicago, Illinois.
20. Breck, D.W., Flanigen, E.M., and Milton, R.M., Abstracts of Papers, 137th Meeting of the ACS, April, 1960.
21. Broughton, D.B., Chem. Eng. Progr. 64, 60 (1968).
22. Broughton, D.B., Lickus, A.G., Petrol. Refiner. 40, 173 (1961).
23. Broughton, D.B., et al., Proc. Amer. Petrol. Inst. Sect. IV 41, 237 (1961).
24. Broughton, D.B., et al., Chem. Eng. Progr. 66, 70 (1970).
25. Broussard, L., and Schoemaker, D.P., J. Am. Chem. Soc., 82, 1041 (1960).
26. Brunauer, S., 'The Adsorption of Gases and Vapors', Vol.1, Physical Adsorption, Princeton, Princeton University Press, 1943.
27. Charles, E.J., U.S. Patent 2,904,507 (Sept. 15, 1959).
28. Chen, N.Y., Lucki, S.J., U.S. Patent 3,668,266 (June 6, 1972).
29. Collins, J.J., Oil Gas J. 60, 97, (1962).
30. Collins, J.J., Chem. Engr. Progr. 64, 66 (1968).

31. Cooper, D.E., et al., Chem. Eng. Progr. 62, 69 (1966).
32. Cronstedt, A., Akad. Handl. Stockholm, 18, 120 (1756).
33. Cundy, H.M., and Rollett, A.P., 'Mathematical Models', 2nd ed., Oxford, London, 106, 104 (1961).
34. Damour, A., Ann. Mines, 17, 191 (1840).
35. Davis, J.C., Chem. Eng. 79, 88 (Oct. 16, 1972).
36. Deer, W.A., Howie, R.A., and Zussman, J., 'Rock Forming Minerals Vol.4; Framework Silicates', John Wiley and Sons, New York, 1963.
37. Dent, L.S., and Smith, J.V., Nature, 181, 1794 (1958).
38. Dorogochinskii, A.Z.,; Mirskii, Ya.V., Chem. Abstr. 77: 64307 (1972).
39. Dosumova, E.Ya., Adylova, T.T., Ryabova, N.D., Chem. Abstr. 76: 16365 (1972).
40. Eichhorn, H., Poggendorf Ann. Phys. Chem., 105:126 (1858).
41. ESSO Research and Engg. Co., British Patent 844,282 (Aug. 10, 1960).
42. ESSO Research and Engg. Co., British Patent 853,530 (Nov. 9, 1960).
43. ESSO Research and Engg. Co., Belg. Patent 637,314 (March 12, 1964).
44. Feldbauer, G.F., Jr., U.S. Patent 3,338,030 (Aug. 29, 1967).
45. Fleck, N., Carlyle, G.W., U.S. Patent 2,921,026 (Jan. 12, 1960).
46. Francis, James O., Lewis, Ralph M., U.S. Patent 3,726,792 (April 10, 1973).

47. Franz, W.R., et al., Petrol. Refiner. 38, 125 (1959).
48. Frid, M.N., Atapina, E.N., Gavrunga, V.E., Chem. Abstr. 78: 138515 (1973).
49. Friedel, Bull. Soc. Fr. Mineral, Cristallogr. 19:14, 96 (1896).
50. Galich, P.N., Kvitkovskii, L.N., Frolova, V.S., Chem. Abstr. 63: 1634 (1965).
51. Galich, P.N., Tabakov, A.V., Dolinskayaya, E.S., Chem. Abstr. 65:2038 (1966).
52. Grandjean, Compt. Rendu, 149: 866 (1909).
53. Griesmer, G.J., et al., Hydrocarbon Proc. 44, 147 (1965).
54. Guiccione, E., Chem. Eng. 72, 104 (April 26, 1965).
55. Gupta, J.C., et al., 68th National Meeting of the AIChE, Houston, Texas, 1971.
56. Hales, G.E., Can. Petrol. (Jan. 1972) 42.
57. Harold, A.R., Zigmond, W.W., Howard, W., U.S. Patent 2,988,502 (June 13, 1961).
58. Harris, T.B., Pipe Line Gas J. (June, 1972) 76.
59. Howard, V.H., Edward, R.C., U.S. Patent 3,007,863 (Nov. 7, 1961).
60. Joubert, J.J., Zwiebel, I., Advances Chem. Ser. 102, 209 (1971).
61. Kvitkovskii, L.V., Inst. Khim. Vysokomolekul Soedin; 45 (1964); Chem. Abstr. 62: 8902 (1965).
62. Loey, R.N., Et al., U.S. Patent 3,201,490 (Aug. 17, 1965).

63. Lee, H., 'Application of Commercial Oxygen to Water and Waste Water Systems' Symposium, University of Texas, Austin, Tex., Nov. 1972.
64. Lee, H., Stahl, D.E., 65th Annual Meeting of the AIChE, New York, N.Y., Nov. 1972.
65. Lee, M.N.Y., Collins, J.J., Safety Air Ammonia Plants 11, 59 (1969).
66. Lee, M.N.Y., Schoofs, R.J., German Patent 1,911,670 (Oct. 9, 1969).
67. Mantell, C.L., 'Adsorption', New York, McGraw-Hill Book Co., 1951.
68. Martin, D.A., Brantley, F.E., U.S. Bur. Mines Rept. 15,6321 (1963).
69. McBain, J.W., 'Sorption of Gases and Vapor by Solids', George Routledge and Sons Ltd., London, 1932.
70. Meier, R.M., Z. Krist., 115, 439 (1961).
71. Milton, R.M., U.S. Patents 2,882,243 and 2,882,244, April 14, 1959.
72. Milton, R.M., 'Molecular Sieves' pp 201, Society of Chemical Industry, London, 1968.
73. Mirskii, Ya. V., et al., Chem. Abstr. 60: 14309 (1964).
74. Mirskii, Ya. V., et al., U.S.S.R. Patent 172,443 (June 29, 1965).
75. Morey, G.W., and Ingerson, E., Econ. Geol. Supplement to No. 5, 32, 607 (1937).

76. Neuzil, R.W., U.S. Patent 3,558,732 (Jan. 26, 1971).
77. Neuzil, R.W., U.S. Patent 3,626,820 (Dec. 9, 1971).
78. Neuzil, R.W., U.S. Patent 3,663,638 (May 16, 1972).
79. Neuzil, R.W., deRosset, A.J., South African Patent 692,327 (April 5, 1968).
80. Neuzil, R.W., deRosset, A.J., British Patent 1,236,691 (June 23, 1971).
81. Pauling, L., Proc. Nat. Acad. Sci., U.S., 16, 453 (1930).
82. Pierce, J.E., Stieghan, D.L., Hydrocarbon Proc., 45, 170 (1966).
83. Plachenov, T.G., Redin, V.I., Zh.Prikl.Khim., 47(4), 907 (1974) Chem. Abstr. 81: 16998 (1974).
84. Plachenov, T.G., Redin, V.I., Seballo, A.A., Zh.Prikl.Khim. 47(5) 1028 (1974); Chem. Abstr. 81: 111706 (1974).
85. Reed, T.B., and Break, D.W., J.Am.Chem.Soc. 78, 5972 (1956).
86. Richards, H.A., et al., U.S. Patent 2,988,502 (June 13, 1961).
87. Ries, H.C., 'n-Paraffins', Process Economics Program Report No.55, 1969, Standford Research Institute, Menlo Park, Calif.
88. Schoofs, R.J., Gas 42, 85 (1966).
89. Shell Internationale, British Patent 1,059,879 (Feb. 22, 1967).
90. Shreve, R.N., Green Sand Bibliography to 1930, U.S. Bureau of Mines Bulletin 328 (1930).
91. Skarstrom, C.W., U.S. Patent 2,944,627 (July 12, 1960).

92. Skarstrom, C.W., U.S. Patent 3,237,377 (March 1, 1966).
93. Smith, J.V., Mineralogical Society of America, Special Paper No.1, 1963.
94. Sterba, M.J., Proc. Amer. Petrol. Inst. Sect. IV 45, 209 (1965).
95. Takahashi, H., et al., Ed. 'Zeolites and Their Applications' pp 96, Gihodo, Tokyo, 1967.
96. Tamura, T., British Patent 1,258,418 (Dec.30, 1971).
97. Taylor, W.H., Z.Krist., 74, 1 (1930).
98. Thompson, H.S., J. Roy. Agr. Soc. Engl., 11:68 (1850).
99. Tunescu, R.C., Caros, R., Petrol. Gaze (Bucharest), 16(7), 410 (1965); Chem. Abstr. 64:495 (1966).
100. Volf, M.B., Alekseeva, R.V., Prokopyuk, L.G., Chem. Abstr. 60 341 (1964).
101. Way, J.T., Roy. Agr. Soc. Engl. 11: 313 (1850).
102. Webber, D.A., Chem. Eng. (Jan. 1972), 18.
103. Wehner, K., et al., British Patents 1,135,801 and 1,135,802 (Dec. 4, 1968).
104. Weigel, O., and Steinhof, E., Z. Krist., 61, 125 (1925).
105. Yeo, A.A., Hicks, C.L., British Patents 898,058 and 898,059 (June 6, 1962).
106. Yeo, A.A., et al., World Petrol. Congr. 6th Sect. IV (1963) 161.

## CHAPTER 3

### EXPERIMENTAL RESULTS ON ADSORPTION OF PURE COMPONENTS

#### 3.1 INTRODUCTION:

Demand for n-paraffins has been steadily increasing in pure form as well as mixtures because of a variety of novel applications. N-Octane is used in fermentation process for the manufacture of citric acid. Use of n-paraffins in the manufacture of biodegradable detergents has increased very rapidly over past several years. Molecular sieve adsorption processes which are very effective, efficient and cheap are becoming popular for the separation of n-paraffins from petroleum fractions. For the design of adsorption columns, one needs the basic data on liquid phase adsorption of these n-paraffins on molecular sieves. Although several workers [4-8] have studied the vapor phase adsorption of pure and binary paraffins, practically no reliable data is available on liquid phase pure component adsorption of n-paraffins in published literature. Sundstrom and Krautz [9] have reported single component adsorption capacities for  $C_7$ ,  $C_{10}$ ,  $C_{12}$  and  $C_{14}$  n-paraffins. However, these authors have not given the adsorption isotherms, which are necessary for design. This has motivated undertaking the present study where adsorption isotherms have been measured for

$C_5$  to  $C_8$  n-paraffins using LMS-5A as an adsorbent. A temperature range of  $6^\circ$  to  $42^\circ C$  has been covered in this study.

### 3.2 EXPERIMENTAL:

The molecular sieves used were LMS-5A; 1/16' inch pellets containing 20 per cent inert clay binder. Benzene (A.R. grade, B.D.H.) and n-paraffins (G.R. grade; E. Merk/B.D.H.) had a minimum purity of 99.0 per cent. To study the effect of liquid concentration on the adsorption, pure n-paraffins were diluted with benzene. Due to its critical diameter ( $6.8 \text{ } \overset{\circ}{\text{A}}$ ), benzene is essentially excluded from the pores (equilibrium loading of benzene on LMS-5A has been reported as 0.002 g/g zeolite [2]).

The experiments were conducted in a pyrex glass assembly, shown in Figure 3.1. which consisted of a 100 ml. adsorption cell attached to a 3-way vacuum stop cock. The molecular sieves were heated at  $450^\circ C$  for 48 hours and then transferred to the preheated cell maintained at  $150^\circ C$  which was then stoppered. The assembly containing the molecular sieves was then evacuated to  $10^{-3}$  torr at  $200^\circ C$  for 4 hours to remove any water vapor or air left in the cell. The evacuated cell was then cooled to room temperature. A weighted quantity of liquid paraffin and benzene mixture was then added to the adsorption cell under vacuum with the help of the

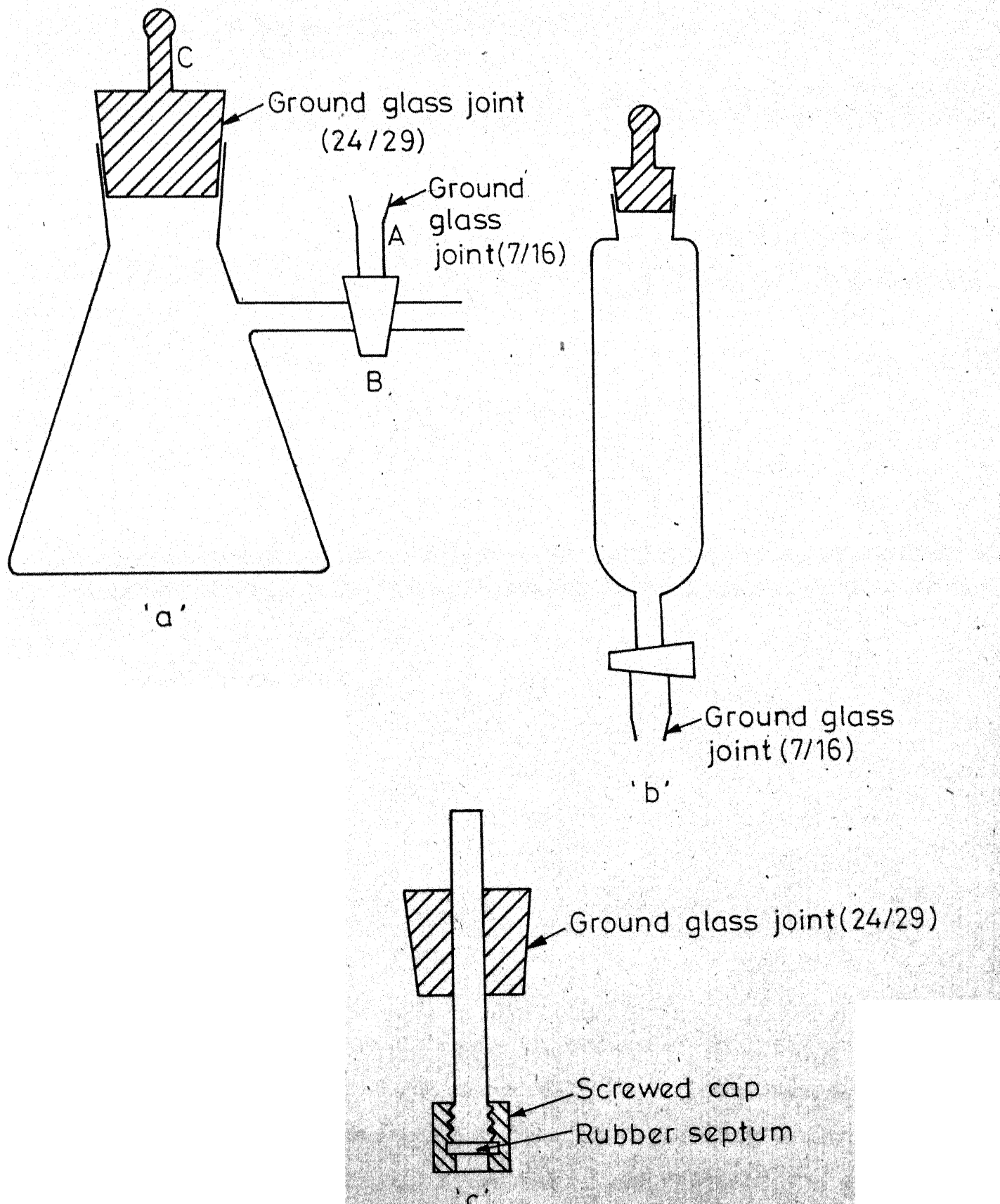


Fig. 3.1 -Assembly of adsorption cell.

assembly shown in Figure 3.1b which was connected to the cell at A (Figure 3.1a). Since the cell was under vacuum, the liquid sample was almost instantaneously sucked and the stopcock B (Figure 3.1a) was then closed. The adsorption cell was then transferred to a controlled temperature water bath with a shaker (Model G-86; New Brunswick Scientific Co., New Jersey) which was maintained at the desired temperature of adsorption within  $\pm 0.25^{\circ}\text{C}$ . Preliminary experiments were conducted with varying amounts of molecular sieves, shaker speeds and volume of sample. From these runs, nearly 30 g of molecular sieves, about 50 ml. of liquid sample and a shaker speed of 300 rpm were chosen as the operating conditions for the main runs.

The breakthrough curves were first determined to establish the time taken to attain equilibrium. To facilitate periodic withdrawal of liquid samples for chromatographic analysis, the assembly shown in Figure 3.1c was attached to the adsorption cell in place of stopper c (Figure 3.1a). This had a rubber septum through which the needle of a microlitre syringe could be pierced to reach the liquid in the cell. These samples were subsequently analysed on a thermal conductivity gas chromatograph (Chromatographic Instrumentation Company; Baroda). A 30 ft long column of 20 per cent bentone on chromosorb W was used for the analysis.

Detailed conditions for analysis are given in Appendix A3.1. Breakthrough runs were terminated when the composition of two successive samples were identical. In general, breakthrough point was reached in approximately 24 hours.

To ensure complete equilibration during adsorption studies, each run was continued for 48 hours and the liquid sample was then analysed to get the final concentration of n-paraffin in the solution. Each reported point on the adsorption isotherm was determined by averaging the results of two experiments conducted simultaneously in two identical cells.

### 3.3 RESULTS AND DISCUSSION:

#### 3.3.1 Breakthrough Curves:

The effect of temperature on the breakthrough curve, for n-heptane is shown in Figure 3.2. Data are tabulated in Appendix A3.2). This figure shows that the time for reaching equilibrium decreases with increasing temperature. This is to be expected because adsorption is a mass transfer process and increasing the temperature increases the mass transfer coefficient, resulting in the breakthrough point being reached earlier.

#### 3.3.2 Adsorption Isotherms:

Figures 3.3 to 3.6 (Data are tabulated in Appendices A3.3 to A3.6) show the adsorption isotherms for n-pentane,

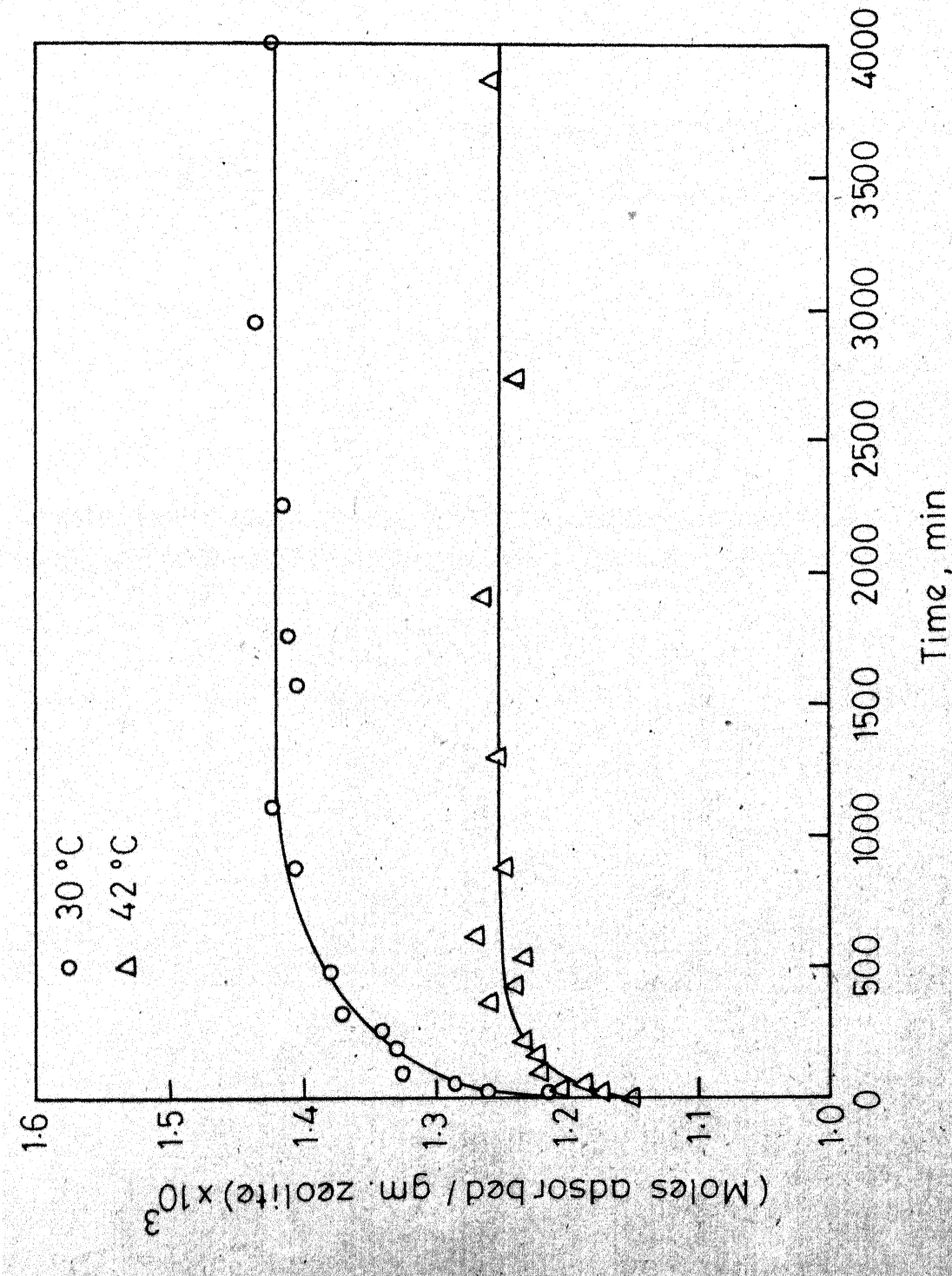


Fig. 3.2 - Breakthrough curves for n-heptane.

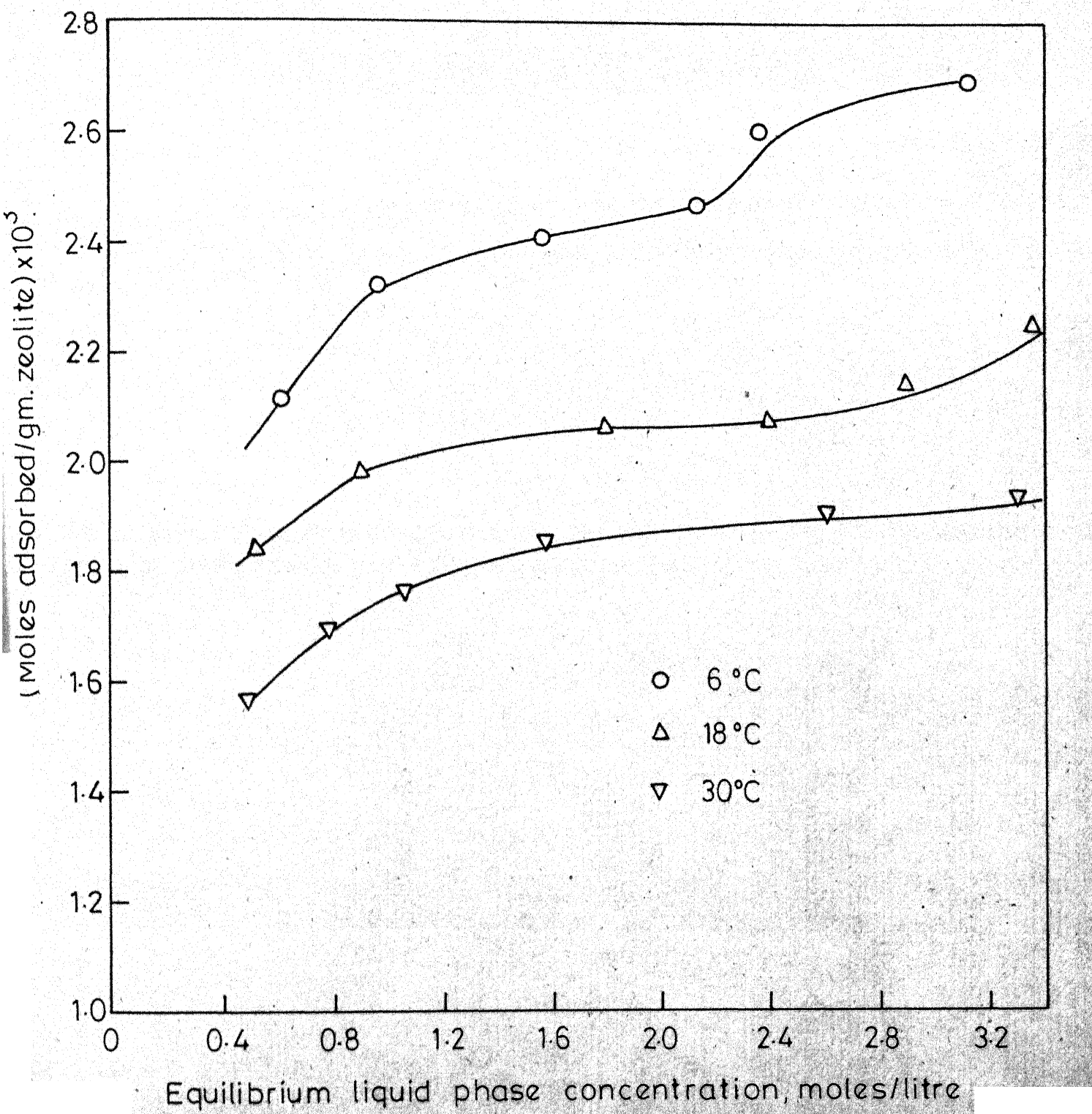


Fig. 3.3 - Adsorption isotherms of n-pentane.

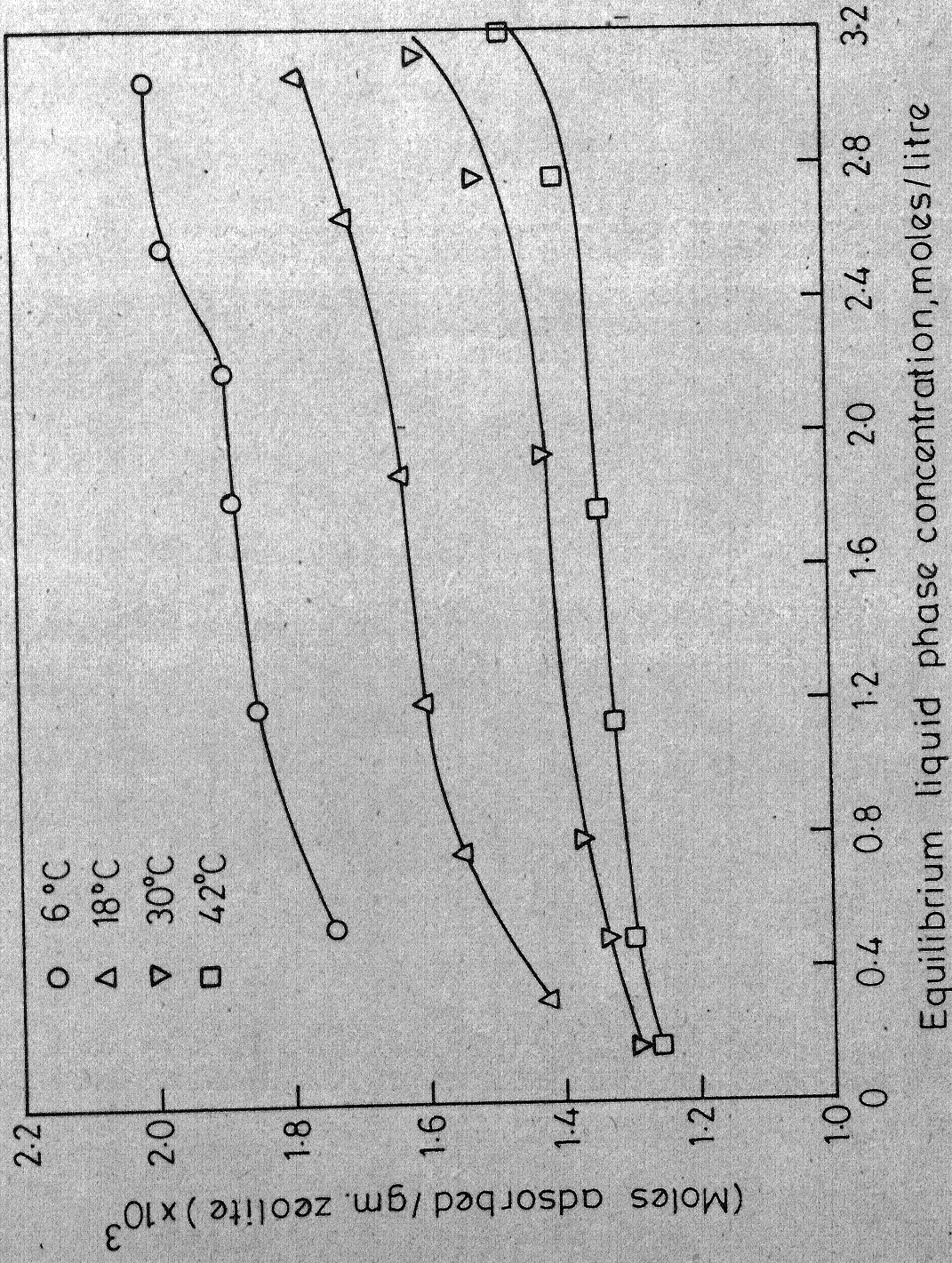


Fig. 3.4 - Adsorption isotherms of n-hexane.

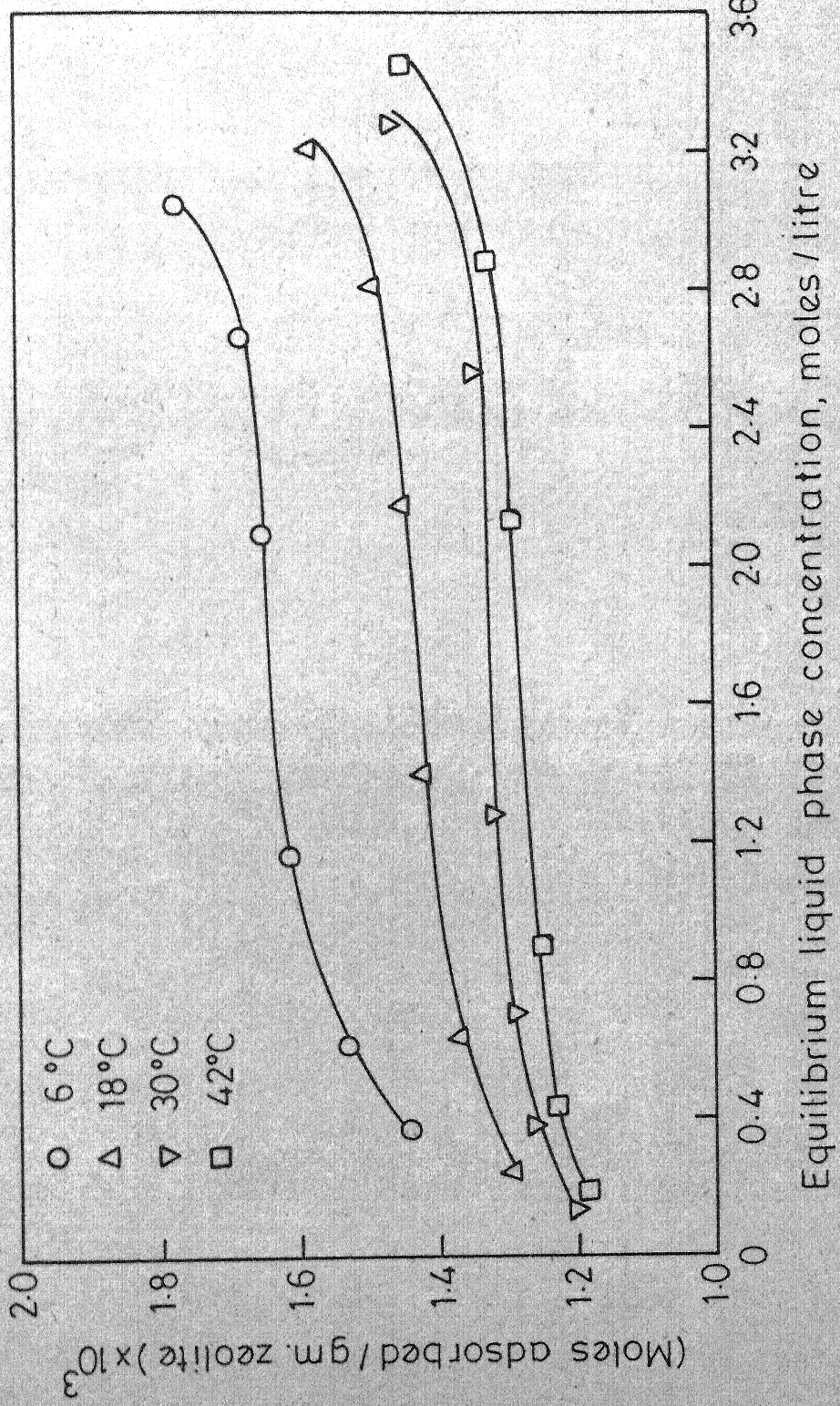


Fig. 3.5 - Adsorption isotherms of n-heptane.

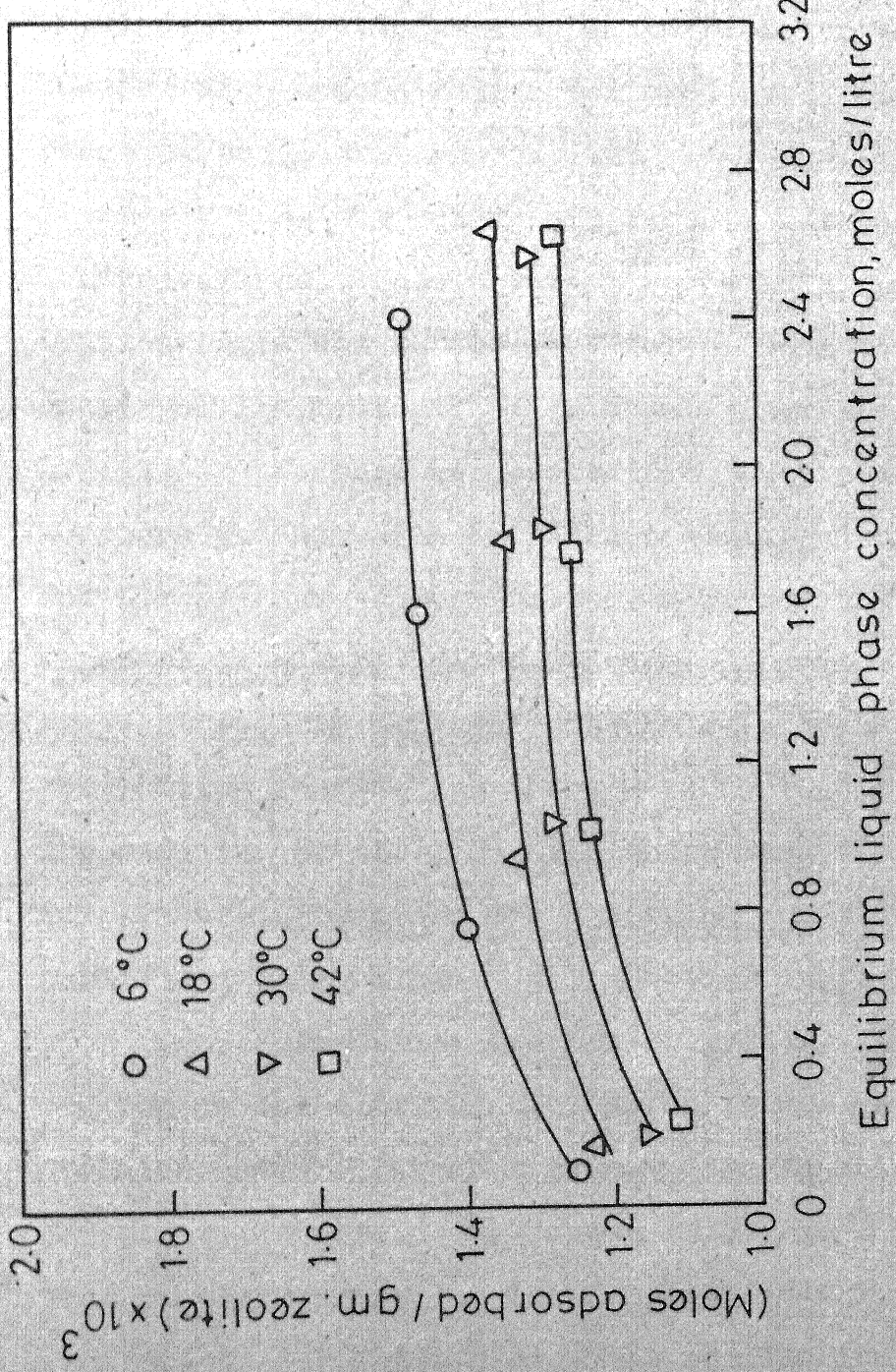


Fig. 3.6 - Adsorption isotherms of n-octane.

n-hexane, n-heptane and n-octane respectively. The general trend of the isotherms show an initial increase in equilibrium loading with concentration followed by a relatively large range of concentration over which the equilibrium loading is nearly constant and then a further increase at high concentrations. This upward trend at high paraffin concentration could not be observed for n-octane because of some practical limitations. This upward increase in equilibrium loading is probably associated with adsorption on external surfaces and not with intra-crystalline adsorption. Barrer and Lee [1] have also reported an upward inflexion in the vapor phase adsorption of hydrocarbons near the condensation temperature. As expected, at the same concentration, the equilibrium loading decreases with increasing temperature. A comparison of these Figures shows that the effect of temperature is maximum for n-pentane and reduces for higher paraffins, being minimum for n-octane in the present study.

For a particular temperature, the effect of concentration on the equilibrium loading is most significant for n-pentane and decreases with increase in molecular size. A typical plot at 30°C is shown in Figure 3.7. This shows that as the equilibrium liquid paraffin concentration changes from 0.4 to 3.2 moles/litre, the equilibrium loading for n-pentane increases from 10.87 to 13.82 g/100 g zeolite which amounts to approximately 28 per cent. For n-heptane, the

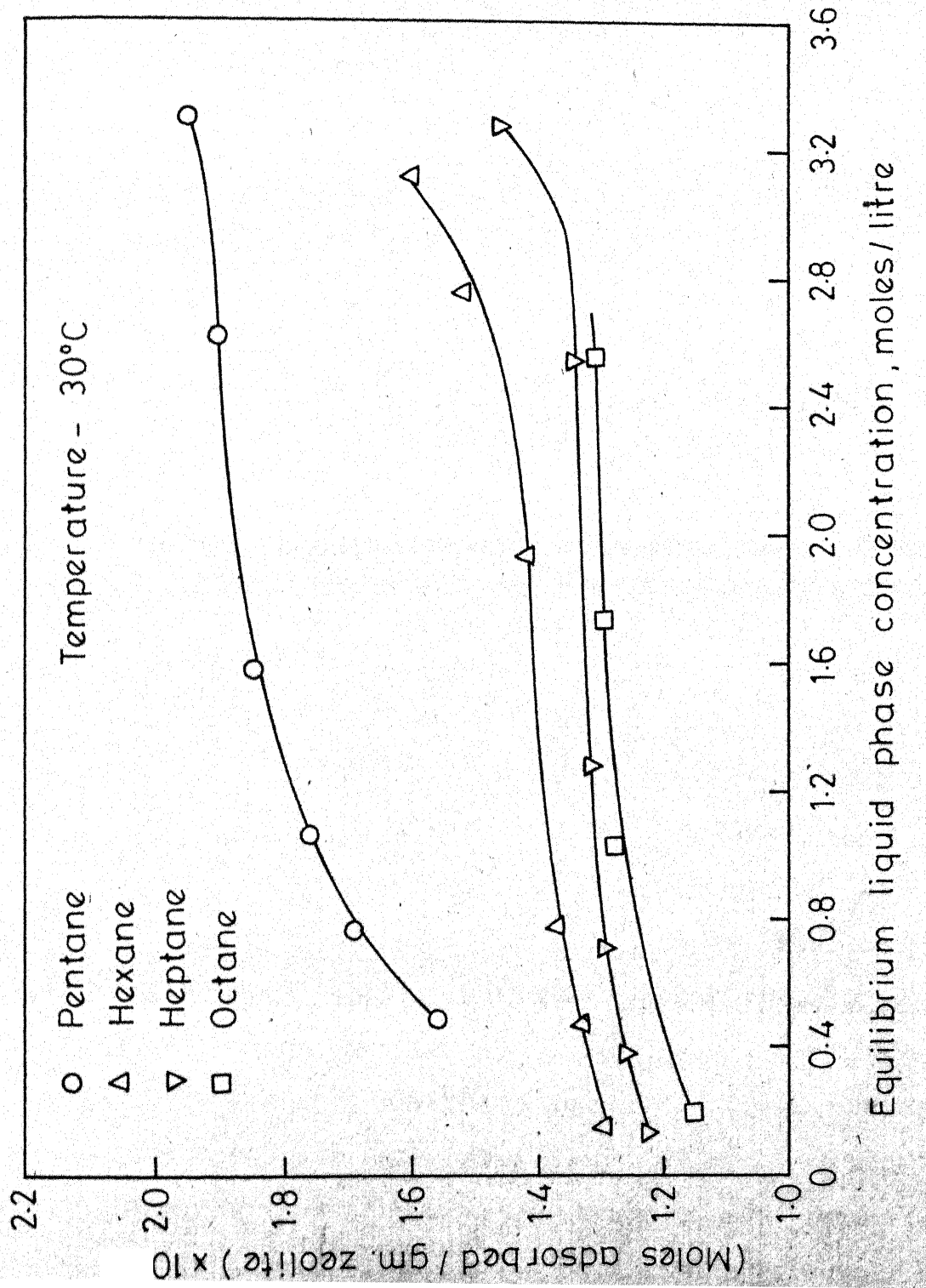


Fig. 3.7 - Adsorption isotherms of different n-paraffins at 30°C.

equilibrium loading increased from 12.50 to 14.30 g/100 g zeolite in the same range of concentration, which is only a 14.4 per cent increase. The results of equilibrium loading for n-heptane are in good agreement with those of Sundstrom and Krautz [9], who have reported a loading of 12.5 g/100 g zeolite at 30°C. These authors did not observe any change in the equilibrium loading with concentration; however, the concentration ranges have not been reported in their paper and it is possible that they did not cover as wide a concentration range.

For the same temperature and liquid concentration, the equilibrium loading decreases with increase in molecular size i.e. the lower molecular weight paraffin is preferentially adsorbed. With increasing molecular weight, the effect of size diminishes. Thus, at 18°C, the equilibrium loading for n-pentane is  $2.03 \times 10^{-3}$  moles/g zeolite at an equilibrium concentration of 1.6 moles/litre compared to  $1.62 \times 10^{-3}$ ,  $1.43 \times 10^{-3}$  and  $1.34 \times 10^{-3}$  moles/g zeolite for n-hexane, n-heptane and n-octane respectively. Peterson and Redlich [3] have also shown that liquid phase sorbability decreases with increasing number of carbon atoms for n-paraffins having 5 or more carbon atoms. This violates Traube's rule which states that higher molecular weight adsorbate should be preferentially adsorbed. The reason

for the preferential adsorption of lower molecular weight hydrocarbons on 5A molecular sieves is that in the zeolites both physico chemical adsorption and steric effects are important. Since type 5A molecular sieves have a pore opening of  $5\text{\AA}^{\circ}$  and n-paraffins have critical diameter of  $4.9\text{\AA}^{\circ}$ , steric effect will play an important role. In shorter chain compounds (lower molecular weight n-paraffins) steric effects will be less in comparison to larger chain compounds.

In the present investigation, an experimental technique, for the liquid phase adsorption of hydrocarbons on zeolite has been perfected. Adsorption isotherms have been measured for different liquid paraffins in the temperature range 6 to  $42^{\circ}\text{C}$ . These data can be used to design single or multiple component adsorption plants.

## REFERENCES

1. Barrer, R.M., and Lee, J.A., Surface Sci., 12, 341 (1968).
2. Breck, D.W., Eversole, W.G., Milton, R.M., Reed, T.B., and Thomas, T.L., J. Am. Chem. Soc., 78, 5963 (1956).
3. Peterson, D.L., Redlich, O., J. Chem. Eng. Data, 7, 570 (1962).
4. Ruthven, D.M., Nature Phys. Sci., 232, 70 (1971).
5. Ruthven, D.M., and Loughlin, K.F., J. Chem. Soc. Faraday Trans., 68, 696 (1972).
6. Ruthven, D.M., Loughlin, K.F., and Derrah, R.I., Advan. Chem., 121, 330 (1973).
7. Ruthven, D.M., Loughlin, K.F., and Holborow, K.A., Chem. Eng. Sci., 28, 701 (1973).
8. Ruthven, D.M., A.I.Ch.E. J., 22, 753 (1976).
9. Sundstrom, D.W., and Krautz, F.G., J. Chem. Eng. Data, 13, 223 (1968).

## CHAPTER 4

### EXPERIMENTAL RESULTS ON ADSORPTION OF MULTICOMPONENT SYSTEMS

#### 4.1 INTRODUCTION:

n-Paraffins form an integral part of various petroleum fractions available in a refinery. In any fraction there are more than one component and any separation process has to be designed to remove mixture of these n-paraffins. In molecular sieve process also different components will adsorb simultaneously in different proportions according to their relative affinity. In order to design these separation systems, multicomponent adsorption data is, therefore required. Very little information is available in published literature on multicomponent liquid phase adsorption of n-paraffins on molecular sieves. Sundstrom and Krautz [3] have reported some data on the liquid phase adsorption of binary systems of  $C_7$ ,  $C_{10}$ ,  $C_{12}$  and  $C_{14}$  n-paraffins on LMS-5A. For all the systems studied, they found that the paraffin with the lower molecular weight was preferentially adsorbed and that the temperature had a negligible effect on the composition of adsorbate in equilibrium for a given liquid composition. Satterfield and Cheng [1] studied the adsorption of a wide variety of liquid binary hydrocarbon systems on NaY zeolite. Satterfield and Smeets [2] have reported the

liquid adsorption data on binary systems of n-octane either with n-decane, or n-dodecane, or n-tetradecane on NaY zeolite. They found that the lower molecular weight paraffin was preferentially adsorbed. They have suggested that the packing characteristics of the higher molecular weight paraffin, rather than the physico-chemical characteristic, play a dominant role in the adsorption selectivity on a zeolite.

In the present investigation, liquid phase adsorption of binary systems, namely, pentane-hexane, hexane-heptane, heptane-octane, pentane-heptane, and pentane-octane on synthetic zeolite LMS-5A have been studied. The ternary systems studied were pentane-hexane-heptane, pentane-hexane-octane and pentane-heptane-octane. Benzene was used as a diluent in all the measurements since its adsorbability on the zeolite used is negligible. The equilibrium curves (mole fraction of lower molecular weight paraffin in liquid vs mole fraction of the same in the adsorbed phase) for all the binary systems were obtained by varying hydrocarbon concentration over a wide range. Measurements were made at 6°, 18°, 30° and 42°C to study the effect of temperature on the equilibrium curves. For all the binary systems, the effect of concentration and temperature on conventional separation factor, K, defined below was also investigated.

$$K = \frac{y_L/x_L}{y_H/x_H} \quad (4.1)$$

where  $x_L$  and  $x_H$  are molefractions of lighter and heavier paraffins in liquid phase and  $y_L$  and  $y_H$  are corresponding molefractions in adsorbed phase when the system is in equilibrium.

#### 4.2 EXPERIMENTAL:

The experimental apparatus and procedure was the same as that for pure components described earlier (Chapter 3).

#### 4.3 RESULTS AND DISCUSSION:

##### 4.3.1 Equilibrium Curves for Binary Systems:

Figures 4.1 through 4.5 show the equilibrium curves for the various binary systems investigated (experimental data are tabulated in Appendices A4.1 through A4.4).

Temperature seems to have very little effect on equilibrium loading of hexane and heptane in hexane-heptane and heptane-octane systems as evidenced from Figures 4.2 and 4.3.

Sundstrom and Krautz [3] have also reported (for binary systems of higher paraffins) that temperature has a negligible effect on the composition of an adsorbate in equilibrium with a given liquid composition. There is a decrease in the amount of pentane adsorbed at 30°C compared to the lower temperatures for pentane-hexane, pentane-heptane and pentane octane systems (Figures 4.1, 4.4 and 4.5). Since

T.I.T KANPUR  
CENTRAL LIBRARY  
62147  
No. A

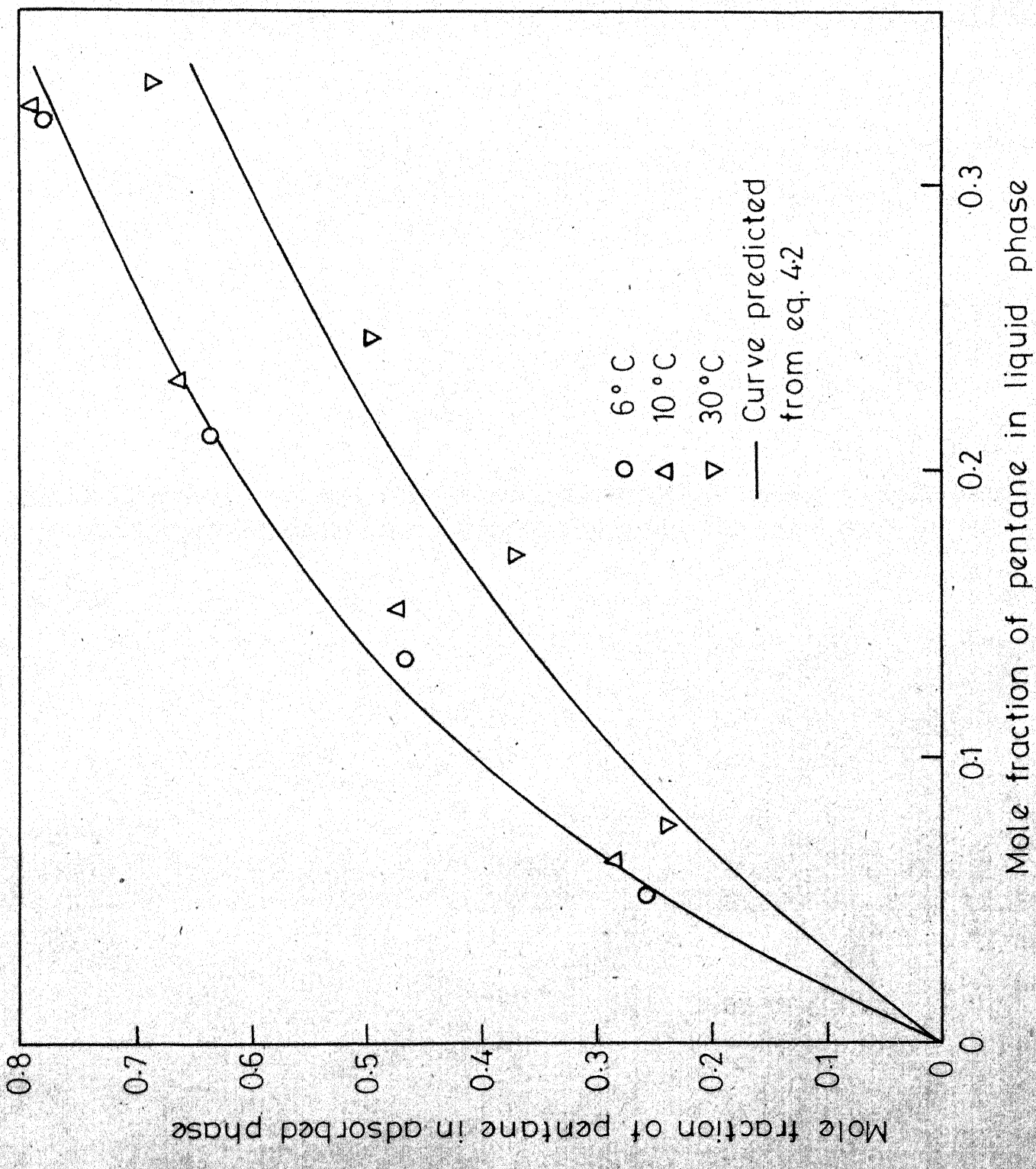


Fig. 4.1 - Equilibrium curves for pentane-hexane system at different temperatures.

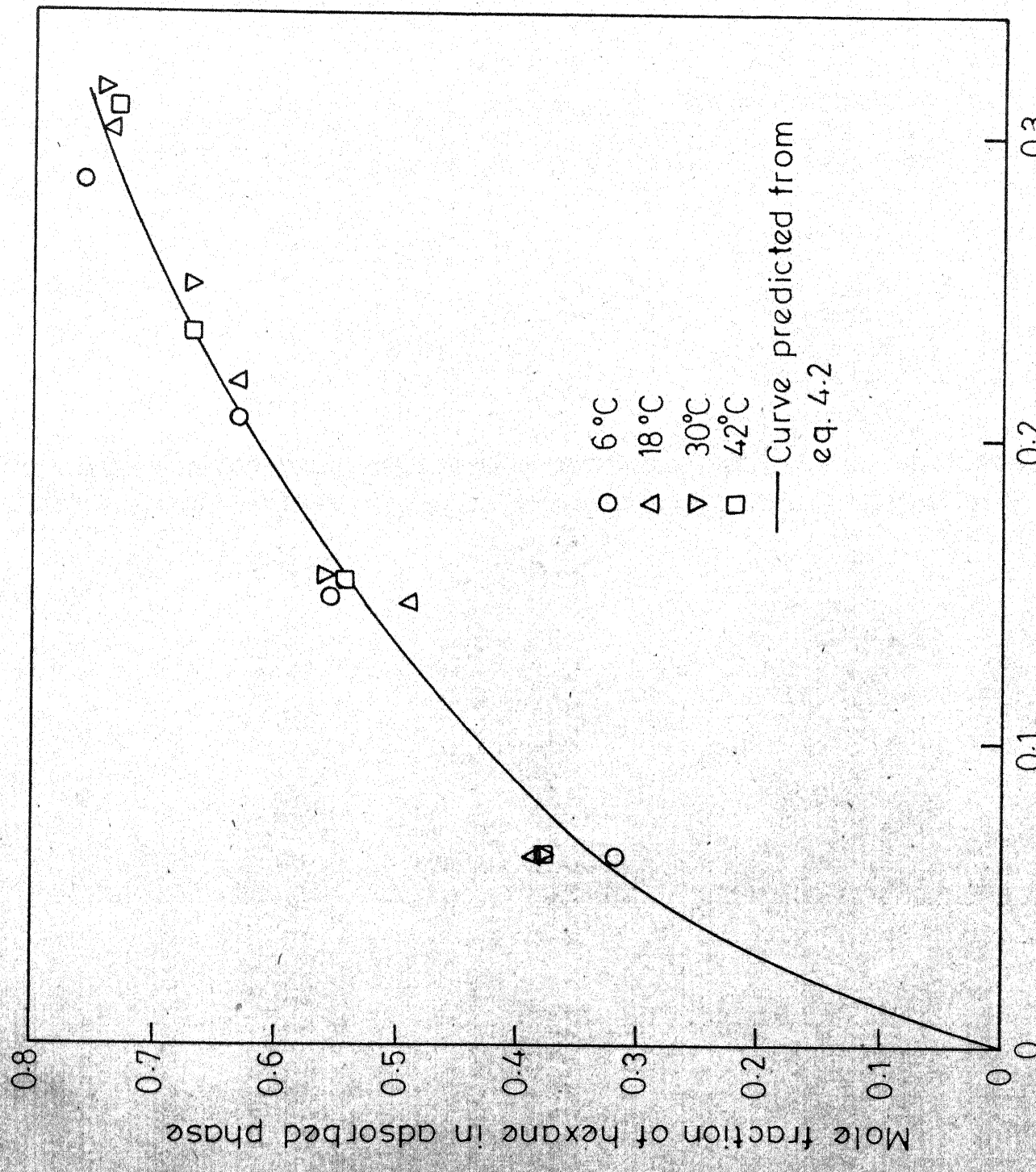


Fig. 4.2 - Equilibrium curves for hexane-heptane system at different temperatures.

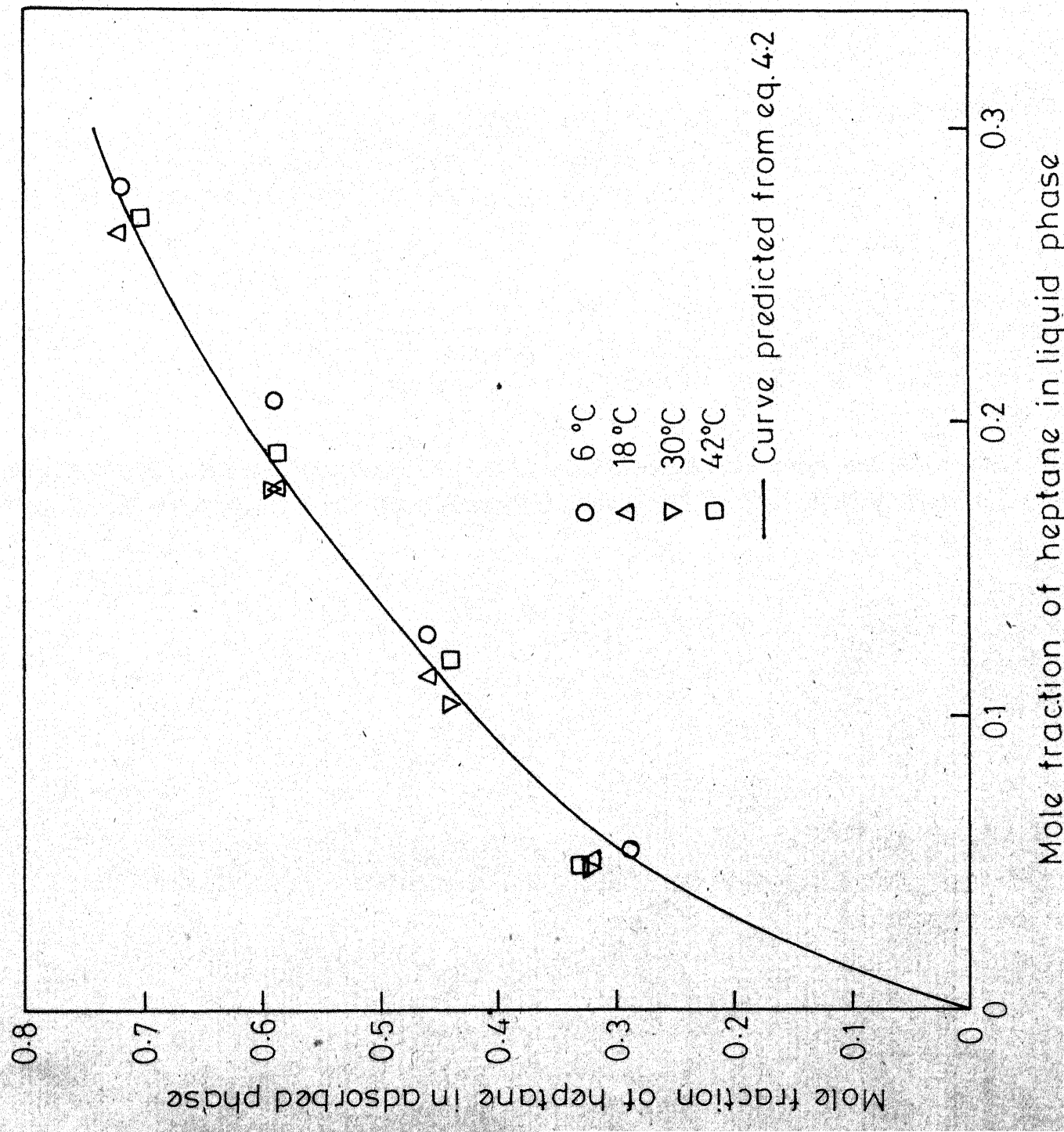


Fig. 4.3 - Equilibrium curves for heptane-octane system at different temperatures.

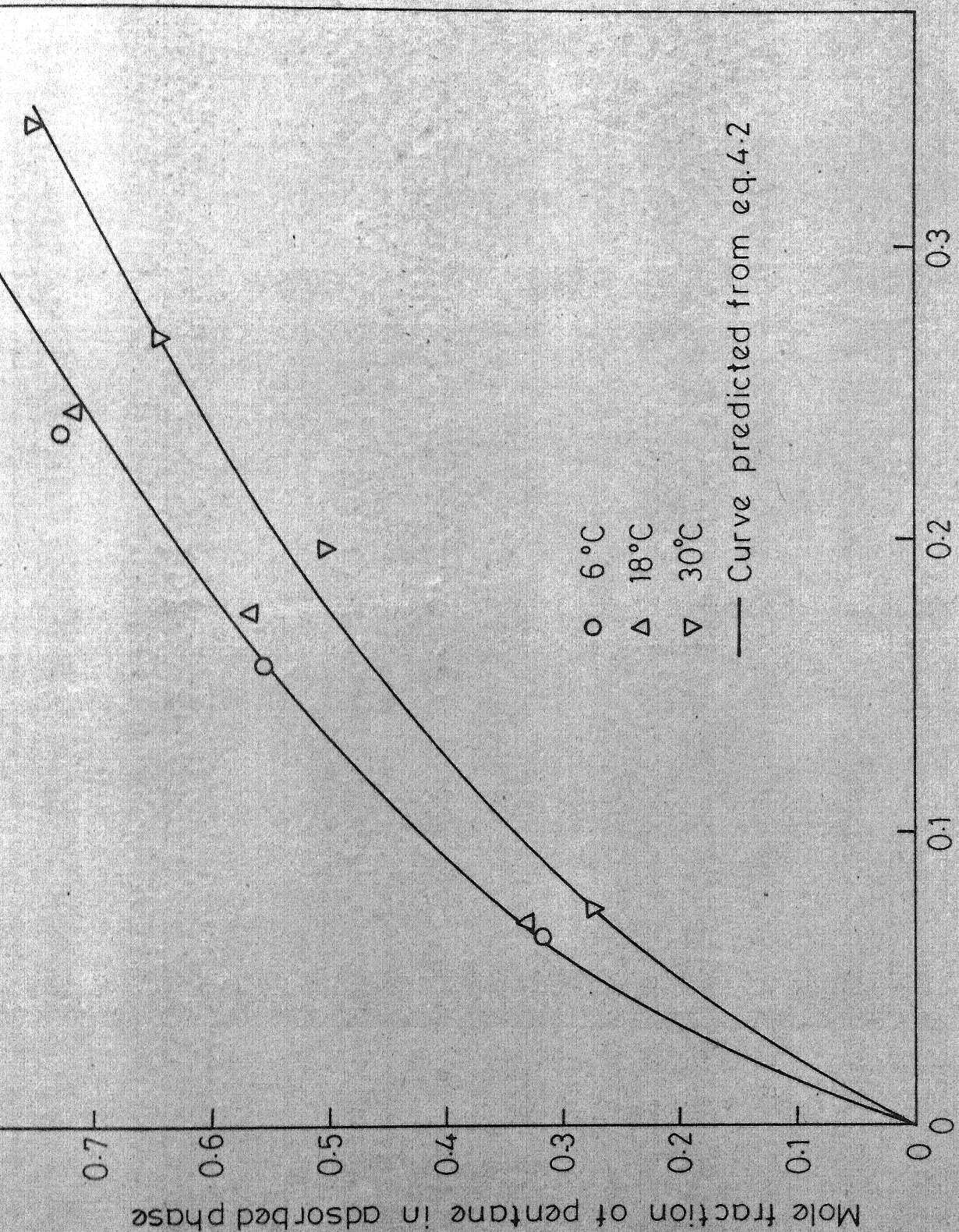


Fig. 4.4 - Equilibrium curves for pentane-heptane system at

this temperature of  $30^{\circ}\text{C}$  is close to the boiling point of pentane, it is possible that due to the increased thermal motion, the probability of an adsorbed pentane molecule escaping from a cavity is higher, thus giving a lower adsorption of pentane at equilibrium. A comparison between Figures 4.1, 4.4 and 4.5 show that while for each system, equilibrium curves for  $6^{\circ}$  and  $18^{\circ}$  coincide,  $30^{\circ}\text{C}$  curve is distinct from  $6^{\circ}$  and  $18^{\circ}$  curve, separation increasing as we move from pentane-octane system through pentane-heptane to pentane-hexane system. A possible explanation for this is that for pentane-hexane system more unadsorbed space is left in the cavity in comparison to that in pentane-heptane system, resulting in more freedom of movement for the pentane molecule and hence more desorption of pentane occurs in pentane-hexane system. A plausible reason for negligible effect of temperature for pentane-octane system could be that with octane, pentane is so tightly packed leaving little or no space for free thermal motion and subsequent desorption. Equilibrium curves at  $30^{\circ}\text{C}$ , for binary systems containing pentane as one of the components are given in Figure 4.6. Adsorption of pentane is highest for pentane-octane system and is the least for pentane-hexane system. Satterfield and Smeets [2] have suggested that the heavier molecule finds its favourable packing while smaller molecule takes up the remaining space which it can do more readily because it is smaller. Similar

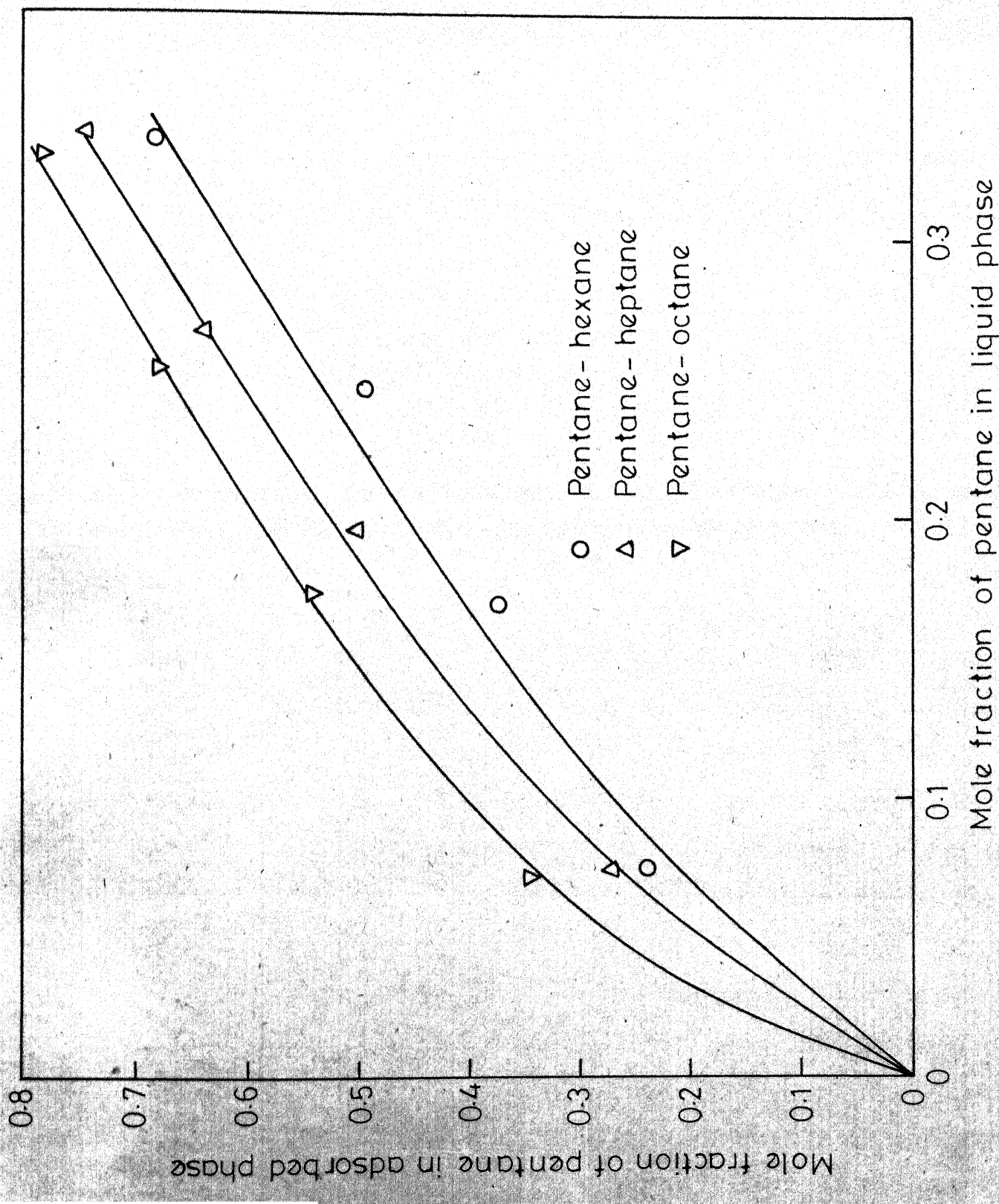


Fig. 4.6 - Equilibrium curves for binary systems containing pentane at 30°C.

argument holds for the present case. Of the three systems shown in Figure 4.6, pentane-octane makes the most tight packing whereas pentane-hexane system the least for the simple reason that there is maximum size difference in the former case and minimum in the latter.

#### 4.3.2 Separation Factors for Binary Systems:

Figures 4.7 to 4.11 show the variation of separation factor  $K$ , as a function of molefraction of lighter hydrocarbon in liquid phase on benzene free basis. However, the values of  $K$  will be the same even if the liquid phase mole fractions were defined inclusive of benzene. In all the cases,  $K$  increases with decrease in composition of lower molecular weight paraffin for all temperatures. Figure 4.7 shows that at  $6^\circ$  and  $18^\circ\text{C}$ , temperature has a negligible effect on  $K$  for pentane-hexane system. At  $30^\circ\text{C}$ , there is a drop in separation factor which may be because of desorption of pentane molecules at  $30^\circ\text{C}$  as already discussed earlier (sec. 4.3.1). Values of  $K$  were independent of temperature for all other systems except pentane-heptane where at  $30^\circ\text{C}$  the separation factor was lower than that at  $6^\circ$  or  $18^\circ\text{C}$ .

For all the systems studied,  $K$  was found to depend on the liquid phase concentration and assumed values less than or greater than one depending on this concentration. However, Sundstrom and Krautz [3] have reported  $K$  to be independent of

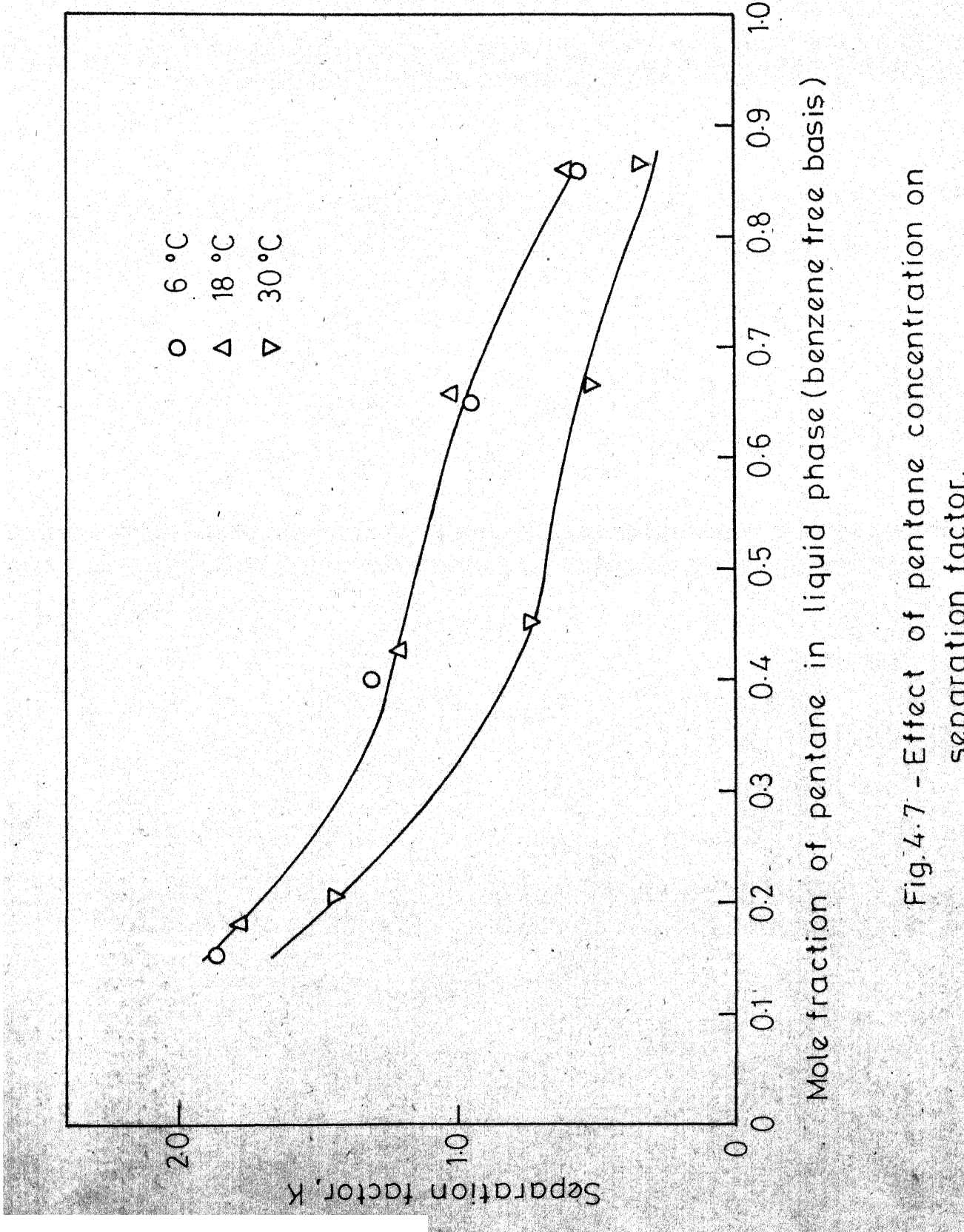


Fig. 4.7 - Effect of pentane concentration on separation factor.  
System :- Pentane-hexane.

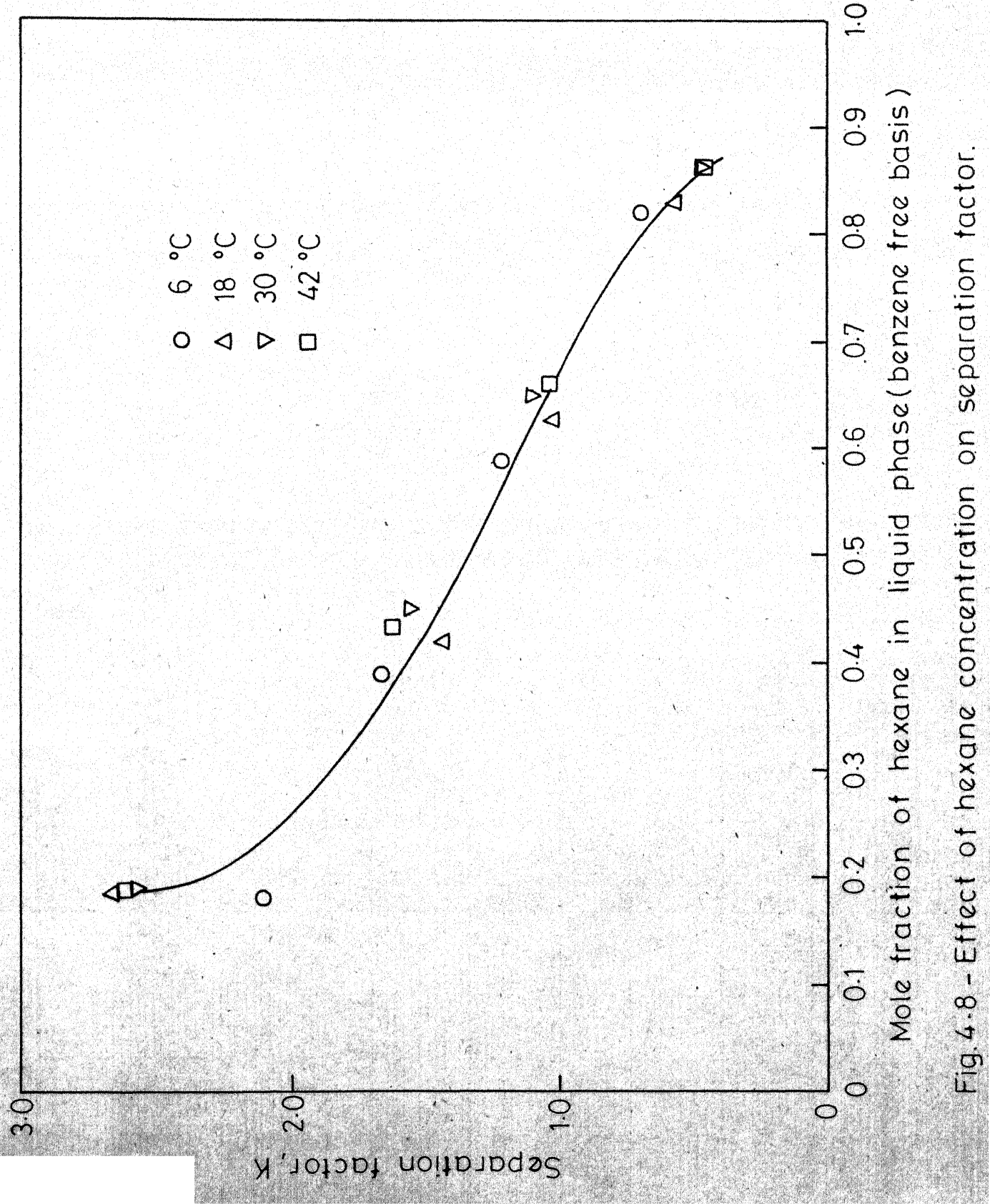


Fig. 4.8 - Effect of hexane concentration on separation factor.  
 System:— Hexane- heptane.

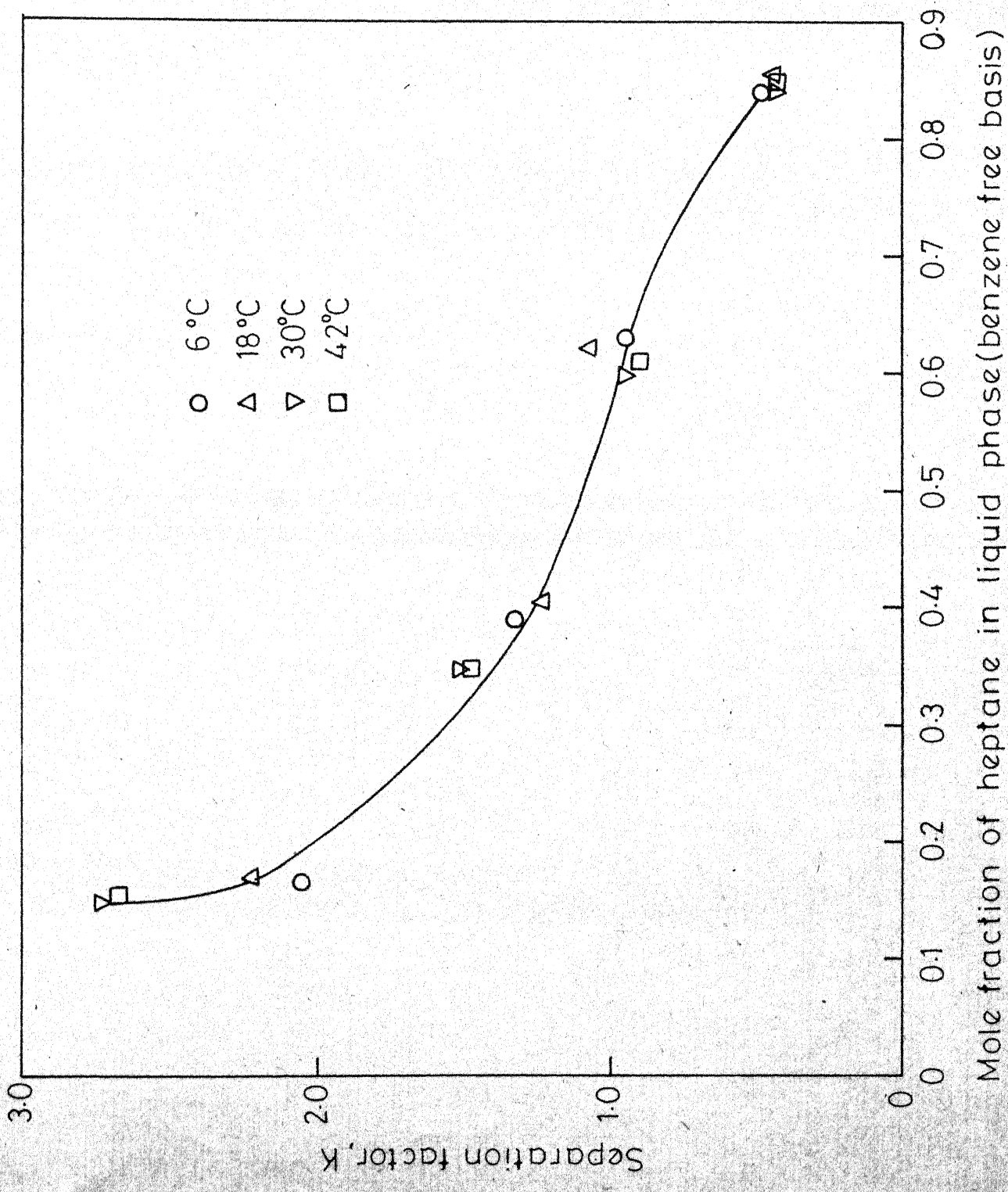


Fig. 4.9 - Effect of heptane concentration on separation factor.  
System : Heptane-octane.

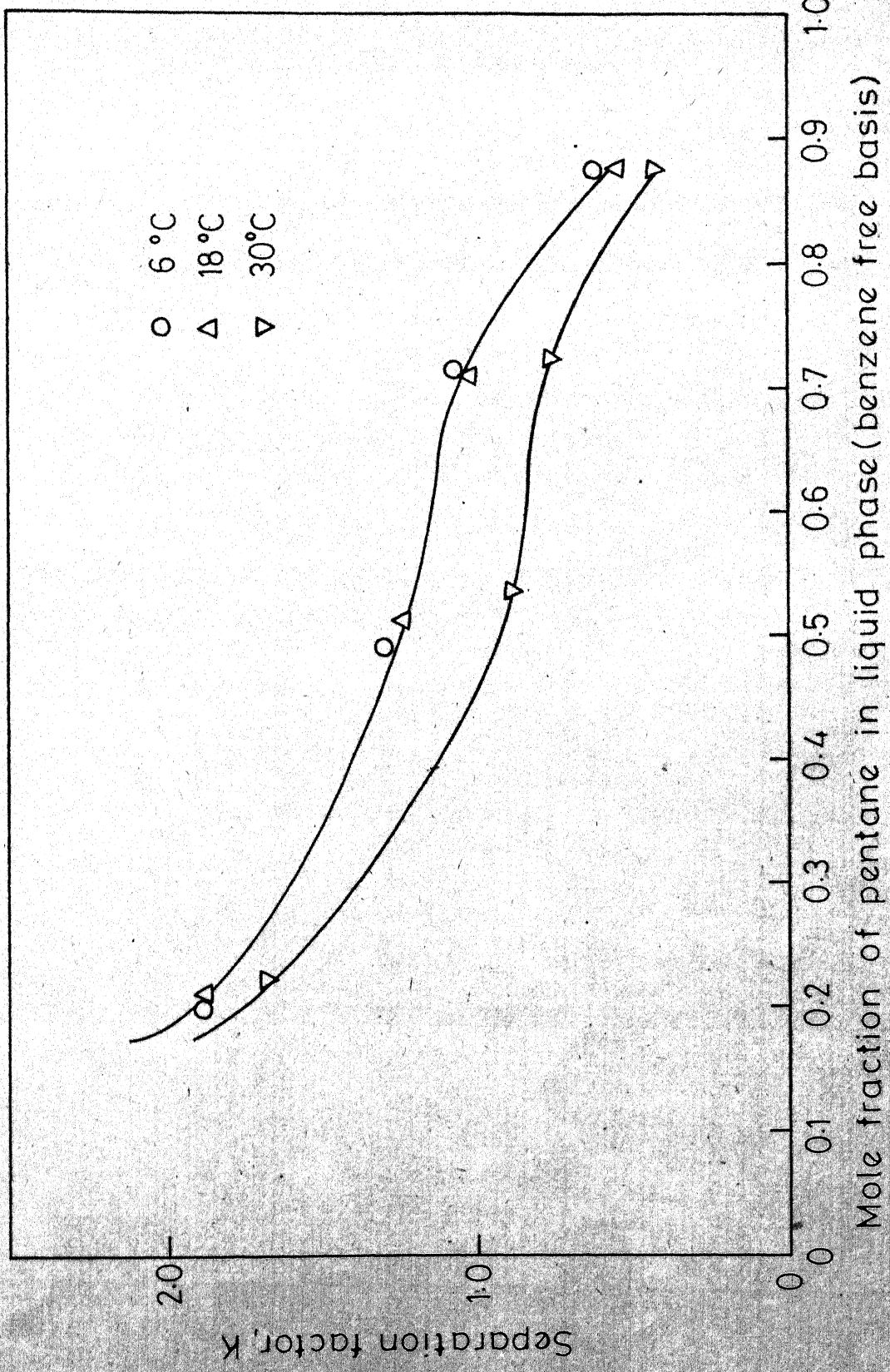


Fig. 4.10 - Effect of pentane concentration on separation factor.  
System : Pentane - heptane.

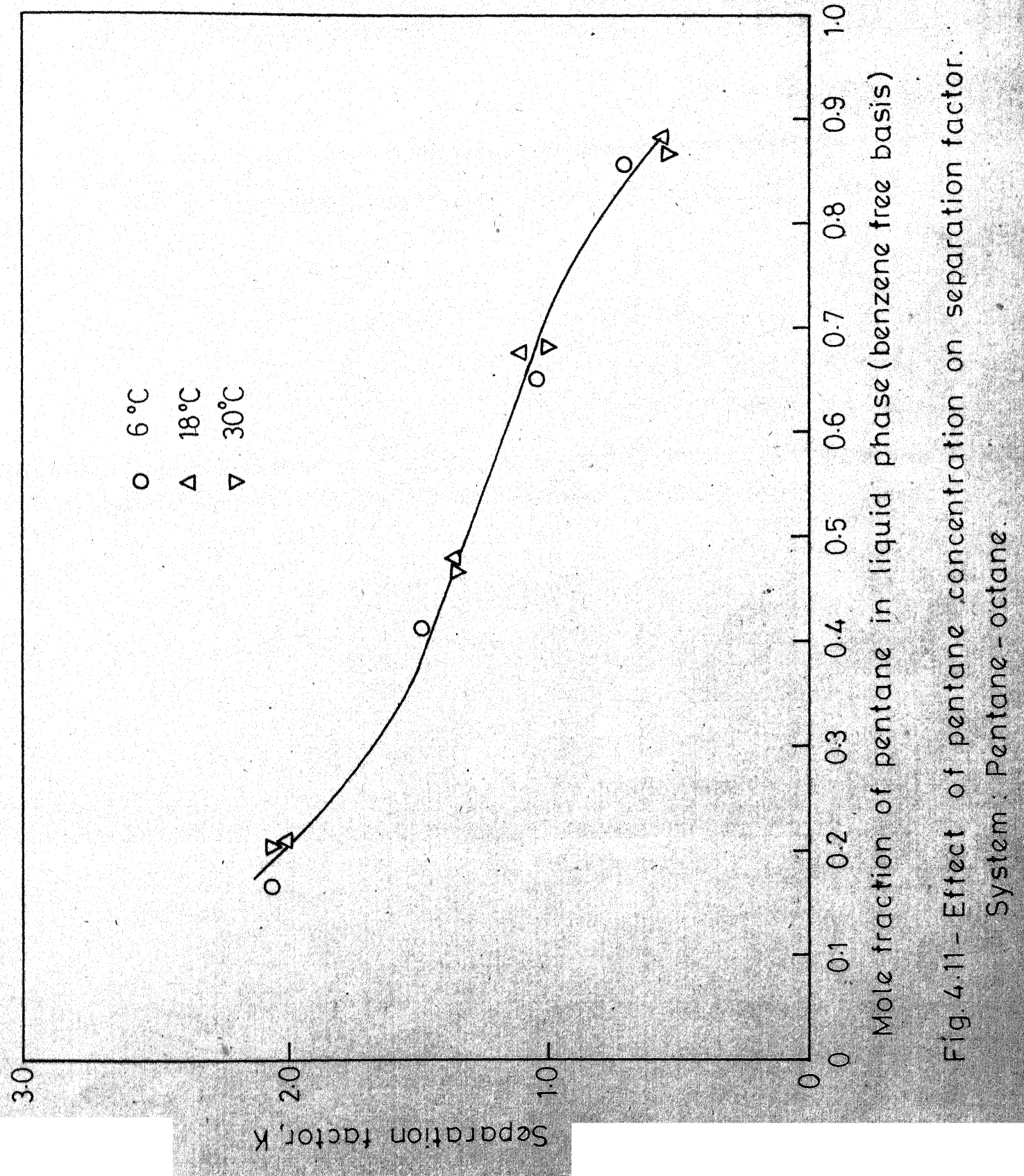


Fig. 4.11 - Effect of pentane concentration on separation factor.  
System: Pentane - octane.

concentration and always greater than unity. The reason for this discrepancy becomes clear if one realises that in the present case (Figures 4.7 through 4.11) the abscissa does not represent the actual mole fraction of lighter paraffin as is normally understood. Usual practice is to define the mole fractions such that  $x_L$  and  $x_H$  will add to unity, whereas in this study, because of an inert component being present in the form of benzene,  $x_L + x_H + x_B = 1$ ; where  $x_B$  is the mole fraction of benzene. However, by redefining the separation factor, it was possible to make it independent of concentration. The new separation factor  $K_r$  was expressed as:

$$K_r = \frac{y_L/x_L}{y_H/(x_H+x_B)} \quad (4.2)$$

The values of  $K_r$ , for all the systems have been calculated and tabulated in Table 4.1. These values are the average of  $K_r$  calculated for different liquid phase concentrations at a fixed temperature. All values of  $K_r$ , thus calculated, are greater than unity. In Figures 4.1 through 4.5 the solid lines represent the calculated equilibrium curves using average values taken from this table in conjunction with eq. 4.2. Since the values of  $K_r$  at 30°C for the three binary systems that contains pentane as one component were much lower than those at other temperatures, the predicted curves have been drawn using values of

TABLE 4.1: SEPARATION FACTOR,  $K_r$ , FOR BINARY SYSTEMS

System	Separation Factor, $K_r$				
	6°C	18°C	30°C	42°C	Average
BPX	6.3	6.5	3.5 <sup>a</sup>	-	6.4
BXH	6.8	6.9	6.5	6.6	6.7
BHO	6.8	7.3	6.6	6.8	6.9
BPH	7.2	7.4	5.0 <sup>a</sup>	-	7.3
BPO	7.6	7.4	6.8 <sup>a</sup>	-	7.5

<sup>a</sup>These values have not been included in calculating the average values of  $K_r$ .

Notes: BPX = Pentane-heXane

BXH = heXane-Heptane

BHO = Heptane-Octane

BPH = Pentane-Heptane

BPO = Pentane-Octane

$K_r$  at this temperature rather than average values. The fact that these predicted curves represent the experimental data well is the proof that the redefined  $K_r$  is indeed independent of concentration. For binary systems containing pentane, the average  $K_r$  values increased with an increasing molecular weight of the heavier component. This shows that separation is easiest, for the systems studied, in pentane-octane system and most difficult in pentane-hexane system.

#### 4.3.3 Adsorption in Ternary Systems:

The three ternary systems studied were pentane-hexane-heptane, pentane-hexane-octane and pentane-heptane-octane at 6°, 18° and 30°C. Adsorption results are presented in Tables 4.2 through 4.4 (operating conditions are tabulated in Appendices A4.5 to A4.7). Total number of molecules adsorbed per cavity decreased with increase in temperature. It was not possible to define a separation factor as was done for binary systems and these data were used to validate the multicomponent adsorption model as discussed later (Chapter 5).

TABLE 4.2: EXPERIMENTAL RESULTS FOR TERNARY SYSTEMS AT 60°C

Run	Equilibrium composition in liquid phase, mole fraction			Molecules adsorbed per cavity			Total number of molecules adsorbed per cavity
	1	2	3	1	2	3	
PXH-1	0.235	0.047	0.083	3.29	1.26	1.29	5.84
PXH-2	0.082	0.174	0.089	1.45	2.46	1.30	5.21
PXH-3	0.053	0.139	0.165	1.20	2.02	1.72	4.94
PXH-4	0.134	0.087	0.141	1.99	1.61	1.60	5.20
PXO-1	0.207	0.046	0.045	3.49	1.27	1.15	5.91
PXO-2	0.082	0.149	0.045	1.67	2.50	1.13	5.30
PXO-3	0.052	0.132	0.086	1.35	2.26	1.47	5.08
PXO-4	0.124	0.088	0.088	2.11	1.64	1.44	5.19
PHO-1	0.223	0.056	0.050	3.60	1.16	1.19	5.95
PHO-2	0.082	0.086	0.086	1.66	1.44	1.62	4.72
PHO-3	0.051	0.162	0.045	1.32	2.17	1.23	4.72
PHO-4	0.055	0.130	0.075	1.35	1.83	1.51	4.69

Notes: PXH = Pentane-hexane-heptane; PHO = Pentane-hexane-octane; PHO = Pentane-heptane-octane

1 is the lightest hydrocarbon in given ternary system and 3 is the heaviest hydrocarbon

TABLE 4.3: EXPERIMENTAL RESULTS FOR TERNARY SYSTEMS AT 18°C

Run	Equilibrium Composition in liquid phase, mole fraction			Molecules adsorbed per cavity			Total number of molecules adsorbed per cavity
	1	2	3	1	2	3	
PXH-5	0.113	0.051	0.165	1.66	1.17	1.86	4.69
PXH-6	0.119	0.123	0.108	1.62	1.61	1.37	4.60
PXH-7	0.216	0.121	0.028	2.74	1.54	0.99	5.27
PXH-8	0.129	0.168	0.029	1.85	2.04	0.98	4.87
-----							
PXO-5	0.045	0.048	0.170	1.22	1.23	1.96	4.41
PXO-6	0.221	0.073	0.023	3.15	1.31	1.03	4.49
PXO-7	0.114	0.144	0.040	1.80	2.04	1.07	4.91
PXO-8	0.056	0.153	0.089	1.21	2.07	1.29	4.57
-----							
PHO-5	0.101	0.042	0.143	1.70	1.09	1.73	4.52
PHO-6	0.216	0.044	0.025	3.42	1.11	1.02	5.55
PHO-7	0.063	0.103	0.092	1.33	1.58	1.38	4.29
PHO-8	0.167	0.099	0.036	2.47	1.46	1.06	4.99

Note: Notations are same as in Table 4.2

TABLE 4.4: EXPERIMENTAL RESULTS FOR TERNARY SYSTEMS AT 20°C

Run	Equilibrium composition in liquid phase, mole fraction			Molecules adsorbed per cavity			Total number of molecules adsorbed per cavity
	1	2	3	1	2	3	
PXH-9	0.077	0.221	0.044	1.04	2.54	1.04	4.62
PXH-10	0.260	0.055	0.042	2.28	1.32	1.12	4.72
PXH-11	0.184	0.135	0.046	1.54	1.90	1.08	4.52
PXH-12	0.170	0.056	0.103	1.67	1.30	1.42	4.39
PXH-13	0.072	0.144	0.115	1.09	1.96	1.30	4.35
PXH-14	0.123	0.037	0.181	1.43	1.16	1.80	4.39
PXH-15	0.142	0.111	0.083	1.44	1.78	1.24	4.46
PXH-16	0.150	0.138	0.103	1.38	1.80	1.23	4.41
PXO-9	0.071	0.216	0.050	1.06	2.62	0.99	4.67
PXO-10	0.165	0.113	0.045	1.62	1.96	0.97	4.55
PXO-11	0.254	0.041	0.049	2.59	1.30	1.02	4.91
PXO-12	0.168	0.044	0.099	1.90	1.36	1.25	4.51

Table 4.4 (contd)

Run	Equilibrium composition in liquid phase, mole fraction	Molecules adsorbed per cavity			Total number of molecules adsorbed per cavity		
		1	2	3			
PHO-9	0.070	0.043	0.185	1.30	1.16	1.87	4.33
PHO-10	0.160	0.101	0.055	1.91	1.56	1.09	4.56
PHO-11	0.168	0.046	0.114	2.01	1.18	1.30	4.49
PHO-12	0.270	0.039	0.054	2.84	1.08	1.05	4.97

Note: Notations are same as in Table 4.2

## REFERENCES

1. Satterfield, C.N., and Cheng, C.S., A.I.Ch.E.J., 18, 720 (1972a).
2. Satterfield, C.N., and Smeets, J.K., A.I.Ch.E.J. 20, 618 (1974).
3. Sundstrom, D.W., and Krautz, F.G., J. of Chem. Eng. Data 13 (2), 223 (1968).

## CHAPTER 5

### MATHEMATICAL MODEL FOR ADSORPTION OF PURE AND MULTICOMPONENT HYDROCARBON SYSTEMS

#### 5.1 INTRODUCTION:

The phenomenon of adsorption has been widely studied and extensive experimental data are now available for pure component vapor phase adsorption of light hydrocarbons and other compounds on different zeolites. However, industrial separation processes generally involve multicomponent adsorption, data for which are scanty. In any petroleum fraction, there are large number of combinations of hydrocarbons and it is, therefore, not possible to experimentally study all these systems. Hence, for the design of any adsorption process, a reliable method for predicting equilibrium adsorption data for mixtures from the isotherm of the pure components is essential.

The conventional adsorption models (Langmuir, Volmer, etc.) are not applicable to zeolite adsorption because the basic assumptions from which the models are derived are generally not fulfilled [2,3,19]. Other available approaches are potential theory and thermodynamic methods. According to the Dubinin-Polanyi potential theory [20], potential curves for adsorption of different gases, measured at different values of temperature and surface coverage on the same adsorbent, may be coalesced into a single curve

by a suitable choice of the coefficient of affinity. The usual choice for this coefficient is the molar volume of the liquified adsorbate. This property of pure-gas adsorption has been used by various investigators [6, 11,12] to predict adsorption equilibria for gas mixtures. The key assumption is that the characteristic potentials for various components of the mixture, and hence their fugacities in the gas phase are given by characteristic curves for adsorption of the pure gases. The extensions of the Dubinin-Polanyi theory to the case of mixtures is valid only when the surface potentials of pure adsorbates are equal at the state of saturated vapor [20]. The thermodynamic methods are those that are independent of any particular theory of the adsorption. Thermodynamic methods of estimating adsorption equilibria of gas mixtures include those of Myers and Prausnitz [13], Kidnay and Myers [8], Lewis, et al. [11], Arnold [1] and Cook and Basmadjian [5]. The basic postulate, common to all these models, is that the adsorbed phase forms an ideal adsorbed solution, but the methods differ in their choice of standard states. However, only the method of Myers and Prausnitz [13] is thermodynamically consistent and hence extensively used.

The structural regularity of zeolite lattices and the existence of well defined cavities within which the sorbate molecules are occluded, suggests that it should be possible

to develop a satisfactory theoretical equilibrium isotherm from the principles of statistical thermodynamics. Ruthven and co-workers, using this approach have proposed pure component [14] and binary gas phase [15-18] models. Binary model proposed by them is valid only for low concentrations.

No attempt has been made so far to develop theoretical models for adsorption in liquid phase even for pure components. However, since in the present study, liquid phase adsorption of single and multicomponent hydrocarbon systems has been investigated, for reasons already mentioned, it is necessary that a liquid phase prediction procedure is developed. Since no clues are available in literature on starting with liquid phase adsorption models, in this first attempt, use has been made of vapor-phase theory. It has been assumed that adsorption from liquid phase will be the same as that from vapor phase if this vapor is in equilibrium with the liquid. In otherwords, if we take a closed vessel partially filled with the liquid adsorbate, a vapor phase will be formed which will reach equilibrium with the liquid after sufficient time has elapsed. If an adsorbent is now placed in this closed system either in liquid phase or in vapor phase, the adsorption will be the same. It is assumed that if the adsorbent is placed in vapor phase, adsorption will disturb the equilibrium temporarily but molecules will come out of the liquid phase and restore vapor phase equilibrium almost

instantaneously. This assumption is usually valid since adsorption at vapor-liquid interface is negligible. This implies that one can use a vapor phase adsorption model to predict liquid phase adsorption if use is made of saturation vapor pressure at the given temperature in place of pressure for pure components. In case of multicomponent systems, partial pressures are obtained using Raoult's law since mixture of paraffins can be taken as an ideal solution.

## 5.2 MATHEMATICAL MODEL FOR ADSORPTION OF PURE n-PARAFFINS:

Consider a system of zeolite lattice with  $M$  cavities and an adsorbate. Because of the structural regularity of the zeolite it may be assumed that these cavities are separate subsystems each of which can adsorb any number of molecules  $s$ , from zero to a maximum of  $m$ . The canonical ensemble partition function for the system is [7]

$$Q = \sum_{s=0}^m q(s) \lambda^s, \quad \lambda = e^{\mu/kT} \quad (5.1)$$

where  $q(s)$  is the partition function for a cavity containing  $s$  sorbate molecules,  $\mu$  is the chemical potential,  $k$  is the Boltzmann constant and  $T$  is the absolute temperature. When all the sites are equivalent (as in molecular sieves), the macroscopic system of  $M$  cavities may be regarded as a grand ensemble of subsystems. The grand partition function for this case is

$$G = Q^M = \left[ \sum_{s=0}^m q(s) \lambda^s \right]^M \quad (5.2)$$

The average number of molecules for this macroscopic system is given by [7]

$$\bar{N} = \lambda \left( \frac{\partial \ln G}{\partial \lambda} \right) = M \lambda \frac{\partial \ln Q}{\partial \lambda}$$

or

$$C = \frac{\bar{N}}{M} = \lambda \frac{\partial \ln Q}{\partial \lambda} = \frac{\sum_{s=0}^m s q(s) \lambda^s}{\sum_{s=0}^m q(s) \lambda^s}$$

where  $C$  is the average number of molecules adsorbed per cavity.

The above equation can be written in terms of configuration integrals  $Z(s)$ , as

$$C = \frac{\sum_{s=0}^m s Z(s) a^s}{\sum_{s=0}^m Z(s) a^s} \quad (5.3)$$

where  $Z(s)$  is the configuration integral for a subsystem of  $s$ -sorbate molecules occluded within a single zeolite cavity and is defined as

$$Z(s) = \frac{1}{s!} \frac{1}{V} \int \exp \{ -U_s(r_1 \dots r_s) / kT \} dr_1 \dots dr_s \quad (5.4)$$

where  $r_i$  is the position vector,  $V$  is the volume of the zeolite cavity,  $U_s$  is the potential energy for the subsystem,  $a$  is the activity of the sorbate ( $= p/kT$ ) for an ideal gas.

When there is no sorbate molecule occluded, we get

$$Z(0) = 1$$

and for one molecule,

$$Z(1) a = \alpha p$$

where  $\alpha$  is the Henry's constant and  $p$  is the pressure.

Expansion of equation (5.3) gives

$$c = \frac{Z(1)a + 2Z(2)a^2 + \dots + m Z(m)a^m}{1 + Z(1)a + Z(2)a^2 + \dots + Z(m)a^m} \quad (5.5)$$

Equation (5.5) defines the adsorption isotherm for the system in terms of configuration integrals defined by equation (5.4). In order to compare theory with experiment, it is necessary to express configuration integrals in terms of measurable quantities. The following approximations are made.

- (i) It is assumed that the form of the potential field within a zeolite cavity is independent of the number of molecules occluded within the cavity.
- (ii) When two or more molecules are present within a given cavity, it is assumed that the molecules move randomly and independently in the potential field resulting from the combined effects of sorbate-sorbent and sorbate-sorbate potentials.

(iii) The effect of sorbate molecules in neighbouring cavities is neglected.

(iv) The energy of interaction between sorbate molecules in the same cavity is represented by Sutherland potential, defined as

$$U_s(r) = \infty, r < \sigma ; \quad U_s(r) = -\epsilon(\sigma/r)^6, \quad r \geq \sigma$$

where  $\epsilon$  and  $\sigma$  are the molecular constants. With these approximations the configuration integrals may be written as

$$Z(s) = \frac{Z(1)^s}{s!} \left(1 - \frac{s\beta}{v}\right)^s \exp\left(\frac{s\beta\epsilon}{v k T}\right), \quad 2 \leq s \leq v/\beta \quad (5.6)$$

where  $\beta = \frac{2}{3} \pi \sigma^3$  is the effective co-volume of the sorbate.

In this expression, the factor  $(1-s\beta/v)$  accounts for the reduction in free volume of the cavity while the exponential term represents the increase in adsorption potential due to the mutual attraction of the sorbate molecules. Substitution of eq.(5.6) in eq. (5.5) gives

$$Z(1)a + Z(1)^2 a^2 (1-2\beta/v)^2 \exp\left(\frac{2\beta\epsilon}{v k T}\right) + \dots +$$

$$C = \frac{\frac{Z(1)^s a^s}{(m-1)!} \left(1 - \frac{m\beta}{v}\right)^m \exp\left(\frac{m\beta\epsilon}{v k T}\right)}{1 + Z(1)a + \frac{Z(1)^2 a^2}{2!} (1-2\beta/v)^2 \exp\left(\frac{2\beta\epsilon}{v k T}\right) + \dots +}$$

$$\frac{Z(1)^s a^s}{m!} \left(1 - \frac{m\beta}{v}\right)^m \exp\left(\frac{m\beta\epsilon}{v k T}\right)$$

Substitution of  $Z(l)a = \alpha p$  in above equation gives

$$\alpha p + (\alpha p)^2 (1-2\beta/v)^2 \exp\left(\frac{2\beta\epsilon}{v k T}\right) + \dots +$$

$$\frac{(\alpha p)^m}{(m-1)!} (1-m\beta/v)^m \exp\left(\frac{m\beta\epsilon}{v k T}\right)$$

$$C = \frac{1 + \alpha p + \frac{(\alpha p)^2}{2!} (1-2\beta/v)^2 \exp\left(\frac{2\beta\epsilon}{v k T}\right) + \dots +}{\frac{(\alpha p)^m}{m!} (1-m\beta/v)^m \exp\left(\frac{m\beta\epsilon}{v k T}\right)} \quad (5.7)$$

This is the theoretical equation for the isotherm for a pure component in terms of Henry's constant,  $\alpha$ , and effective molecular volume,  $\beta$ . Some difficulty arises in the choice of appropriate value for  $\beta$ , since the molecular volume of the sorbate, and hence the saturation capacity of the zeolite, varies with temperature. Dubinin [16] has suggested that the molar volume of the intracrystalline fluid may be approximated by a linear interpolation between the molar volume of the saturated liquid sorbate at its normal boiling point,  $T_B$ , and the vander Waals co-volume at the critical temperature,  $T_C$ . This approximation has been used by Ruthven and co-workers [14-18] who found it valid only at very low adsorption. With this approximation eq. (5.7) is left with a single parameter  $\alpha$  which, in principle, may be calculated, in terms of molecular constants, by evaluating the configuration integrals for a single sorbate molecule

occluded within a cavity. However, such calculations are only approximate [17, 18] since configuration integrals cannot be exactly calculated. In practice,  $\alpha$  can either be calculated by the slope of the isotherm at low concentration or by matching the theoretical equation to an experimental isotherm. In general, it has been found [16] that the exponential term in eq. (5.7) has a very minor effect. This factor can, therefore, be omitted to give a simpler equation for the isotherm as

$$C = \frac{\alpha p + (\alpha p)^2 (1-2\beta/v)^2 + \dots + (\alpha p)^m (1-m\beta/v)^m / (m-1)!}{1 + \alpha p + \frac{(\alpha p)^2}{2!} (1-2\beta/v)^2 + \dots + \frac{(\alpha p)^m}{m!} (1-m\beta/v)^m} \quad (5.8)$$

This expression is much simpler in comparison to eq. (5.7) and can be handled without much difficulty. Since benzene was used as a diluent, even in pure component systems there were two components in the liquid phase. Application of Raoult's law gives

$$C = \frac{\alpha P x + (\alpha P x)^2 (1-2\beta/v)^2 + \dots + \frac{(\alpha P x)^m}{(m-1)!} (1-m\beta/v)^m}{1 + \alpha P x + \frac{(\alpha P x)^2}{2!} (1-2\beta/v)^2 + \dots + \frac{(\alpha P x)^m}{m!} (1-m\beta/v)^m} \quad (5.9)$$

where  $P$  is the vapor pressure of the paraffin at adsorption temperature and  $x$  is the equilibrium mole fraction of the same in liquid phase.

Equation (5.9) along with the constraint  $m \beta \leq v$  was used with pure component adsorption data to give values of  $\alpha$  and  $\beta$ .

### 5.3 EXTENSION OF THE MODEL TO BINARY SYSTEMS:

The pure component model developed above has been extended for binary systems. In binary systems, there are, two adsorbates and both of them can be occluded individually or simultaneously in any cavity of the zeolite. There will be competition between the two components and the one which has a higher affinity for the adsorbent will be adsorbed preferentially in comparison to the other. The total number of molecules of both components will be restricted by the volume of the cavity. For a binary mixture of components A and B, the grand partition function,  $G_{AB}$  [17] is

$$G_{AB} = \left[ \sum_{j=0} \sum_{i=0} q(i,j) \lambda_A^i \lambda_B^j \right]^M = Q_{AB}^M \quad (5.10)$$

where  $Q_{AB}$  is the canonical ensemble partition function for the system containing components A and B,  $q(i,j)$  is the partition function for a cavity containing  $i$  molecules of A and  $j$  molecules of B,  $\lambda_A = e^{\mu_A/kT}$  and  $\lambda_B = e^{\mu_B/kT}$  ( $\mu_A$  and  $\mu_B$  are the chemical potentials of components A and B and  $T$  is the absolute temperature). The summation in the above equation is carried out over all values of  $i$  and  $j$  given by

$$i \beta_A + j \beta_B \leq v \quad (5.11)$$

where  $\beta_A$  and  $\beta_B$  are the effective molecular volumes of A and B respectively at adsorption temperature. In terms of configuration integrals, eq.(5.10) can be written as

$$G_{AB} = \left[ \sum_j \sum_i Z(i,j) a_A^i a_B^j \right]^M = Q_{AB}^M \quad (5.12)$$

where  $Z(i,j)$  is the configuration integral for system containing  $i$  molecules of A and  $j$  molecules of B and  $a_A$  and  $a_B$  are the activities of component A and B respectively. Average number of molecules of A and B adsorbed per cavity ( $c_A$  and  $c_B$ ) are given by

$$c_A = \frac{n_A}{M} = \lambda_A \left( \frac{\partial \ln Q_{AB}}{\partial \lambda_A} \right)_{\lambda_B, T} \quad (5.13)$$

$$c_B = \frac{n_B}{M} = \lambda_B \left( \frac{\partial \ln Q_{AB}}{\partial \lambda_B} \right)_{\lambda_A, T} \quad (5.14)$$

Substitution of eq. (5.12) in eqs. (5.13) and (5.14) gives

$$c_A = \frac{\sum_j \sum_i i Z(i,j) a_A^i a_B^j}{\sum_j \sum_i Z(i,j) a_A^i a_B^j} \quad (5.15)$$

and

$$c_B = \frac{\sum_j \sum_i j Z(i,j) a_A^i a_B^j}{\sum_j \sum_i Z(i,j) a_A^i a_B^j} \quad (5.16)$$

The configuration integrals for two components, with the same

assumptions as given for pure components (sec.5.2) are given by

$$Z(i,j) = \frac{Z(1,0)^i Z(0,1)^j}{i! j!} \left(1 - \frac{i\beta_A}{v} - \frac{j\beta_B}{v}\right)^{i+j} \exp\left(\frac{i\beta_A \epsilon_A + j\beta_B \epsilon_B}{v k T}\right) \quad (5.17)$$

(where  $\epsilon_A$  and  $\epsilon_B$  are molecular constants for components A and B respectively) with the condition of eq.(5.11).  $Z(1,0)$  is the configuration integral when only one molecule of A and no molecules of B is adsorbed i.e.

$$Z(1,0) = Z_A \quad (5.18)$$

Similarly,

$$Z(0,1) = Z_B \quad (5.19)$$

$$Z(0,0) = Z(0) = 1 \quad (5.20)$$

Therefore,

$$Z(1,0) a_A = Z_A a_A = \alpha_A p_A \quad (5.21)$$

and

$$Z(0,1) a_B = Z_B a_B = \alpha_B p_B \quad (5.22)$$

where  $\alpha_A$  and  $\alpha_B$  are Henry's constants for components A and B respectively and  $p_A$  and  $p_B$  are partial pressures of A and B respectively. Expansion of eq.(5.15) gives

$$C_A = \frac{OZ(0,0) a_A^0 a_B^0 + OZ(0,1) a_A^0 a_B^1 + Z(1,0) a_A a_B^0 + \sum_j \sum_i i Z(i,j) a_A^i a_B^j}{Z(0,0) a_A^0 a_B^0 + Z(1,0) a_A^1 a_B^0 + Z(0,1) a_A^0 a_B^1 + \sum_j \sum_i Z(i,j) a_A^i a_B^j}$$

or

$$c_A = \frac{z(1,0) a_A + \sum_j \sum_i i z(i,j) a_A^i a_B^j}{z(0,0) + z(1,0) a_A + z(0,1) a_B + \sum_j \sum_i z(i,j) a_A^i a_B^j} \quad (5.23)$$

where summations are now carried out over all values of  $i$  and  $j$  satisfying

$$i + j \geq 2 \quad (5.24)$$

$$i\beta_A + j\beta_B \leq v \quad (5.11)$$

Substitution of eqs. (5.20) to (5.22) in eq. (5.23) gives

$$c_A = \frac{\alpha_A p_A + \sum_j \sum_i i z(i,j) a_A^i a_B^j}{1 + \alpha_A p_A + \alpha_B p_B + \sum_j \sum_i z(i,j) a_A^i a_B^j} \quad (5.25)$$

Equations (5.17) and (5.25) give

$$c_A = \frac{\alpha_A p_A + \sum_j \sum_i \frac{i z(1,0)^i a_A^i z(0,1)^j a_B^j}{i! j!} (1 - i\beta_A/v - j\beta_B/v)^{i+j} \times \exp \left( \frac{i\beta_A \varepsilon_A + j\beta_B \varepsilon_B}{v k T} \right)}{1 + \alpha_A p_A + \alpha_B p_B + \sum_j \sum_i \frac{z(1,0)^i a_A^i z(0,1)^j a_B^j}{i! j!} (1 - i\beta_A/v - j\beta_B/v)^{i+j} \times \exp \left( \frac{i\beta_A \varepsilon_A + j\beta_B \varepsilon_B}{v k T} \right)} \quad (5.26)$$

Substitution of eqs. (5.21) and (5.22) in above equation gives

$$\alpha_A p_A + \sum_j \sum_i \frac{(\alpha_A p_A)^i (\alpha_B p_B)^j}{(i-1)! j!} (1-i\beta_A/v - j\beta_B/v)^{i+j} \times \\ \exp \left( \frac{i\beta_A \epsilon_A + j\beta_B \epsilon_B}{v k T} \right)$$

$$C_A = \frac{1 + \alpha_A p_A + \sum_j \sum_i \frac{(\alpha_A p_A)^i (\alpha_B p_B)^j}{i! j!} (1-i\beta_A/v - j\beta_B/v)^{i+j} \times \\ \exp \left( \frac{i\beta_A \epsilon_A + j\beta_B \epsilon_B}{v k T} \right)}{1 + \alpha_A p_A + \alpha_B p_B + \sum_j \sum_i \frac{(\alpha_A p_A)^i (\alpha_B p_B)^j}{i! j!} (1-i\beta_A/v - j\beta_B/v)^{i+j} \times \\ \exp \left( \frac{i\beta_A \epsilon_A + j\beta_B \epsilon_B}{v k T} \right)} \quad (5.27)$$

Similarly equation for  $C_B$  can also be derived, which is

$$\alpha_B p_B + \sum_j \sum_i \frac{(\alpha_A p_A)^i (\alpha_B p_B)^j}{i! (j-1)!} (1-i\beta_A/v - j\beta_B/v)^{i+j} \times \\ \exp \left( \frac{i\beta_A \epsilon_A + j\beta_B \epsilon_B}{v k T} \right)$$

$$C_B = \frac{1 + \alpha_A p_A + \alpha_B p_B + \sum_j \sum_i \frac{(\alpha_A p_A)^i (\alpha_B p_B)^j}{i! j!} (1-i\beta_A/v - j\beta_B/v)^{i+j} \times \\ \exp \left( \frac{i\beta_A \epsilon_A + j\beta_B \epsilon_B}{v k T} \right)}{1 + \alpha_A p_A + \alpha_B p_B + \sum_j \sum_i \frac{(\alpha_A p_A)^i (\alpha_B p_B)^j}{i! j!} (1-i\beta_A/v - j\beta_B/v)^{i+j} \times \\ \exp \left( \frac{i\beta_A \epsilon_A + j\beta_B \epsilon_B}{v k T} \right)} \quad (5.28)$$

The expressions along with constraints (5.11) and (5.24) give the general model for binary mixtures. As in pure component model, when exponential terms are neglected, we get

$$\alpha_A p_A + \sum_j \sum_i \frac{(\alpha_A p_A)^i (\alpha_B p_B)^j}{(i-1)! j!} (1-i\beta_A/v - j\beta_B/v)^{i+j}$$

$$C_A = \frac{1 + \alpha_A p_A + \alpha_B p_B + \sum_j \sum_i \frac{(\alpha_A p_A)^i (\alpha_B p_B)^j}{i! j!} (1-i\beta_A/v - j\beta_B/v)^{i+j}}{1 + \alpha_A p_A + \alpha_B p_B + \sum_j \sum_i \frac{(\alpha_A p_A)^i (\alpha_B p_B)^j}{i! j!} (1-i\beta_A/v - j\beta_B/v)^{i+j}} \quad (5.29)$$

and

$$C_B = \frac{\alpha_A p_A + \sum_j \sum_i \frac{(\alpha_A p_A)^i (\alpha_B p_B)^j}{i! (j-1)!} (1-i\beta_A/v - j\beta_B/v)^{i+j}}{1 + \alpha_A p_A + \alpha_B p_B + \sum_j \sum_i \frac{(\alpha_A p_A)^i (\alpha_B p_B)^j}{i! j!} (1-i\beta_A/v - j\beta_B/v)^{i+j}} \quad (5.30)$$

Equations (5.29) and (5.30) along with constraints (5.11) and (5.24) give simplified form of the model for binary mixtures. Values of  $\alpha_A$ ,  $\alpha_B$ ,  $\beta_A$  and  $\beta_B$  needed in above expressions are obtained from isotherms of pure components. Raoult's law for components A and B gives

$$p_A = P_A x_A \quad \text{and} \quad p_B = P_B x_B$$

where  $P_A$  and  $P_B$  are vapor pressures of components A and B respectively and  $x_A$  and  $x_B$  are molefractions of A and B in liquid phase. Substitution of these in equations (5.29) and (5.30) gives

$$C_A = \frac{\alpha_A p_A x_A + \sum_j \sum_i \frac{(\alpha_A p_A x_A)^i (\alpha_B p_B x_B)^j}{(i-1)! j!} (1-i\beta_A/v - j\beta_B/v)^{i+j}}{1 + \alpha_A p_A x_A + \alpha_B p_B x_B + \sum_j \sum_i \frac{(\alpha_A p_A x_A)^i (\alpha_B p_B x_B)^j}{i! j!} (1-i\beta_A/v - j\beta_B/v)^{i+j}} \quad (5.31)$$

and

$$c_B = \frac{\alpha_B^p x_B + \sum_j \sum_i \frac{(\alpha_A^p x_A)^i (\alpha_B^p x_B)^j}{i! (j-1)!} (1 - \frac{i\beta_A}{v} - \frac{j\beta_B}{v})^{i+j}}{1 + \alpha_A^p x_A + \alpha_B^p x_B + \sum_j \sum_i \frac{(\alpha_A^p x_A)^i (\alpha_B^p x_B)^j}{i! j!} x (1 - \frac{i\beta_A}{v} - \frac{j\beta_B}{v})^{i+j}} \quad (5.32)$$

Equations (5.31) and (5.32) along with the constraints (5.11) and (5.24) were used to calculate average number of molecules of A and B adsorbed per cavity in a binary system of A and B. Values of  $\alpha_A$ ,  $\alpha_B$ ,  $\beta_A$  and  $\beta_B$  needed in above expressions are obtained from isotherms of pure components.

#### 5.4 EXTENSION OF THE MODEL TO TERNARY SYSTEMS:

The above model can be extended to a multicomponent system with any number of components. We extend it here for three components. In this case, there are three components A, B and C with Henry's constants  $\alpha_A$ ,  $\alpha_B$  and  $\alpha_C$  and molecular volumes  $\beta_A$ ,  $\beta_B$  and  $\beta_C$  respectively. The grand partition function,  $G_{ABC}$ , for the system can be written as

$$G_{ABC} = \left[ \sum_{h=0} \sum_{j=0} \sum_{i=0} q(i,j,h) \lambda_A^i \lambda_B^j \lambda_C^h \right]^M = Q_{ABC}^M$$

with constraint

$$i\beta_A + j\beta_B + h\beta_C \leq v$$

where  $q(i,j,h)$  is the partition function of a cavity containing  $i$  molecules of A,  $j$  molecules of B and  $h$  molecules of C.

$Q_{ABC}$  is the canonical ensemble partition function for the system containing components A, B and C.  $\lambda_A = e^{\mu_A/kT}$ ,  $\lambda_B = e^{\mu_B/kT}$  and  $\lambda_C = e^{\mu_C/kT}$  ( $\mu_A$ ,  $\mu_B$  and  $\mu_C$  are chemical potentials for components A, B and C respectively). In terms of configuration integrals above equation can be written as

$$G_{ABC} = \left[ \sum_h \sum_j \sum_i Z(i, j, h) a_A^i a_B^j a_C^h \right] = Q_{ABC}^M \quad (5.33)$$

where  $Z(i, j, h)$  is the configuration integral for a cavity containing  $i$  molecules of A,  $j$  molecules of B and  $h$  molecules of C.  $a_A$ ,  $a_B$  and  $a_C$  are activities of A, B and C respectively. The average number of molecules of A, B and C adsorbed can be written as

$$c_A = \frac{n_A}{M} = \lambda_A \left( \frac{\partial \ln Q_{ABC}}{\partial \lambda_A} \right) \lambda_B, \lambda_C, T \quad (5.34)$$

$$c_B = \frac{n_B}{M} = \lambda_B \left( \frac{\partial \ln Q_{ABC}}{\partial \lambda_B} \right) \lambda_A, \lambda_C, T \quad (5.35)$$

$$c_C = \frac{n_C}{M} = \lambda_C \left( \frac{\partial \ln Q_{ABC}}{\partial \lambda_C} \right) \lambda_A, \lambda_B, T \quad (5.36)$$

Equation (5.33) with equations (5.34 to 5.35) gives

$$c_A = \frac{\sum_h \sum_j \sum_i i Z(i, j, h) a_A^i a_B^j a_C^h}{\sum_h \sum_j \sum_i Z(i, j, h) a_A^i a_B^j a_C^h} \quad (5.37)$$

$$c_B = \frac{\sum_h \sum_j \sum_i j Z(i, j, h) a_A^i a_B^j a_C^h}{\sum_h \sum_j \sum_i Z(i, j, h) a_A^i a_B^j a_C^h} \quad (5.38)$$

$$c_C = \frac{\sum_h \sum_j \sum_i h z(i,j,h) a_A^i a_B^j a_C^h}{\sum_h \sum_j \sum_i z(i,j,h) a_A^i a_B^j a_C^h} \quad (5.39)$$

The configuration integrals for ternary systems, with the usual assumptions as discussed earlier, are approximated by

$$z(i,j,h) = \left[ \frac{z(1,0,0)^i z(0,1,0)^j z(0,0,1)^h}{i! j! h!} \left( 1 - \frac{i\beta_A}{v} - \frac{j\beta_B}{v} - \frac{h\beta_C}{v} \right)^{i+j+h} \times \exp \left( \frac{i\beta_A \epsilon_A + j\beta_B \epsilon_B + h\beta_C \epsilon_C}{v k T} \right) \right] \quad (5.40)$$

where,

$$z(0,0,0) = z(0) = 1 \quad (5.41)$$

$$z(1,0,0) a_A = z_A a_A = \alpha_A p_A \quad (5.42)$$

$$z(0,1,0) a_B = z_B a_B = \alpha_B p_B \quad (5.43)$$

$$z(0,0,1) a_C = z_C a_C = \alpha_C p_C \quad (5.44)$$

where  $p_A$ ,  $p_B$  and  $p_C$  are partial pressures of components A, B and C respectively. Equation (5.37) on expansion gives

$$c_A = \frac{0z(0,0,0) a_A^0 a_B^0 a_C^0 + 0z(0,1,0) a_A^0 a_B^1 a_C^0 + 0z(0,0,1) \times a_A^0 a_B^0 a_C^1 + 1z(1,0,0) a_A^1 a_B^0 a_C^0 + \sum_h \sum_j \sum_i i z(i,j,h) \times a_A^i a_B^j a_C^h}{z(0,0,0) a_A^0 a_B^0 a_C^0 + z(1,0,0) a_A^1 a_B^0 a_C^0 + z(0,1,0) \times a_A^0 a_B^1 a_C^0 + z(0,0,1) a_A^0 a_B^0 a_C^1 + \sum_h \sum_j \sum_i z(i,j,h) \times a_A^i a_B^j a_C^h}$$

with a added constraint  $i+j+h \geq 2$

Equations (5.41) to (5.44) with above equation gives

$$C_A = \frac{\alpha_A p_A + \sum_h \sum_j \sum_i i Z(i, j, h) a_A^i a_B^j a_C^h}{1 + \alpha_A p_A + \alpha_B p_B + \alpha_C p_C + \sum_h \sum_j \sum_i Z(i, j, h) a_A^i a_B^j a_C^h}$$

Substitution of equation (5.40) in above equation gives

$$C_A = \frac{\alpha_A p_A + \sum_h \sum_j \sum_i \frac{Z(1, 0, 0)^i a_A^i Z(0, 1, 0)^j a_B^j Z(0, 0, 1)^h a_C^h}{(i-1)! j! h!} \times (1 - \frac{i\beta_A}{v} - \frac{j\beta_B}{v} - \frac{h\beta_C}{v})^{i+j+h} \exp(\frac{i\beta_A \varepsilon_A + j\beta_B \varepsilon_B + h\beta_C \varepsilon_C}{v k T})}{1 + \alpha_A p_A + \alpha_B p_B + \alpha_C p_C + \sum_h \sum_j \sum_i \frac{Z(1, 0, 0)^i a_A^i Z(0, 1, 0)^j a_B^j Z(0, 0, 1)^h a_C^h}{i! j! h!} \times (1 - \frac{i\beta_A}{v} - \frac{j\beta_B}{v} - \frac{h\beta_C}{v})^{i+j+h} \exp(\frac{i\beta_A \varepsilon_A + j\beta_B \varepsilon_B + h\beta_C \varepsilon_C}{v k T})}$$

Equations (5.42) to (5.44) with above equation gives

$$C_A = \frac{\alpha_A p_A + \sum_h \sum_j \sum_i \frac{(\alpha_A p_A)^i (\alpha_B p_B)^j (\alpha_C p_C)^h}{(i-1)! j! h!} \times (1 - \frac{i\beta_A}{v} - \frac{j\beta_B}{v} - \frac{h\beta_C}{v})^{i+j+h} \exp(\frac{i\beta_A \varepsilon_A + j\beta_B \varepsilon_B + h\beta_C \varepsilon_C}{v k T})}{1 + \alpha_A p_A + \alpha_B p_B + \alpha_C p_C + \sum_h \sum_j \sum_i \frac{(\alpha_A p_A)^i (\alpha_B p_B)^j (\alpha_C p_C)^h}{i! j! h!} \times (1 - \frac{i\beta_A}{v} - \frac{j\beta_B}{v} - \frac{h\beta_C}{v})^{i+j+h} \exp(\frac{i\beta_A \varepsilon_A + j\beta_B \varepsilon_B + h\beta_C \varepsilon_C}{v k T})}$$

(5.45)

With constraints  $i+j+h \geq 2$  and  $i\beta_A + j\beta_B + h\beta_C \leq v$ .

Equation (5.45) gives the molecules of component A adsorbed per cavity of zeolite. Similar expressions for components B and C can be derived and are

$$c_B = \frac{\alpha_A p_A + \sum_h \sum_j \sum_i \frac{(\alpha_A p_A)^i (\alpha_B p_B)^j (\alpha_C p_C)^h}{i! (j-1)! h!} x}{1 + \alpha_A p_A + \alpha_B p_B + \alpha_C p_C + \sum_h \sum_j \sum_i \frac{(\alpha_A p_A)^i (\alpha_B p_B)^j (\alpha_C p_C)^h}{i! j! h!} x} \\ \cdot \frac{(1 - \frac{i\beta_A}{v} - \frac{j\beta_B}{v} - \frac{h\beta_C}{v})^{i+j+h} \exp(\frac{i\beta_A \varepsilon_A + j\beta_B \varepsilon_B + h\beta_C \varepsilon_C}{v k T})}{(1 - \frac{i\beta_A}{v} - \frac{j\beta_B}{v} - \frac{h\beta_C}{v})^{i+j+h} \exp(\frac{i\beta_A \varepsilon_A + j\beta_B \varepsilon_B + h\beta_C \varepsilon_C}{v k T})} \quad (5.46)$$

$$c_C = \frac{\alpha_C p_C + \sum_h \sum_j \sum_i \frac{(\alpha_A p_A)^i (\alpha_B p_B)^j (\alpha_C p_C)^h}{i! j! (h-1)!} (1 - \frac{i\beta_A}{v} - \frac{j\beta_B}{v} - \frac{h\beta_C}{v})^{i+j+h} x}{1 + \alpha_A p_A + \alpha_B p_B + \alpha_C p_C + \sum_h \sum_j \sum_i \frac{(\alpha_A p_A)^i (\alpha_B p_B)^j (\alpha_C p_C)^h}{i! j! h!} x} \\ \cdot \frac{\exp(\frac{i\beta_A \varepsilon_A + j\beta_B \varepsilon_B + h\beta_C \varepsilon_C}{v k T})}{(1 - \frac{i\beta_A}{v} - \frac{j\beta_B}{v} - \frac{h\beta_C}{v})^{i+j+h} \exp(\frac{i\beta_A \varepsilon_A + j\beta_B \varepsilon_B + h\beta_C \varepsilon_C}{v k T})} \quad (5.47)$$

with constraints

$$i\beta_A + j\beta_B + h\beta_C \leq v \quad (5.48)$$

$$i+j+h \geq 2 \quad (5.49)$$

Equations (5.45) to (5.47) along with the constraints (5.48) and (5.49) predict the value of molecules adsorbed per cavity for components A, B and C respectively in a ternary system. When the exponential term representing sorbate-sorbate attraction is neglected, the above equations reduce to

$$c_A = \frac{\alpha_A p_A + \sum_h \sum_j \sum_i \frac{(\alpha_A p_A)^i (\alpha_B p_B)^j (\alpha_C p_C)^h}{(i-1)! j! h!} (1 - \frac{i\beta_A}{v} - \frac{j\beta_B}{v} - \frac{h\beta_C}{v})^{i+j+h}}{1 + \alpha_A p_A + \alpha_B p_B + \alpha_C p_C + \sum_h \sum_j \sum_i \frac{(\alpha_A p_A)^i (\alpha_B p_B)^j (\alpha_C p_C)^h}{i! j! h!} \times (1 - \frac{i\beta_A}{v} - \frac{j\beta_B}{v} - \frac{h\beta_C}{v})^{i+j+h}} \quad (5.50)$$

$$c_B = \frac{\alpha_B p_B + \sum_h \sum_j \sum_i \frac{(\alpha_A p_A)^i (\alpha_B p_B)^j (\alpha_C p_C)^h}{i! (j-1)! h!} (1 - \frac{i\beta_A}{v} - \frac{j\beta_B}{v} - \frac{h\beta_C}{v})^{i+j+h}}{1 + \alpha_A p_A + \alpha_B p_B + \alpha_C p_C + \sum_h \sum_j \sum_i \frac{(\alpha_A p_A)^i (\alpha_B p_B)^j (\alpha_C p_C)^h}{i! j! h!} \times (1 - \frac{i\beta_A}{v} - \frac{j\beta_B}{v} - \frac{h\beta_C}{v})^{i+j+h}} \quad (5.51)$$

$$c_C = \frac{\alpha_C p_C + \sum_h \sum_j \sum_i \frac{(\alpha_A p_A)^i (\alpha_B p_B)^j (\alpha_C p_C)^h}{i! j! (h-1)!} (1 - \frac{i\beta_A}{v} - \frac{j\beta_B}{v} - \frac{h\beta_C}{v})^{i+j+h}}{1 + \alpha_A p_A + \alpha_B p_B + \alpha_C p_C + \sum_h \sum_j \sum_i \frac{(\alpha_A p_A)^i (\alpha_B p_B)^j (\alpha_C p_C)^h}{i! j! h!} \times (1 - \frac{i\beta_A}{v} - \frac{j\beta_B}{v} - \frac{h\beta_C}{v})^{i+j+h}} \quad (5.52)$$

Using Raoult's law to calculate the partial pressures, one gets

$$\alpha_A^{P_A x_A} + \sum_h \sum_j \sum_i \frac{(\alpha_A^{P_A x_A})^i (\alpha_B^{P_B x_B})^j (\alpha_C^{P_C x_C})^h}{(i-1)! j! h!} \times$$

$$(1 - \frac{i\beta_A}{v} - \frac{j\beta_B}{v} - \frac{h\beta_C}{v})^{i+j+h}$$

$$C_A = \frac{\alpha_A^{P_A x_A} + \sum_h \sum_j \sum_i \frac{(\alpha_A^{P_A x_A})^i (\alpha_B^{P_B x_B})^j (\alpha_C^{P_C x_C})^h}{i! j! h!} \times}{1 + \alpha_A^{P_A x_A} + \alpha_B^{P_B x_B} + \alpha_C^{P_C x_C} + \sum_h \sum_j \sum_i \frac{(\alpha_A^{P_A x_A})^i (\alpha_B^{P_B x_B})^j (\alpha_C^{P_C x_C})^h}{i! j! h!} \times (1 - \frac{i\beta_A}{v} - \frac{j\beta_B}{v} - \frac{h\beta_C}{v})^{i+j+h}} \quad (5.53)$$

$$\alpha_B^{P_B x_B} + \sum_h \sum_j \sum_i \frac{(\alpha_A^{P_A x_A})^i (\alpha_B^{P_B x_B})^j (\alpha_C^{P_C x_C})^h}{i! (j-1)! h!} \times$$

$$(1 - \frac{i\beta_A}{v} - \frac{j\beta_B}{v} - \frac{h\beta_C}{v})^{i+j+h}$$

$$C_B = \frac{\alpha_B^{P_B x_B} + \sum_h \sum_j \sum_i \frac{(\alpha_A^{P_A x_A})^i (\alpha_B^{P_B x_B})^j (\alpha_C^{P_C x_C})^h}{i! j! h!} \times}{1 + \alpha_A^{P_A x_A} + \alpha_B^{P_B x_B} + \alpha_C^{P_C x_C} + \sum_h \sum_j \sum_i \frac{(\alpha_A^{P_A x_A})^i (\alpha_B^{P_B x_B})^j (\alpha_C^{P_C x_C})^h}{i! j! h!} \times (1 - \frac{i\beta_A}{v} - \frac{j\beta_B}{v} - \frac{h\beta_C}{v})^{i+j+h}} \quad (5.54)$$

$$\alpha_C^{P_C x_C} + \sum_h \sum_j \sum_i \frac{(\alpha_A^{P_A x_A})^i (\alpha_B^{P_B x_B})^j (\alpha_C^{P_C x_C})^h}{i! j! (h-1)!} \times$$

$$(1 - \frac{i\beta_A}{v} - \frac{j\beta_B}{v} - \frac{h\beta_C}{v})^{i+j+h}$$

$$C_C = \frac{\alpha_C^{P_C x_C} + \sum_h \sum_j \sum_i \frac{(\alpha_A^{P_A x_A})^i (\alpha_B^{P_B x_B})^j (\alpha_C^{P_C x_C})^h}{i! j! h!} \times}{1 + \alpha_A^{P_A x_A} + \alpha_B^{P_B x_B} + \alpha_C^{P_C x_C} + \sum_h \sum_j \sum_i \frac{(\alpha_A^{P_A x_A})^i (\alpha_B^{P_B x_B})^j (\alpha_C^{P_C x_C})^h}{i! j! h!} \times (1 - \frac{i\beta_A}{v} - \frac{j\beta_B}{v} - \frac{h\beta_C}{v})^{i+j+h}} \quad (5.55)$$

where  $x_A$ ,  $x_B$  and  $x_C$  are mole fractions of A, B and C in liquid phase and  $P_A$ ,  $P_B$  and  $P_C$  are vapor pressures of components A, B and C respectively. Equations (5.53), (5.54)

and 5.55 along with the constraints (5.48) and (5.49) were used to calculate average number of molecules adsorbed per cavity of components A, B and C respectively.  $\alpha_A$ ,  $\beta_A$ ,  $\alpha_B$ ,  $\beta_B$ ,  $\alpha_C$  and  $\beta_C$  used in these equations were obtained from isotherms of pure components.

## 5.5 RESULTS AND DISCUSSION:

### 5.5.1 Adsorption of Pure Hydrocarbons:

The equation derived from the model for isotherms of pure component (Eq. (5.9)) has two parameters  $\alpha$  and  $\beta$ .  $\alpha$  can be calculated from the slope of the adsorption isotherm at very low concentrations. The nature of the isotherms (Figures 3. 3 to 3.6) did not permit direct measurement of the slope, because of experimental limitations of finding equilibrium loadings at very low concentrations. It was also observed that, for the n-paraffins studied, equation (5.9) is very sensitive to  $\beta$ , the molecular volume of the adsorbate. The approximation of its value by van der Waals co-volume, as suggested by Dubinin and used by Ruthven and coworkers [14-18]. was found to be unsatisfactory for the systems investigated. Thus it is observed that a more accurate determination of the values of the parameters  $\alpha$  and  $\beta$  is required to predict the adsorption isotherms for the hydrocarbons studied. However, in the absence of better prediction procedures for  $\alpha$  and  $\beta$ , it was decided to obtain these using the experimental

data. Thus, it has been implicitly assumed that our two parameter model is valid for pure hydrocarbon adsorption. Experimental isotherms (Data are taken from A3.3 to A3.6) were matched with the model by a least square minimization procedure, using Blind search Technique to evaluate  $\alpha$  and  $\beta$ . An objective function  $E$  is defined as

$$E = \left[ \sum_{i=1}^n (c_{\text{Cal}} - c_{\text{Expt}})^2 \right]$$

where,  $n$  = number of data points

$c_{\text{Cal}}$  = calculated value of molecules adsorbed per cavity from Eq. (5.9)

$c_{\text{Expt}}$  = experimental value of molecules adsorbed per cavity

$E$  is then minimized over a wide range of the values of parameters  $\alpha$  and  $\beta$  to give minimum value,  $E_{\text{min}}$ , of the objective function.

$$E_{\text{Min}} = \underset{\alpha, \beta}{\text{Min}} \left[ \sum_{i=1}^n (c_{\text{Cal}} - c_{\text{Expt}})^2 \right]$$

The values of  $\alpha$  and  $\beta$  corresponding to  $E_{\text{min}}$  were then taken to represent the best values of these parameters for a given paraffin at a fixed temperature. Figure 5.1 shows typical predicted adsorption isotherms using calculated values of  $\alpha$  and  $\beta$  along with experimentally observed data points at 18°C. Similar plots were obtained at other temperatures also but have not been included here. This

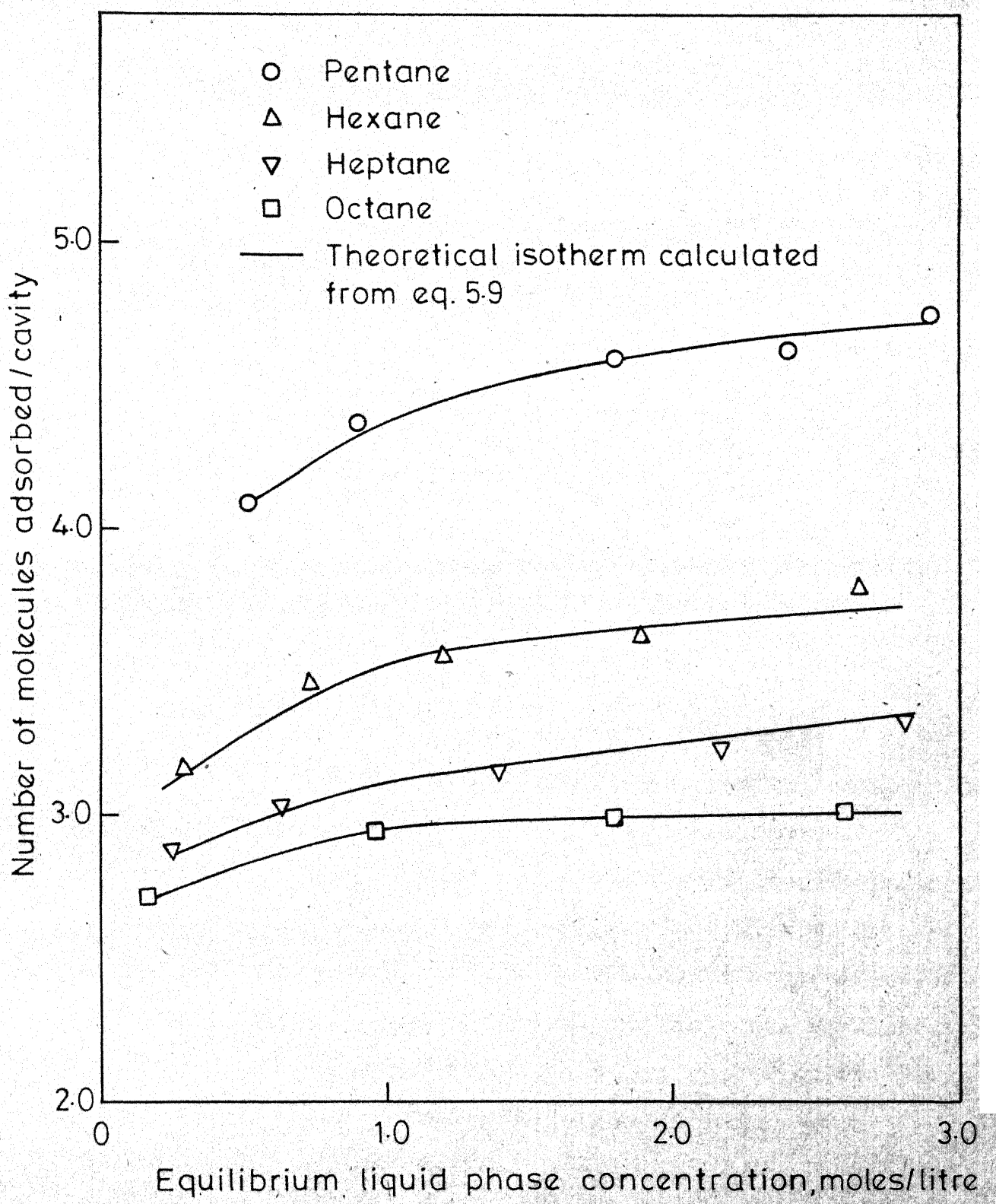


Fig. 5.1 - Comparison between predicted and experimental isotherms at 18°C.

should not be taken as a validation of the model because the prediction is not totally independent of experimental data, rather, it makes use of the latter to calculate the former. The comparison has been made to merely show that the two parameter model is able to represent the experimental data fairly well. As will be seen later, the validation of the pure component model comes from the fact that, for most of the systems **studied**, the predictions made using this model for binary and ternary systems match within 10 per cent of the experimentally observed values.

The values of  $\alpha$  and  $\beta$  along with the minimum error, for all the paraffins studied, at different temperatures are given in Table 5.1.  $\alpha$  was found to decrease with an increase in temperature which means that adsorption decreases with increasing temperature. It was also observed that  $\alpha$  increased with the molecular weight of paraffin. The molecular volume of the adsorbate, as expected, increased with temperature and was higher, at a particular temperature, for higher molecular weight paraffin. The internal consistency in calculated values of  $\alpha$  and  $\beta$  further justifies the way they were obtained. Figure 5.2 shows Arrhenius plots for all the hydrocarbons studied.

TABLE 5.1: VALUES OF  $\alpha$  AND  $\beta$  AT DIFFERENT TEMPERATURES

Paraffin	Temperature, °C	$\alpha$ , (molecules)/(cavity)(torr)	$\beta$ , $\text{Å}^3$	$E_{\min}$
n-pentane	6	4.50	94.50	0.0521
	18	3.96	116.55	0.0487
	30	1.86	129.50	0.0072
n-hexane	6	64.05	136.50	0.0121
	18	50.92	165.71	0.0241
	30	46.03	179.88	0.0465
n-heptane	42	22.46	183.79	0.0333
	6	365.54	166.19	0.0227
	18	222.43	179.31	0.0199
n-octane	30	101.44	183.96	0.0488
	42	36.14	184.99	0.0877
	6	3079.89	181.92	0.0019
n- <sup>13</sup> C	18	824.36	187.41	0.0002
	30	485.90	215.00	0.0063
	42	247.75	225.10	0.0207

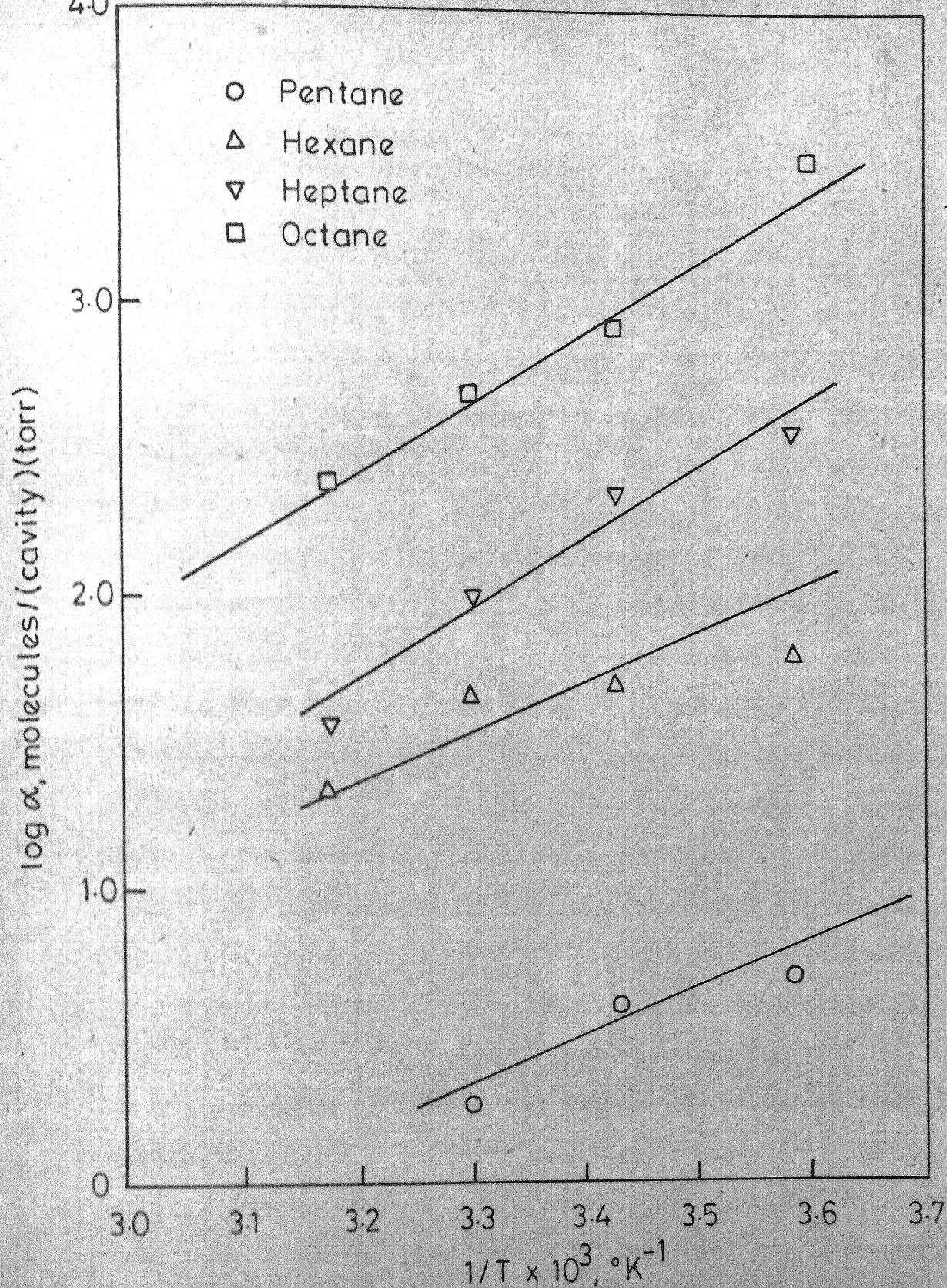


Fig 5.2 -Arrhenius plot for  $\alpha$ .

### 5.5.2 Adsorption of Binary Systems:

Equations (5.31) and (5.32) along with constraints (5.11) and (5.24) were used to predict values of  $C_A$  and  $C_B$ , for all the binary systems studied, using appropriate values of  $\alpha$  and  $\beta$  obtained for pure components. Tables 5.2 to 5.5 (operating data are given in A4.1 to A4.4) give the results of all the systems at  $6^\circ$ ,  $18^\circ$ ,  $30^\circ$  and  $42^\circ\text{C}$  respectively. In general errors are less than 10 per cent, for more than 90 per cent of a total of 136 predictions made. At  $6^\circ\text{C}$ , the maximum error of 10.8 per cent is observed in the case of pentane-hexane system, all others out of a total of 40 predictions showing less than 10 per cent error. At  $18^\circ\text{C}$ , the maximum error of 12.4 per cent is also observed for the pentane-hexane system. There are 3 other predicted values which are more than 10 per cent higher than the experimental values at this temperature. The difference in predicted and experimental value of molecules adsorbed per cavity increases upto about 14 per cent, at  $30^\circ\text{C}$ , for systems having pentane as one component. This large error in case of pentane at  $30^\circ\text{C}$  may be attributed to larger thermal motions of pentane molecules adsorbed at this temperature which is close to its boiling point. Due to these motions some of the adsorbed pentane may come out of the zeolite cavity resulting in smaller loading than predicted. The proposed model does not account for any such desorption and hence predicts higher adsorption than

TABLE 5.2: COMPARISON OF EXPERIMENTAL AND PREDICTED VALUES FOR BINARY SYSTEMS AT 6 °C

Run	Equilibrium composition in liquid phase, mole fraction	Molecules adsorbed per cavity				Per cent, Error 1			
		Experimental		Predicted					
1	2	1	2	1	2				
BPX-1	0.321	0.052	4.75	1.36	4.88	1.32	2.7	2.0	2.5
BPX-2	0.213	0.115	3.20	2.01	3.44	2.00	7.3	0.3	0.3
BPX-3	0.134	0.201	1.96	2.98	2.17	2.95	10.8	1.0	1.0
BPX-4	0.052	0.290	1.51	3.90	1.55	3.88	1.7	0.5	0.5
BXH-1	0.063	0.284	1.36	2.91	1.41	2.95	3.6	1.4	1.4
BXH-2	0.138	0.214	2.02	2.13	2.06	2.17	1.9	2.0	2.0
BXH-3	0.206	0.144	2.75	1.59	2.81	1.64	2.0	3.3	3.3
BXH-4	0.285	0.062	3.69	1.18	3.78	1.21	2.3	3.4	3.4
BHO-1	0.055	0.278	1.17	2.89	1.25	2.92	6.7	1.1	1.1
BHO-2	0.127	0.198	1.61	2.24	1.69	2.30	5.4	2.7	2.7
BHO-3	0.208	0.122	2.31	1.61	2.35	1.70	1.6	5.7	5.7
BHO-4	0.280	0.053	3.04	1.20	3.11	1.27	2.2	6.1	6.1

Table 5.2 (contd)

Run	Equilibrium composition in liquid phase, mole fraction	Molecules adsorbed per cavity			Per cent, Error	
		Experimental	Predicted		1	2
	1	2		1	2	
BPH-1	0.302	0.042	5.00	1.13	5.14	1.16
BPH-2	0.237	0.094	3.92	1.47	4.15	1.45
BPH-3	0.157	0.164	2.62	2.11	2.85	2.04
BPH-4	0.065	0.263	1.44	3.10	1.57	3.05
—	—	—	—	—	—	—
BPO-1	0.054	0.275	1.20	2.94	1.28	2.93
BPO-2	0.141	0.203	2.05	3.22	2.17	3.29
BPO-3	0.219	0.117	3.27	1.59	3.44	1.65
BPO-4	0.314	0.052	4.77	1.11	4.85	1.21

Note: 1 represents the lighter hydrocarbon in a given binary mixture and 2 represents the remaining component.

BPX= Pentane-hexane  
 BXH= hexane-heptane  
 BHO= heptane-octane  
 BPH= pentane-heptane  
 BPO= pentane-octane

TABLE 5.3: COMPARISON OF EXPERIMENTAL AND PREDICTED VALUES FOR BINARY SYSTEMS AT 18°C

Run	Equilibrium composition in liquid phase, mole fraction	Molecules adsorbed per cavity				Per cent, Error 1/2			
		Experimental		Predicted					
1	2	1	2	1	2				
BPX-5	0.327	0.052	*	4.05	1.07	4.17	1.20	3.0	12.4
BPX-6	0.231	0.119	*	3.04	1.55	3.14	1.64	3.2	5.4
BPX-7	0.152	0.203	*	1.99	2.23	2.11	2.32	6.2	4.2
BPX-8	0.064	0.288	*	1.22	3.10	1.36	3.19	11.6	2.9
BXH-5	0.064	0.279	*	1.26	2.00	1.39	2.10	10.4	5.1
BXH-6	0.146	0.201	*	1.84	1.90	2.01	1.98	9.1	4.1
BXH-7	0.219	0.130	*	2.51	1.46	2.63	1.52	4.7	4.4
BXH-8	0.302	0.061	*	3.14	1.13	3.29	1.20	4.9	6.4
BHO-5	0.052	0.248	*	1.16	2.49	1.23	2.52	6.4	1.2
BHO-6	0.114	0.166	*	1.57	1.85	1.65	1.93	5.3	4.0
BHO-7	0.178	0.108	*	2.03	1.42	2.17	1.50	6.8	5.6
BHO-8	0.264	0.045	*	2.82	1.08	2.89	1.16	2.3	7.2

Table 5.3 (contd)

Run	Equilibrium composition in liquid phase, mole fraction		Molecules adsorbed per cavity		Per cent, Error 1 2
	1	2	Experimental 1	Predicted 2	
BPH-5	0.320	0.045	4.13	4.29	1.14
BPH-6	0.243	0.098	3.39	3.45	1.42
BPH-7	0.177	0.168	2.36	1.82	2.51
BPH-8	0.070	0.264	1.29	2.63	1.42
BPO-5	0.067	0.249	1.36	2.54	1.48
BPO-6	0.156	0.170	2.25	1.81	2.38
BPO-7	0.237	0.114	3.10	1.35	3.32
BPO-8	0.327	0.045	4.26	1.05	4.33

Note: Notations are same as used in Table 5.2

TABLE 5.4:

COMPARISON OF EXPERIMENTAL AND PREDICTED VALUES FOR BINARY SYSTEMS AT 30°C

Run	Equilibrium composition in liquid phase, mole fraction	Molecules adsorbed per cavity				Per cent, Error		
		Experimental	Predicted	1	2			
	1	2	1	2	1	2		
BPX-9	0.074	0.288	1.04	2.80	1.19	3.06	14.4	9.3
BPX-10	0.170	0.205	1.42	2.39	1.56	2.54	9.9	6.7
BPX-11	0.247	0.123	1.88	1.92	2.09	2.04	10.9	6.0
BPX-12	0.335	0.052	2.96	1.34	3.13	1.44	5.6	7.6
BXH-9	0.317	0.050	3.04	1.04	3.14	1.10	3.1	6.0
BXH-10	0.251	0.135	2.54	1.24	2.62	1.32	3.1	5.9
BXH-11	0.155	0.189	1.98	1.55	2.07	1.62	4.2	4.5
BXH-12	0.064	0.274	1.33	2.20	1.41	2.30	6.2	4.4
BHO-9	0.049	0.280	1.12	2.36	1.20	2.41	7.1	2.2
BHO-10	0.104	0.197	1.43	1.81	1.52	1.88	6.4	3.8
BHO-11	0.180	0.119	1.93	3.53	2.06	1.42	6.5	5.1
BHO-12	0.270	0.050	2.55	1.06	2.68	1.14	5.2	7.1

Table 5.4 (contd)

Run	Equilibrium composition in liquid phase, mole fraction		Molecules adsorbed per cavity		Per cent, error 1/2
	1	2	Experimental 1	Predicted 2	
BPH-9	0.339	0.047	3.38	1.16	3.58 1.24 6.2 7.1
BPH-10	0.268	0.102	2.67	1.49	2.75 1.58 2.8 5.9
BPH-11	0.197	0.171	1.89	1.88	2.06 2.00 8.8 6.1
BPH-12	0.075	0.265	1.20	2.56	1.35 2.70 12.5 5.2
BP0-9	0.071	0.279	1.26	2.39	1.44 2.47 13.8 3.2
BP0-10	0.173	0.200	1.96	1.67	2.17 1.78 10.5 6.2
BP0-11	0.254	0.120	2.73	1.29	2.91 1.37 6.6 6.4
BP0-12	0.330	0.051	3.75	1.05	3.73 1.13 0.4 7.4

Note: Notations are same as used in Table 5.2

TABLE 5.5: COMPARISON OF EXPERIMENTAL AND PREDICTED VALUES FOR BINARY SYSTEMS AT 42°C

Run	Equilibrium composition in liquid phase, mole fraction	Molecules adsorbed per cavity				Per cent, Error
		Experimental		Predicted		
1	2	1	2	1	2	1
BXH-13	0.063	0.271	1.22	2.01	1.39	13.5
BXH-14	0.148	0.193	1.80	1.44	2.01	11.4
BXH-15	0.236	0.120	2.32	1.14	2.52	1.24
BXH-16	0.308	0.050	2.69	0.98	2.92	1.08
BHO-13	0.050	0.275	1.10	2.25	1.20	2.35
BHO-14	0.120	0.224	1.40	1.78	1.50	1.86
BHO-15	0.190	0.120	1.90	1.34	2.01	1.41
BHO-16	0.271	0.050	2.49	1.06	2.58	1.14

Note: Notations are same as used in Table 5.2

that actually taking place. At  $42^{\circ}\text{C}$ , maximum error is found in hexane-heptane system which is 13.5 per cent, for hexane. This can also be justified with the same reasoning as for pentane.

### 5.5.3 Adsorption of Ternary Systems:

Equations (5.53) to (5.55) along with constraints (5.48) and (5.49) were used to predict values of  $C_A$ ,  $C_B$  and  $C_C$ , for all the ternary systems studied, using appropriate values of  $\alpha$  and  $\beta$  obtained for pure components. Tables 5.6 to 5.8 (Operating conditions are taken from Appendices A4.5 to A4.7) give the results of all the ternary systems studied at  $6^{\circ}$ ,  $18^{\circ}$  and  $30^{\circ}\text{C}$  respectively. Since pentane was present in all the systems, temperatures higher than  $30^{\circ}\text{C}$  were not studied. It has been observed that for about 85 per cent of a total of 120 predictions made, errors are less than 10 per cent. At  $6^{\circ}\text{C}$ , maximum error is 14 per cent and there are two more predictions for which errors are more than 10 per cent. At  $18^{\circ}\text{C}$ , there are 5 predicted values which are more than 10 per cent higher than the experimental values. Errors increase upto 18.5 per cent, at  $30^{\circ}\text{C}$ . There are 11 more predictions at this temperature for which the error is more than 10 per cent. At  $30^{\circ}\text{C}$ , 25 per cent of the predicted values are 10 per cent higher than the experimentally observed values. This does not mean that the ternary

TABLE 5.6: COMPARISON OF EXPERIMENTAL AND PREDICTED VALUES FOR TERNARY SYSTEMS AT 60°C

Run	Equilibrium composition in liquid phase, mole fraction			Molecules adsorbed per cavity			Per cent. Error					
	1	2	3	Experimental	1	2	3	1	2	3		
PXH-1	0.235	0.047	0.083	3.29	1.26	1.29	3.68	1.32	1.31	11.9	4.6	1.6
PXH-2	0.082	0.174	0.089	1.45	2.46	1.30	1.66	2.60	1.33	14.1	5.5	2.3
PXH-3	0.053	0.139	0.165	1.20	2.02	1.72	1.32	2.15	1.76	9.9	6.7	2.4
PXH-4	0.134	0.087	0.141	1.99	1.61	1.60	2.27	1.66	1.61	14.0	3.0	1.0
PXO-1	0.207	0.046	0.045	3.49	1.27	1.15	3.62	1.37	1.24	3.7	8.5	7.6
PXO-2	0.082	0.149	0.045	1.67	2.50	1.14	1.76	2.59	1.25	5.6	3.4	9.6
PXO-3	0.052	0.132	0.086	1.35	2.26	1.47	1.44	2.31	1.54	7.0	2.3	5.0
PXO-4	0.124	0.088	0.088	2.11	1.64	1.44	2.22	1.74	1.50	5.1	6.0	4.1
PHO-1	0.223	0.056	0.050	3.60	1.16	1.19	3.75	1.23	1.25	4.2	5.7	5.2
PHO-2	0.082	0.086	0.086	1.66	1.44	1.62	1.80	1.53	1.70	8.5	5.9	4.5
PHO-3	0.017	0.162	0.045	1.32	2.17	1.23	1.45	2.31	1.32	9.7	6.5	7.7
PHO-4	0.055	0.130	0.075	1.35	1.83	1.51	1.46	1.91	1.57	8.3	4.2	3.7

Note: 1 is the lightest hydrocarbon in a given ternary system and 3 is the heaviest hydrocarbon.

PXH = Pentane-Hexane-Heptane; PXO = Pentane-hexane-Octane; PHO = Pentane-Heptane-Octane

TABLE 5.7: COMPARISON OF EXPERIMENTAL AND PREDICTED VALUES FOR TERNARY SYSTEMS AT 18°C

Run	Equilibrium composition in liquid phase, mole fraction			Molecules adsorbed per cavity						Per cent, Error	
				Experimental			Predicted				
	1	2	3	1	2	3	1	2	3		
PXH-5	0.114	0.051	0.165	1.66	1.17	1.86	1.80	1.27	1.90	8.4	
PXH-6	0.119	0.123	0.108	1.62	1.60	1.37	1.79	1.72	1.46	10.3	
PXH-7	0.216	0.121	0.028	1.74	1.54	0.99	2.85	1.63	1.09	3.9	
PXH-8	0.129	0.168	0.029	1.85	2.04	0.98	1.96	2.17	1.11	5.8	
PXO-5	0.045	0.048	0.170	1.22	1.23	1.96	1.33	1.34	2.10	9.1	
PXO-6	0.221	0.073	0.023	3.15	1.31	1.03	3.29	1.41	1.08	4.3	
PXO-7	0.114	0.144	0.040	1.80	2.04	1.07	1.89	2.09	1.15	4.9	
PXO-8	0.056	0.153	0.089	1.21	2.07	1.29	1.34	2.19	1.36	10.2	
PHO-5	0.101	0.042	0.143	1.70	1.09	1.73	1.86	1.21	1.83	9.3	
PHO-6	0.216	0.044	0.025	3.42	1.11	1.01	3.60	1.21	1.10	5.2	
PHO-7	0.063	0.103	0.092	1.33	1.58	1.38	1.51	1.67	1.50	13.4	
PHO-8	0.166	0.099	0.036	2.47	1.46	1.06	2.62	1.54	1.15	6.2	

Note: Notations are same as used in Table 5.6

TABLE 5.8: COMPARISON OF EXPERIMENTAL AND PREDICTED VALUES FOR TERNARY SYSTEMS AT 30°C

Run	Equilibrium composition in liquid phase, mole fraction	Molecules adsorbed per cavity						Per cent, Error 1 2 3				
		Experimental			Predicted							
		1	2	3	1	2	3					
PXH-9	0.077	0.221	0.044	1.04	2.54	1.04	1.23	2.67	1.11	18.5	5.2	6.4
PXH-10	0.259	0.055	0.042	2.28	1.32	1.12	2.49	1.46	1.17	9.1	10.6	4.8
PXH-11	0.184	0.135	0.046	1.54	1.90	1.08	1.72	2.04	1.14	11.8	7.4	5.7
PXH-12	0.170	0.056	0.103	1.67	1.30	1.42	1.85	1.45	1.47	10.8	11.3	3.6
PXE-13	0.072	0.144	0.115	1.09	1.96	1.30	1.25	2.09	1.38	14.9	6.4	5.9
PXE-14	0.123	0.037	0.181	1.43	1.16	1.80	1.57	1.26	1.93	9.7	8.5	7.1
PXH-15	0.142	0.111	0.083	1.44	1.78	1.24	1.58	1.88	1.30	9.8	5.6	4.4
PXH-16	0.150	0.138	0.103	1.38	1.86	1.23	1.52	1.93	1.31	9.7	7.3	6.0
---	---	---	---	---	---	---	---	---	---	---	---	---
FXO-9	0.071	0.216	0.050	1.06	2.62	0.99	1.24	2.74	1.08	16.8	4.4	8.3
FXO-10	0.165	0.113	0.045	1.62	1.96	0.97	1.79	2.06	1.08	10.1	5.0	11.0
FXO-11	0.254	0.041	0.049	2.59	1.30	1.02	2.71	1.38	1.11	4.8	6.2	8.2
FXO-12	0.168	0.044	0.099	1.90	1.36	1.25	2.11	1.44	1.28	10.9	6.1	2.3

Table 5.8 (contd)

Run	Equilibrium composition in liquid phase, mole fraction			Molecules adsorbed per cavity			Per cent. Error		
				Experimental			Predicted		
	1	2	3	1	2	3	1	2	3
PHO-9	0.070	0.045	0.185	1.30	1.16	1.87	1.49	1.24	1.92
PHO-10	0.160	0.101	0.055	1.91	1.56	1.09	2.08	1.65	1.15
PHO-11	0.168	0.046	0.114	2.01	1.18	1.30	2.20	1.26	1.38
PHO-12	0.270	0.039	0.054	2.84	1.08	1.05	3.02	1.20	1.13

Note: Notations are same as used in Table 5.6

adsorption model is not holding good. Many predicted values are more than 10 per cent only because all of the ternary systems studied had pentane as one of the component, for which thermal vibrations and hence errors are more at 30°C. From the comparison between predicted and experimental values for binary and ternary systems, it seems that maximum discrepancy lies in systems, at 30°C, having pentane as one of the components.

## REFERENCES

1. Arnold, J.R., J.Am.Chem.Soc., 71, 104 (1949).
2. Barrer, R.M., Lee, J.A., Surface Sci., 12, 354 (1968).
3. Barrer, R.M., Davies, J.A., Proc. Roy. Soc. A, 320, 289 (1970).
4. Brauer, P., Lopatkin, A.A., Stepanez, G.Ph., Adv. Chem., 102, 97 (1971).
5. Cook, W.H., Basmadjian, D., Can. J. Chem. Engng., 43, 78 (1965).
6. Grant, R.J., Manes, M., Ind. Engng. Chem. Fundls., 3, 221 (1964).
7. Hill, T.L., Introduction to Statistical Thermodynamics, Addison Wesley, Mass. 1960.
8. Kidney, A.J., Myers, A.L., A.I.Ch.E. J., 12, 981 (1966).
9. Kippling, J.J., Adsorption from Solutions of Non-Electrolytes Academic Press, Inc. London (1965).
10. Kiselev, A.V., Adv. Chem., 102, 37 (1971).
11. Lewis, W.K., Gilliland, E.R., Chertow, B., Cadogen, W.P., Ind. Engng. Chem. 42, 1319 (1950).
12. Malson, F.D., Altman, M., Alberth, E.R., Phys. Chem., 57, 106 (1953).
13. Myers, A.L., Prausnitz, J.M., A.I.Ch.E.J., 11, 121 (1965).
14. Ruthven, D.M., Nature Physical Science, 232 (29), 70 (1971).
15. Ruthven, D.M., Loughlin, K.F., J.C.S. Faraday Trans., 68, 696 (1972).

16. Ruthven, D.M., Loughlin, K.F., Derrah, R.I., *Advan. Chem.*, 121, 330 (1973).
17. Ruthven, D.M., Loughlin, K.F., Holborow, K.A., *Chem. Eng. Sci.*, 28, 701 (1973).
18. Ruthven, D.M., *A.I.Ch.E. J.*, 22 (4), 753 (1976).
19. Schirmer, W., Fiedrich, G., Grossman, A., Stach, H., *Ist Conf. Molecular Sieve Zeolites* (London, 1967); *Proceedings (Soc. Chem. Ind.)*, 1968, p.276.
20. Sircar, S., Myers, A.L., *Chem. Eng. Sci.*, 28, 489 (1973).

## CHAPTER 6

### CONCLUSIONS AND RECOMMENDATIONS

#### 6.1 CONCLUSIONS:

The following conclusions were made from this study:

1. An adsorption cell was developed and used for liquid phase adsorption studies on pure and multicomponent systems. Pure, binary and ternary systems of n-pentane, n-hexane, n-heptane and n-octane, with benzene as a diluent, were studied at 6, 18, 30 and 42°C.
2. In adsorption of single components, lower molecular weight paraffins were preferentially adsorbed. For all the paraffins studied, adsorption decreased with increase in temperature; the decrease was largest for the lightest component.

3. Up to 18°C, for all the binary systems studied, temperature had no effect on the equilibrium adsorption. At 30°C, there was a decrease in adsorption of pentane for all the systems containing it as one of the components. For the systems studied this decrease was highest for pentane-hexane system and the lowest for pentane-octane system. Because of benzene as a diluent, conventional separation factor was found to be concentration dependent. The separation factor was redefined to make it independent of

concentration. Except for binary systems at 30°C containing pentane, the redefined separation factor was independent of temperature. At 30°C it was found to decrease for pentane containing binaries, being the lowest for pentane-hexane system.

4. A two parameter statistical model was developed to represent pure component adsorption data. This model was then extended for binary and ternary systems and was validated by experimental data. Predictions by proposed model, for all the binary and ternary systems, were in good agreement with experimental adsorption data for temperatures upto 18°C. Errors were more for the systems containing pentane at 30°C.

#### 6.2 RECOMMENDATIONS:

The present study does not cover all the n-paraffins of industrial importance. It is, therefore, recommended to perform adsorption studies on the remaining paraffins present in petroleum fractions like naphtha, kerosene, etc. With complete data on pure systems one should be able to predict multicomponent equilibrium loadings necessary for the design of industrial separation systems. The proposed model, with no clues available for liquid phase adsorption, seems to be a reasonable first attempt. In this model

sorbate-sorbate attraction term has been neglected which may be critical near the boiling point of a component and hence for future it is recommended to take this into account also. Since in any petroleum fraction, there are more than three components present, it is, therefore, recommended to test the model for the systems with more components.

APPENDIX A3.1

## CALIBRATION OF GAS CHROMATOGRAPH

In the present study, for all the cases, benzene was used as a reference material. Standardization curves, for all the components, were obtained using known mixtures of paraffin in benzene. The peak areas were measured by a disc integrator attached to the recorder. The plot of peak area ratio of paraffin to benzene versus respective known weight ratio gave a linear standardization curve for each paraffin. A typical chromatogram is shown in Figure A3.1 and these calibration curves are shown in Figure A3.2.

Operating conditions for analysis were:

Chromatograph: Chromatography and Instruments Co.

Baroda, India

Carrier gas: Nitrogen

Flow rate: 25 ml/min

Column dimensions: 1/8 inch x 30 ft, S.S.

Packing: 20 per cent bentone on Chromosorb W

Column and detector temperature: 90°C

Bridge current: 100 mA

Detector: Thermal conductivity (Katharometer)

1. n-pentane
2. n-hexane
3. n-heptane
4. n-octane
5. Benzene

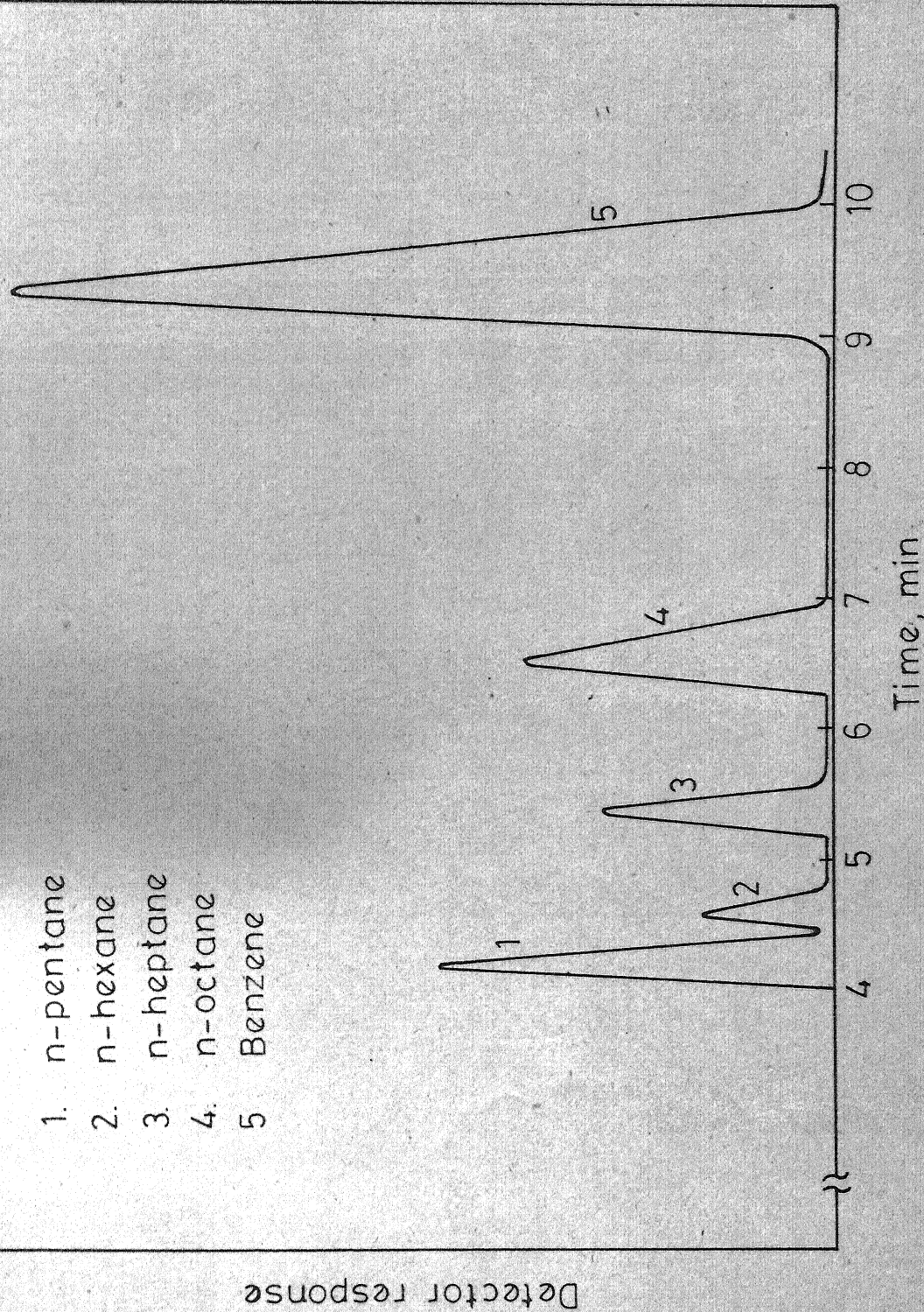


Fig.A3.1 - A typical chromatogram for n-paraffins-benzene mixture.

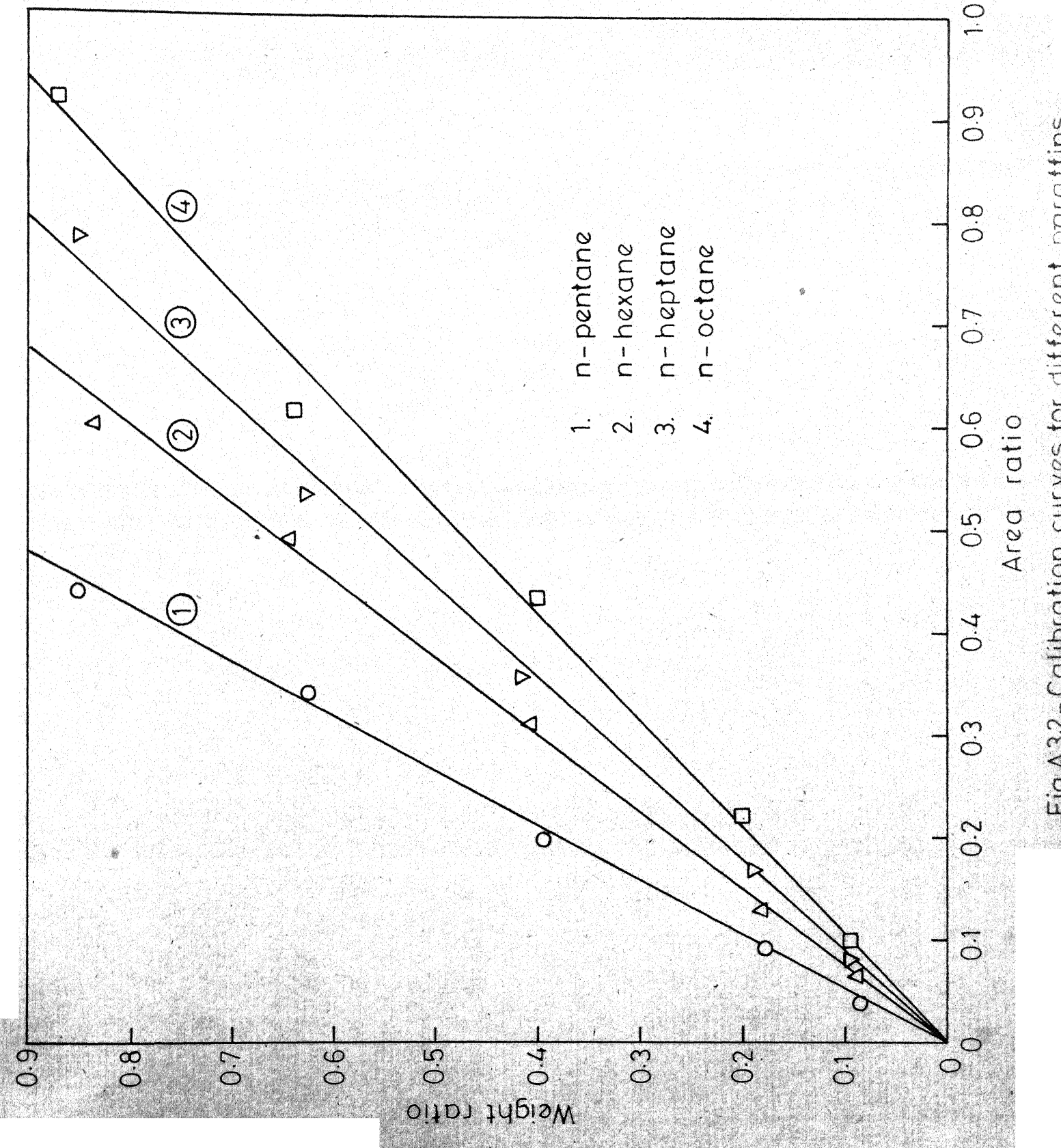


Fig A3.2 - Calibration curves for different paraffins

APPENDIX A3.2: EXPERIMENTAL RESULTS FOR BREAKTHROUGH  
CURVES OF n-HEPTANE

30°C42°C

Weight of adsorbent=30.1692 gms

Weight of adsorbent=30.2937 gms

Initial concentration = 4.05moles/  
litreInitial concentration = 2.35mol/  
litre

Time, min.	Amount adsorbed, gms/gm adsorbent	Time, min.	Amount adsorbed, gms/gm. adsorbent
5	0.081	5	0.072
13	0.114	16	0.121
30	0.117	33	0.127
40	0.120	65	0.129
60	0.119	110	0.133
105	0.122	180	0.133
165	0.122	250	0.134
205	0.123	310	0.137
340	0.125	500	0.138
425	0.124	860	0.140
555	0.123	1120	0.142
675	0.127	1560	0.140
880	0.124	1650	0.141
1370	0.125	2250	0.141
1900	0.126	2950	0.142
2740	0.123	4005	0.141
3860	0.125		

APPENDIX A3.3: EXPERIMENTAL RESULTS FOR PURE COMPONENTS AT 60°C

Run	Initial weight of parafin, gms.	Weight of benzene, gms.	Weight of adsorbent, gms.	Equilibrium composition in liquid phase, moles/litre	Amount adsorbed $\times 10^3$ , moles/gm. adsorbent
PCP-1	6.2266	34.6860	28.8314	0.613	2.11
PCP-2	7.9232	32.0250	30.5984	0.957	2.34
PCP-3	9.9353	29.4294	31.1904	1.571	2.41
PCP-4	11.5071	27.3132	30.0712	2.135	2.46
PCP-5	12.2716	26.0300	29.5984	2.359	2.60
PCP-6	14.7726	22.5500	30.8231	3.134	2.69
PCX-1	6.4389	34.6949	30.3089	0.531	1.74
PCX-2	8.9915	31.2825	30.0537	1.184	1.85
PCX-3	11.1530	27.6715	30.1619	1.808	1.88
PCX-4	12.4690	25.9012	30.2414	2.177	1.90
PCX-5	14.0024	24.1504	30.1572	2.562	1.98
PCX-6	15.5839	21.5524	30.1579	3.052	2.00

Appendix A3.3 (contd)

Run	Initial weight of paraffin, gms.	Weight of benzene, gms.	Weight of adsorbent, gms.	Equilibrium composition in liquid phase, moles/litre	Amount adsorbed $\times 10^3$ , moles/gm. adsorbent
PCH-1	5.9552	37.0112	30.0612	0.369	1.44
PCH-2	7.3584	34.6630	30.9299	0.612	1.53
PCH-3	9.6718	31.1180	30.0182	1.159	1.61
PCH-4	13.6947	25.9943	30.1776	2.093	1.65
PCH-5	15.5407	21.6310	30.1525	2.667	1.68
PCH-6	19.2762	23.1126	29.9446	3.040	1.77
—	—	—	—	—	—
PCO-1	4.7286	39.4436	29.4436	0.102	1.25
PCO-2	8.6003	35.0220	29.7638	0.757	1.40
PCO-3	13.3325	30.5282	29.8819	1.598	1.46
PCO-4	18.1627	26.1594	30.1518	2.408	1.48

Notes: PCP = Pentane ; PCX = hexane ; PCH = Heptane ; PCO = Octane

APPENDIX A3.4: EXPERIMENTAL RESULTS FOR PURE COMPONENTS AT 18°C

Run	Initial weight of paraffin, gms.	Weight of benzene, gms.	Weight of adsorbent, gms.	Equilibrium composition in liquid phase, moles/litre	Amount adsorbed x 10 <sup>3</sup> , moles/gm. adsorbent
PCP-7	5.5164	34.2741	30.1516	0.514	1.84
PCP-8	6.8696	32.1562	29.8920	0.897	1.97
PCP-9	9.7070	28.3424	29.8155	1.805	2.06
PCP-10	11.6121	26.1195	30.4224	2.396	2.08
PCP-11	13.0938	23.8120	30.0950	2.900	2.14
PCP-12	14.6541	21.5422	30.3362	3.381	2.26
PCX-7	4.8062	35.8121	30.2010	0.305	1.42
PCX-8	6.6721	33.3212	30.1327	0.738	1.55
PCX-9	8.4502	33.1627	29.7911	1.204	1.60
PCX-10	10.8467	27.0012	30.2712	1.888	1.63
PCX-11	13.6404	23.4124	30.1124	2.645	1.71
PCX-12	15.2694	21.4993	30.3313	3.056	1.77

Appendix A3.4 (contd)

Run	Initial weight of paraffin, gms.	Weight of benzene, gms.	Weight of adsorbent, gms.	Equilibrium composition in liquid phase, moles/litre	Amount adsorbed $\times 10^3$ , moles/gm. adsorbent
PCH-7	4.9563	37.8911	30.1224	0.240	1.29
PCH-8	6.8680	34.6521	30.0763	0.635	1.37
PCH-9	10.2145	29.7512	29.9427	-	1.42
PCH-10	13.7656	25.8162	30.2729	2.181	1.45
PCH-11	16.7123	22.6412	29.7539	2.813	1.49
PCH-12	19.4322	21.5222	30.1862	3.199	1.58
-----	-----	-----	-----	-----	-----
PCO-5	5.0870	39.4436	29.8127	0.173	1.23
PCO-6	9.5649	35.0220	29.7638	0.945	1.33
PCO-7	14.6110	30.5282	29.8819	1.799	1.34
PCO-8	20.3376	26.1594	30.1518	2.644	1.36

Note: Notations are same as used in Appendix A3.3

APPENDIX A3.5: EXPERIMENTAL RESULTS FOR PURE COMPONENTS AT 30°C

Run	Initial weight of paraffin, gms.	Weight of benzene, gms.	Weight of adsorbent, gms.	Equilibrium composition in liquid phase, moles/litre	Amount adsorbed x 10 <sup>2</sup> , moles/gm. adsorbent
PCP-13	4.9792	36.8414	30.1627	0.491	1.56
PCP-14	6.1819	35.4624	30.2117	0.774	1.69
PCP-15	7.1965	33.6217	29.9648	1.067	1.76
PCP-16	8.7734	29.8030	29.8984	1.580	1.85
PCP-17	11.3450	23.0523	30.2504	2.616	1.90
PCP-18	13.2071	20.1176	30.3348	3.298	1.95
PCX-13	3.9664	38.2135	30.2250	0.159	1.29
PCX-14	5.2980	36.6232	30.2590	0.476	1.33
PCX-15	6.5841	34.8473	30.1720	0.787	1.37
PCX-16	10.8198	27.6433	30.1517	1.938	1.42
PCX-17	14.4555	24.3121	30.2237	2.764	1.52
PCX-18	15.1436	20.8467	30.0917	3.126	1.60

Appendix A3.5 (contd)

Run	Initial weight of paraffin, gms.	Weight of benzene, gms.	Weight of adsorbent, gms.	Equilibrium composition in liquid phase, moles/litre	Amount adsorbed $\pi$ 1, moles/gm. ad sorbent
PCH-13	4.1599	38.6491	29.6542	0.129	1.20
PCH-14	5.4954	36.4382	30.1355	0.384	1.26
PCH-15	6.9523	34.7820	29.1270	0.713	1.29
PCH-16	9.6658	31.2298	29.8075	1.290	1.32
PCH-17	15.0776	23.1127	30.2279	2.564	1.34
PCH-18	19.2518	20.1729	30.1617	3.280	1.46
---	---	---	---	---	---
PCO-9	5.0126	39.4436	29.8127	0.205	1.15
PCO-10	9.4363	35.0220	29.7638	0.938	1.28
PCO-11	14.1260	30.5282	29.8819	1.734	1.29
PCO-12	19.7864	26.1594	30.1518	2.571	1.31

Note: Notations are same as used in Appendix A3.3

APPENDIX A3.6: EXPERIMENTAL RESULTS FOR PURE COMPONENTS AT 42°C

Run	Initial weight of paraffin, gms.	Weight of benzene, gms.	Weight of adsorbent, gms.	Equilibrium composition in liquid phase, moles/litre	Amount adsorbed x 10 <sup>3</sup> moles/gm. adsorbent
PCX-19	3.9565	38.4122	30.1729	0.173	1.26
PCX-20	5.2359	36.8409	29.7009	0.488	1.29
PCX-21	7.9588	33.1919	30.3013	1.144	1.32
PCX-22	10.5224	29.9335	30.6614	1.771	1.34
PCX-23	14.7546	25.0412	30.0920	2.771	1.40
PCX-24	16.3813	22.4673	29.8512	3.188	1.47
PCX-19	4.4595	38.5281	30.2214	0.183	1.19
PCX-20	5.6869	36.3121	29.8729	0.444	1.23
PCX-21	7.8807	33.6171	29.9253	0.908	1.25
PCX-22	13.5459	26.1927	30.0625	2.142	1.29
PCX-23	18.0898	23.7676	30.3016	2.873	1.33
PCX-24	22.0978	21.0921	30.2842	3.451	1.45
PCO-13	5.0558	39.4436	29.8127	0.236	1.11
PCO-14	9.9295	35.0220	29.7638	1.022	1.25
PCO-15	14.4930	30.5282	29.8819	1.770	1.25
PCO-16	20.6542	26.1594	30.1518	2.626	1.27

Note: Notations are same as used in Appendix A3.3

Appendix A4.1 (contd)

Run	Initial weight of paraffins, gms. 1	Weight of benzene, gms. 2	Weight of adsorbent, gms.	Equilibrium composition in liquid phase, mole fraction 1 2	Adsorbed phase composition, mole fraction, 1 2	Separation factor, K
BPH-1	14.1358	3.3475	21.7080	30.3614 0.877	0.123 0.815	0.185 0.62
BPH-2	10.9897	5.9411	21.7019	30.5584 0.716	0.284 0.727	0.273 1.06
BPH-3	7.2624	9.6524	21.6857	30.8941 0.510	0.490 0.554	0.446 1.29
BPH-4	3.3264	15.0246	21.6963	29.5329 0.198	0.802 0.318	0.682 1.88
—	—	—	—	—	—	—
BPO-1	2.8074	17.5999	21.7013	30.2394 0.165	0.835 0.290	0.710 2.06
BPO-2	6.2894	14.7825	21.6429	30.1516 0.409	0.591 0.506	0.494 1.48
BPO-3	9.7731	8.0076	21.7214	29.8294 0.653	0.347 0.673	0.327 1.09
BPO-4	14.5298	4.3224	21.7398	29.7286 0.857	0.143 0.811	0.189 0.72

<sup>a</sup>These mole fractions are on benzene free basis.

Note: 1 represents the lighter hydrocarbon in a given binary mixture and 2 presents the other component.

BPX = Pentane-hexane; BXH = hexane-Heptane; BHO = Heptane-Octane; BPH = Pentane-Heptane  
BPO = Pentane-Octane

APPENDIX A4.2: EXPERIMENTAL RESULTS FOR BINARY SYSTEMS AT 18°C

Run	Initial weight of paraffins, gms. 1	Weight of benzene, adsorbent, gms. 2	Weight of benzene, adsorbent, gms.	Equilibrium composition in liquid phase, mole fraction: 1 2	Adsorbed phase composition, mole fraction: 1 2	Separation Factor, K
BPX-5	14.4761	3.2372	21.6802	30.0021 0.863	0.137 0.791	0.209 0.60
BPX-6	10.0973	6.1969	21.6915	30.1527 0.660	0.340 0.662	0.338 1.01
BPX-7	6.6587	10.1203	21.6929	29.9284 0.428	0.572 0.472	0.528 1.19
BPX-8	3.1750	14.2555	21.6815	30.2721 0.182	0.818 0.283	0.717 1.78
BXH-5	3.7799	14.5023	21.6613	29.8827 0.186	0.814 0.387	0.613 2.76
BXH-6	7.4778	11.1023	21.6902	29.7625 0.421	0.579 0.492	0.508 1.33
BXH-7	10.9669	7.5245	21.7107	30.1895 0.628	0.372 0.632	0.368 1.02
BXH-8	15.0007	4.2015	21.6992	30.1029 0.831	0.169 0.736	0.264 0.56
BHO-5	3.6281	15.0288	21.6364	29.8816 0.174	0.826 0.318	0.682 2.22
BHO-6	6.5250	10.1608	21.6825	29.9222 0.407	0.593 0.458	0.542 1.23
BHO-7	9.7213	7.0137	21.7127	30.1713 0.622	0.378 0.589	0.411 0.87
BHO-8	14.4419	3.7221	21.7038	29.7727 0.854	0.146 0.723	0.277 0.44

## Appendix A4.2 (contd.)

Run	Initial weight of paraffins, gms.	Weight of benzene, gms.	Weight of adsorbent, gms.	Equilibrium composition in liquid phase, mole fraction <sup>a</sup>		Adsorbed phase composition, mole fraction	Separation factor, K		
				1	2				
BPH-5	14.1038	3.4302	21.6807	29.8817	0.876	0.124	0.793	0.207	0.54
BPH-6	10.6794	5.9672	21.6892	30.1516	0.712	0.288	0.716	0.284	1.02
BPH-7	7.7114	9.5931	21.6712	30.2910	0.513	0.487	0.565	0.435	1.23
BPH-8	3.3628	14.5987	21.6698	30.0152	0.209	0.791	0.329	0.671	1.85
-----	-----	-----	-----	-----	-----	-----	-----	-----	-----
BPO-5	3.2892	15.4744	21.7185	29.8326	0.212	0.788	0.349	0.651	1.99
BPO-6	6.8179	10.7777	21.6623	29.8129	0.479	0.521	0.554	0.446	1.35
BPO-7	10.2713	7.6230	21.6629	29.5027	0.675	0.325	0.696	0.304	1.11
BPO-8	14.5588	3.8900	21.6903	30.0089	0.879	0.121	0.802	0.198	0.56

<sup>a</sup>These mole fractions are on benzene free basis

Note: Notations are same as used in Appendix A4.1

APPENDIX A4.3: EXPERIMENTAL RESULTS FOR BINARY SYSTEMS AT 30°C

Run	Initial weight of paraffins, gms. 2	Weight of benzene, gms.	Weight of adsorbent, gms.	Equilibrium compo- sition in liquid phase, mole fraction a		Adsorbed phase composition, mole fraction 1	Separation factor, K 2
				1	2		
BPX-9	3.3295	13.9764	21.5863	29.8627	0.205	0.795	0.241
BPX-10	6.8686	10.6777	21.8855	30.1690	0.453	0.547	0.373
BPX-11	9.7702	6.9730	21.9107	30.0854	0.667	0.333	0.494
BPX-12	13.9554	3.6111	21.9169	30.0989	0.866	0.134	0.689
BXH-9	15.4862	3.6045	21.7025	29.8314	0.863	0.137	0.745
BXH-10	12.6950	7.7851	21.6817	29.7729	0.650	0.350	0.671
BXH-11	7.9399	10.1209	21.6939	29.9238	0.450	0.550	0.561
BXH-12	3.8784	14.5098	21.6898	30.1122	0.190	0.810	0.377
BHO-9	3.5132	16.7999	21.6396	29.7622	0.148	0.852	0.322
BHO-10	6.0619	11.7229	21.7012	29.8320	0.345	0.655	0.442
BHO-11	9.7249	7.4713	21.6988	29.9698	0.601	0.399	0.588
BHO-12	14.4074	3.9464	21.6628	29.7440	0.843	0.157	0.706

Appendix A4.3 (contd)

Run	Initial weight of paraffins, gms. 1	Weight of benzene, gms. 2	Weight of adsorbent, gms.	Equilibrium compo- sition in liquid phase, mole fraction		Separation factor, K			
				1	2				
BPH-9	14.3499	3.7235	21.6517	30.1516	0.877	0.123	0.744	0.256	0.41
BPH-10	11.1221	6.5071	21.6899	30.2912	0.725	0.275	0.643	0.357	0.68
BPH-11	8.0645	10.0740	21.6712	30.0459	0.534	0.466	0.501	0.499	0.88
BPH-12	3.4456	14.6269	21.6025	30.1127	0.220	0.780	0.279	0.721	1.66
—	—	—	—	—	—	—	—	—	—
BPO-9	3.4364	17.3266	21.6626	30.1124	0.204	0.796	0.346	0.654	2.07
BPO-10	7.4217	12.6457	21.6439	29.8826	0.465	0.535	0.539	0.461	1.35
BPO-11	10.7569	8.0406	21.6827	29.8412	0.679	0.321	0.679	0.321	1.00
BPO-12	14.3044	4.2407	21.6836	29.9018	0.866	0.134	0.781	0.219	0.55

<sup>a</sup>These mole fractions are on benzene free basis

Note: Notations are same as used in **Appendix A4.1**

APPENDIX A4.1: EXPERIMENTAL RESULTS FOR BINARY SYSTEMS AT 42°C

Run	Initial weight of paraffins, gms.	Weight of benzene, gms adsorbent, gms.	Equilibrium composition in liquid phase, mole fraction <sup>a</sup>		Adsorbed phase composition, mole fraction	Separation factor, K
			1	2		
BXH-13	3.6740	13.9992	21.6717	29.8010	0.189	0.811
BXH-14	7.4603	10.0817	21.6829	29.7700	0.434	0.566
BXH-15	11.4451	6.7269	21.6528	30.1217	0.662	0.338
BXH-16	14.6661	3.5147	21.7512	30.0129	0.860	0.140
BHO-13	3.5617	16.4160	21.6538	30.1616	0.154	0.846
BHO-14	6.9718	13.5424	21.7216	29.8517	0.349	0.651
BHO-15	10.2128	7.5678	21.6982	29.9114	0.613	0.387
BHO-16	14.4486	3.9645	21.6724	29.8434	0.844	0.156
					0.701	0.299
					0.43	

<sup>a</sup>These mole fractions are on benzene free basis

Note: Notations are same as used in Appendix A4.1

APPENDIX A4.5: OPERATING CONDITIONS FOR TERNARY SYSTEMS AT 60°C

Run	Initial weight of paraffins, gms.	1	2	3	Weight of benzene, gms.	Weight of adsorbent, gms.
PXH-1	10.6388	3.2586	5.3818		21.6916	30.2192
PXH-2	3.9274	9.2417	5.5638		21.6836	30.1814
PXH-3	2.8052	7.4966	9.4497		21.6876	29.9384
PXH-4	6.1566	5.1188	8.3040		21.6746	30.0446
---	---	---	---	---	---	---
PXO-1	9.2721	3.0436	3.8059		21.6265	29.8626
PXO-2	3.8967	7.8161	3.7385		21.6629	29.8884
PXO-3	2.7226	6.9346	5.9805		21.6778	29.9254
PXO-4	5.6098	4.9040	6.1882		21.6828	30.1146
---	---	---	---	---	---	---
PHO-1	10.1738	3.8783	4.1975		21.7108	29.9827
PHO-2	3.8141	5.1505	6.1502		21.6927	30.0839
PHO-3	2.6733	9.0024	3.8486		21.6634	30.2256
PHO-4	2.8028	7.3864	5.5603		21.7088	30.1617

Note: 1 is the lightest hydrocarbon in a given ternary system and 3 is the heaviest hydrocarbon.

PXH = Pentane-hExane-Heptane; PXO = Pentane-hExane-Octane;

PHO = Pentane-Heptane-Octane

APPENDIX A4.6: OPERATING CONDITIONS FOR TERNARY SYSTEMS AT 18°C

Run	Initial weight of paraffins, gms	Weight of benzene, gms	Weight of adsorbent, gms
	1	2	3
PXH-5	5.0132	3.1772	9.3806
PXH-6	5.2235	6.3778	6.4338
PXH-7	9.4934	6.3666	2.5716
PXH-8	5.6149	8.3080	2.5063
PXO-5	2.4187	2.9722	10.2961
PXO-6	9.5309	4.0827	2.6465
PXO-7	4.9743	7.2392	3.4290
PXO-8	2.7661	7.5776	5.9953
PHO-5	4.4916	3.1085	9.0036
PHO-6	9.3936	3.2041	2.6660
PHO-7	3.0125	6.0269	6.1011
PHO-8	7.1677	5.9279	3.2853

Note: Notations are same as used in Appendix A4.5

APPENDIX A4.7: OPERATING CONDITIONS FOR TERNARY SYSTEMS AT 30°C

Run	Initial weight of paraffins, gms.			Weight of benzene, gms.	Weight of adsorbent, gms.
	1	2	3		
PXH-9	3.6674	11.8669	3.3120	21.8955	30.2529
PXH-10	12.1527	3.5771	3.2395	21.8900	29.9740
PXH-11	8.5445	7.5332	3.5182	21.9500	30.2944
PXH-12	7.9277	3.6292	6.2008	21.9147	29.6884
PXH-13	3.5245	7.9038	6.7744	21.8947	30.0294
PXH-14	5.9696	2.7866	10.4366	21.8869	30.2339
PXH-15	6.5736	6.2677	5.2552	21.8929	30.2514
PXH-16	7.1555	7.7968	6.4614	21.8749	29.9409
---	---	---	---	---	---
PXO-9	3.1831	10.8408	3.9158	21.7015	29.9297
PXO-10	6.4726	6.2920	3.6184	21.6927	29.9765
PXO-11	10.2570	3.0167	4.5387	21.6998	29.8965
PXO-12	6.7440	3.1244	6.4821	21.6886	30.1028

Appendix A4.7 (contd)

Run	Initial weight of paraffins, gms			Weight of benzene, gms	Weight of adsorbent, gms.
	1	2	3		
PHO-9	3.2666	3.2886	11.2380	21.6813	30.2216
PHO-10	6.6120	6.2257	4.2156	21.6602	29.9107
PHO-11	6.9678	3.5144	7.3890	21.6912	29.8635
PHO-12	11.2332	3.1689	4.2958	21.7002	29.9234

Note: Notations are same as used in Appendix A4.5

ADDENDUM

The term "breakthrough time" has been somewhat inappropriately used in the text. It is usually meant to represent the time required for the first appearance of a species from the exit of an adsorption column. In this work, it has been used to describe the time required for the attainment of adsorption equilibrium.